Project Number: SYS-0078
Mechanical Engineering

Redesign of the Restrainer band for a Horse Leg Protective Device Based on a Static Analysis

A Major Qualifying Project Report
Submitted to the Faculty of the

Worcester Polytechnic Institute

in partial fulfillment of the requirements for the
Degree of Bachelor of Science
By

Xiaolin Zhen
_____

Xiaowen Zhen
_____

Date: April 18, 2012

Sponsoring Organization:
Dr. Carl Kirker-Head
Cummings School of Veterinary Medicine at Tufts University

Project Advisor:
_____
Professor Satya Shivkumar

Project Advisor:
_____
Professor Allen H. Hoffman

Keywords:
1. Equine biomechanics 2. Tension force 3. MCPJ angle

Abstract

Conventional horse leg protectors, such as bandage-wrapped boots, are not energy dissipative and require operation by professionals. Manta Design, Inc. designed a protective device intended to minimize the hyperextension of the flexor tendons in a horse's forelimb by providing counter tensions with an attached restrainer band. However, the current band design does not provide consistent tension and is insufficient at protecting the metstarsophalangeal joint (MCPJ) from injury. This project studied the static performance of the MCPJ to determine the required restrainer band tensions needed for Manta Design's protectant. It was found that restrainer band should be designed to counter the tension of the suspensory ligament tendon, which contributed to most of the MCPJ tension. The allowed minimum and maximum restrainer band tensions were determined to be 87N and 1620N, respectively, in order to reduce MCPJ moment by 10 percent. The improved restrainer band achieves an 8.4% MCPJ moment reduction at maximum extension.

Table of Contents

List of Figures

List of Tables

List of Equations

1.0. Introduction

Horses are large running mammals, weighing 450-500 kg (990-1100 lbs). They are capable of rapid acceleration and attaining upper speeds of 20 m/s (44 mph) [1]. Each year, a great amount of time and money is invested to breed and raise racing horses. Horse racing has become one of the worldwide popular sports from an aristocratic entertainment during the cultural developments. Although horse racing involves close cooperation between the jockeys and the horses, it depends more on the speed and racing ability of the horses.

The tendons in horse forelimb are more susceptible to injuries because they are responsible for energy absorption and emission. When a horse gallops, the lead leg is flexed under the body of the horse and rotates forward while two other legs support the body to propel it forward [2]. The forelimbs of the horse function primarily for weight-bearing, which could support approximately 60% of the body weight [1], rather than propulsion. On the other hand, the non-boney structures such as muscles, tendons and ligaments, are principally responsible for enabling the locomotion by providing propulsive forces and storing energy. The metacarpophalangeal joint (MCPJ, fetlock joint) supports overall locomotion by acting as a passive spring.

The horse's large body size, slender limb structure and occasional need for high speed or rapid acceleration expose the lower limbs to risks of injury, mostly due to a misstep of the hoof or from repeated loading of the limb during racing. Even though the horse's third metacarpal (cannon) bone (Figure 1) is one of the strongest in the entire skeleton, the MCPJ or the mid--metacarpal region of the superficial digital flexor tendons (SDFT) (Figure 1) are locations frequently affected in racing horses [3]. It requires extensive recovery periods before the horse can return to normal activity. In most of the cases, the healing process can be aggravated due to competitive use of horses. As a result, the tendon injury will fail to fully resolve, causing life-long limitation of use.

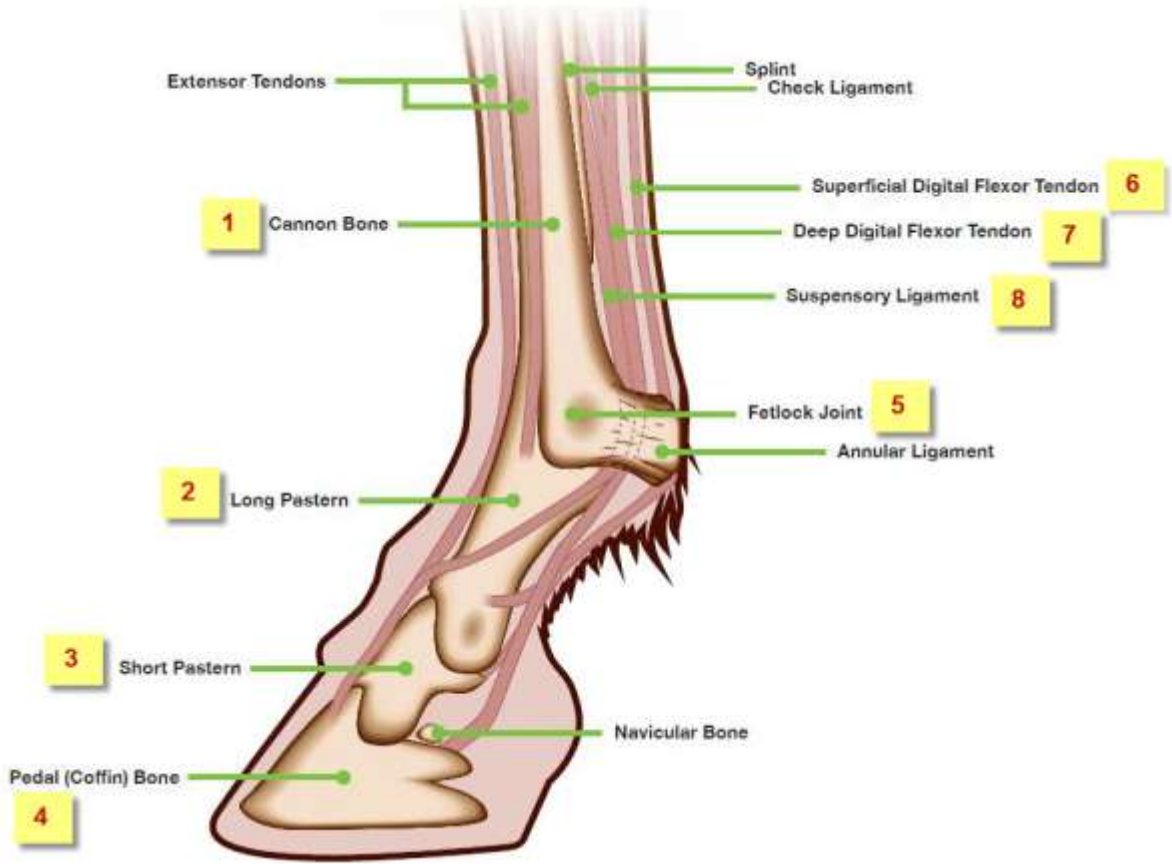

Figure 1: Bones and tendons of the equine forelimb, lateral view, left side. [4]

Some researchers have been looking for methods of reducing the incidences of lower limb injuries and improving functional outcomes following lower limb injuries, such as by modifying ground surface and reducing the training regimens [3]. Conventional methods such as bandage wrapped boots were widely used to prevent horse leg tendon injuries. However, bandage wrapped boots had more disadvantages than advantages to the horse legs because the bandage has to be wrapped by professionals. The bandage wrapped boots are also not energy dissipative [4].

A better sleeve is necessary for horses to enable them to compete at a high level while protecting their forelimbs. A firm understanding of horse limb biomechanics will allow the researchers to significantly reduce injuries in horse lower forelimbs by better predicting biological and non-biological material behaviors during locomotion. Cummings School of Veterinary Medicine at Tufts University is partnering with Manta Design Inc. in developing a horse leg protective device through MCPJ moment reduction by using a restrainer band attachment. However the restrainer band does not provide constant tension and therefore does not sufficiently protect the horse leg. In this project, the restrainer band was biomechanically analyzed and design an improved band has been developed.

2.0. Background Research

This chapter discusses many aspects of the biomechanics of the horse forelimb. A few scholars found that the hyperextension of horse leg tendons is positively associated with the MCPJ moment. One way to protect tendons is through usage of horse leg protective device. This chapter also describes the benchmarks and philosophy of the horse leg protective device. The horse leg protective device with a restrainer band attachment designed by Tufts Cummings School of Veterinary will limit the MCPJ moment of the horse forelimb and eventually protect horse leg tendons from hyperextension.

2.1 Equine Forelimb Anatomy

The horse leg protective device covers areas from ¾ of the 3rd metacarpal bone (cannon bone) to distal area of the short pastern bone. The device was designed to cover the indicated area because the flexor tendons responsible for the extension of the horse leg are located in these areas. In this section, the structure of the horse forelimb, including the bones and the tendons was discussed. The range of motion (ROM) of the MCPJ was also included as it was the benchmark in designing the horse leg protective device.

2.1.1 Bones

Figure 2 presents the bone structures of a horse forelimb. The bones provide support for the body weight and help form the shape. The top bone of the forelimb, scapula is a flat triangular bone that joins onto the humerus. The spine of the scapula (a ridge) divides it into two halves, providing attachment for the shoulder muscles. Next is the humerus. Scapula and humerus forms the shoulder joint. Humerus forms the elbow joint with radius and ulna. Below the radius and ulna is the carpus, which is treated as the knee in horses. It consists of seven bones. These bones are called the carpal bones, except for the seventh bone which is referred to as the accessory carpal bone.

The carpal bones the metacarpal bones are shown in Figure 2. In human, there are five metacarpal bones, however, in horses, only 2nd, 3rd, and 4th metacarpals are present. In horse legs, the 1st and 5th metacarpals have disappeared while the 2nd and 4th metacarpals are greatly reduced in accordance with the streamlining and lengthening of the limb for speed. The third metacrapal, also known as cannon bone, is well developed robust bone that carries the entire weight assigned to the limb. The 2nd and 4th metacarpals, also known as the splint bones, appear slender and about a third shorter than the cannon bone. The splint bones are connected to cannon bones by fibrous tissue and located behind the cannon bone [1].

The proximal, middle, and distal phalanges form the supporting skeleton at the bottom of the forelimb. The three phalanges correspond to the three phalanges of a human finger, thus we can think horses are standing with its fingers [2]. The proximal phalanx, also known as long pastern, is the longest of the three. The middle phalanx or short pastern is half as long as the preceding. The distal phalanx or the coffin bone consists of spongy bone throughout [1].

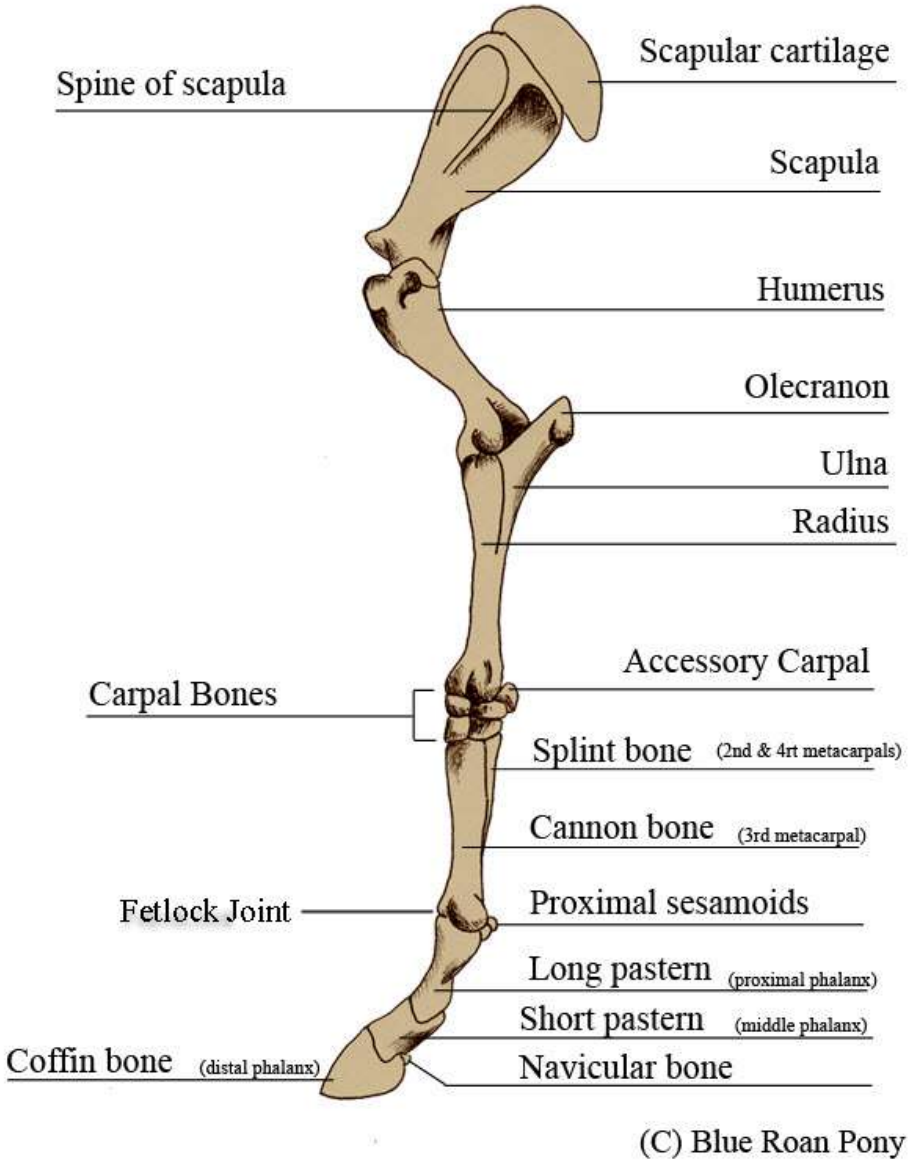

Figure 2 Bones of horse forelimb, lateral view, left side [6].

The fetlock (also known as metacarpophalangeal joint, MCPJ) of horses corresponds to human knuckles, such as the ball of the foot. The fetlock is formed by the junction of cannon bone and the proximal phalanx. The fetlock is a hinge joint, allowing flexion and extension, but limit rotation, adduction and abduction [5]. At the back of the fetlock there is a pair of sesamoid bones (medial and lateral). The sesamoid bones are to keep the tendons and ligaments that run between them correctly functioning [5].

2.1.2 Tendons and Ligaments

Tendons and ligaments are another important because tendon and ligament strains and sprains are very common injuries in the lower leg of performance horses. The most common of these injuries affects the weight bearing digital flexor tendons at the back of the canon bone and fetlock. Not only do these

injuries result in a high level of wastage in performance horses, they also have a high rate of re-occurrence [3].

Tendons and ligaments are made up of elastic fibers, primarily composed of collagen. These fibers can stretch to a limited degree, and each tendon or ligament is composed of many parallel elastic collagen fibers [3]. Tendons join muscle to bone so that when the muscle contracts the bone moves. Most tendons are described as either flexor or extensor. Flexor tendons allow a joint to bend inward toward to body (close), while flexor tendons allow a joint to extend (open) Ligaments are strong, flexible connective-tissue band that join bone to bone. Most ligaments are composed of dense fibrous tissues formed by parallel bundles of collagen fibers. They have a shiny white appearance and are flexible, strong and noncompliant. Ligaments are stabilizing structures that hold the bones together and stop them from overextending, over-flexing or over-rotating [7].The main tendons and ligaments of an equine forelimb is shown in Figure 3.

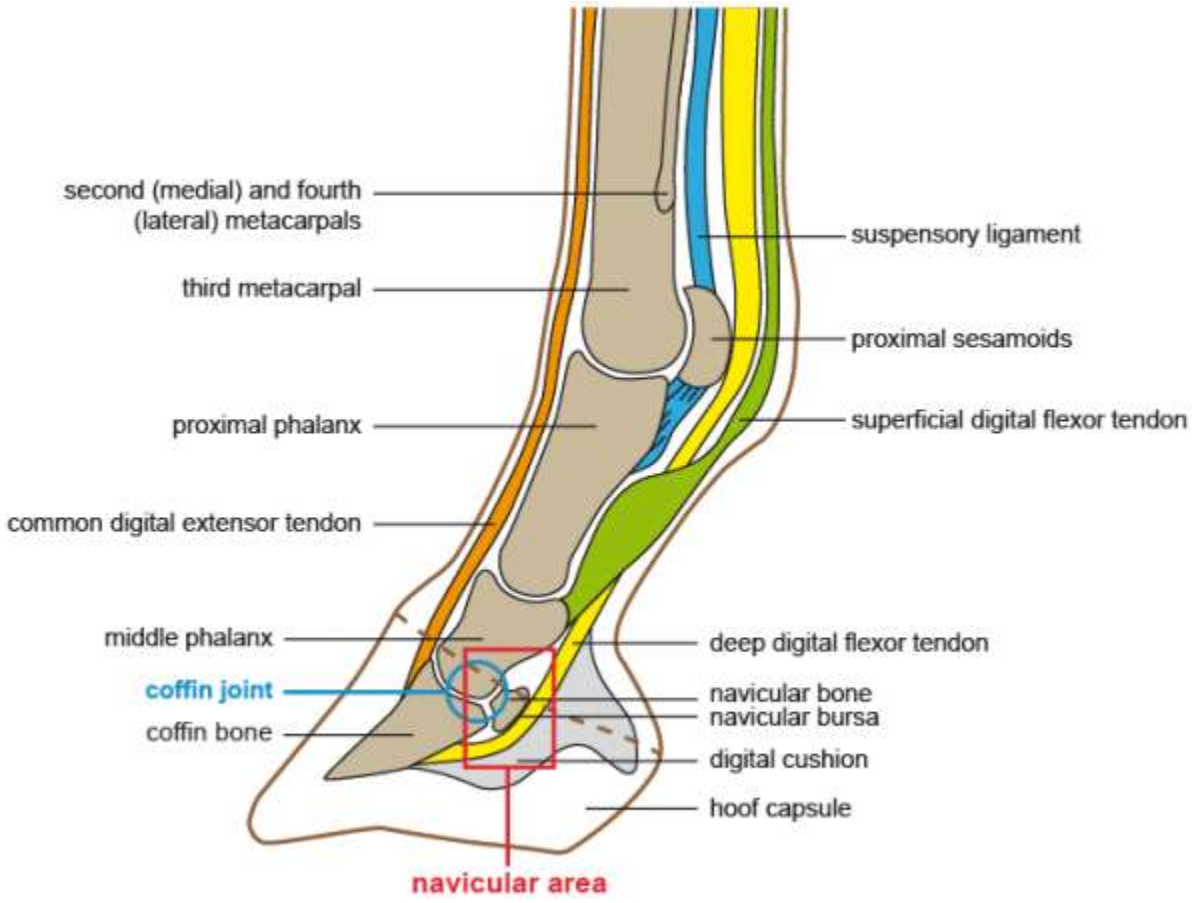

Figure 3 -Tendons and Ligaments of Equine Forelimb [8].

The four principal tendons and ligaments in the horse forelimb are: 1) Superficial digital flexor tendon (colored green in Figure 3), deep digital flexor tendon (colored yellow in Figure 3), suspensory ligament (colored blue in Figure 3) and common digital flexor tendon (colored orange in Figure 3). The superficial and deep digital flexors and the common digital extensor work together with the suspensory ligament to add additional stability to the fetlock, pastern and coffin joints [8].

The flexor tendons (including the superficial digital flexor tendon, SDFT and the deep digital flexor tendon, DDFT) run down from the radius above the MCPJ. The SDFT ends on the proximal and middle phalanges, while the DDFT ends of the lower surface of the coffin bone [1]. A suspensory ligament is a band of fibrous tissue that supports an organ or body part. In horses, the suspensory ligament consists of a strong band of tendon-like tissue that lies along the back of the cannon bone between the splint bones. It originates from the top of the back of the cannon bone and continues down to the fetlock region. About two-thirds of the way down the cannon bone, the suspensory ligament splits into two branches (medial and lateral); each branch inserts into one of the paired (medial and lateral) proximal sesamoid bones. The primary function of the suspensory ligament is to prevent excessive extension of the MCPJ during the weight-bearing or stance phase of the stride [7]. The common digital flexor tendon starts from the bottom third of the radius and continues down the front of the leg. [2]. The SDFT and DDFT as well as the suspensory ligament control the "extension" of the forelimb while the common digital flexor tendon controls the "flexion" of the forelimb.

2.1.3 Range of Motion (ROM) of the horse MCPJ

In kinesiology, extension is a movement of a joint that results in increased angle between two bones or body surfaces at a joint. Extension usually results in straightening of the bones or body surfaces involved. While on the other hand, a flexion movement can result in the decrease in angle of a joint. A horse flexes its limbs backward while extends its limbs forward (**Error! Reference source not found.**).

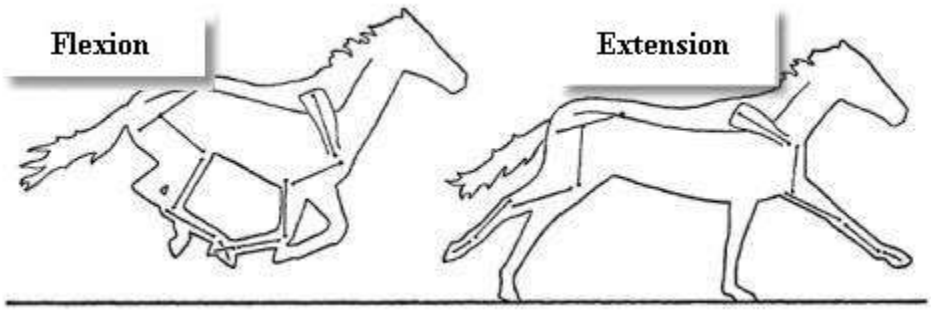

Figure 4 - Schematic illustration of various positions during the galloping of a horse [9].

According to Ratzlaff, normal horses moving at the trot have the maximum range of motion in the fetlock is from 36.8 °(flexion) to -81.2 °(extension) (Figure 5) [9].

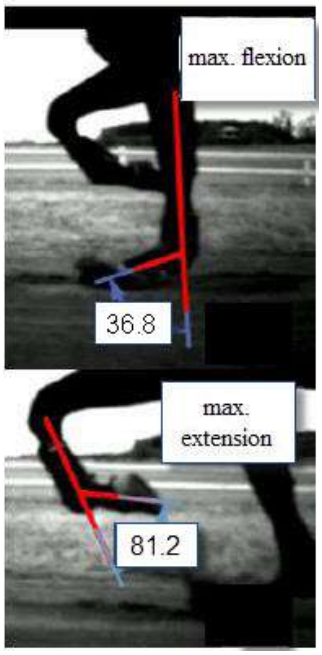

Figure 5 - Range of Motion (ROM) of MCPJ of a horse forelimb. The maximum flexion angle is 36.8 °and the maximum extension angle is -81.2 °[9].

If a part of the body such as a joint is overstretched or "bent backwards" because of exaggerated extension motion, then one speaks of a hyperextension. This puts a lot of stress on the ligaments of the joint, and need not always be a voluntary movement, but may occur as part of accidents, falls, or other causes of trauma [10].

2.2 Common tendon injury locations on the horse forelimb

The tendons and ligaments of horse forelimb have high tensile strength and great elasticity. When loaded, the tendons demonstrate a large increase in length for a small increment in load, resulting in a nonlinear relationship as seen on a stress-strain graph, and later followed by a linear loading region in which the tendon can return to its original form. The hysteretic characteristics reflect the actions such as energy dissipation and restoring forces at the nonlinear locations of the structure. Figure 6 shows an example depicting the hysteresis characteristics of tendons in a repeated strain cycling to different strain levels on one sample of horse flexor tendon [3]. The area inside the hysteresis loop equals the amount of energy dissipated in that cycle of deformation. As higher loads are applied, a nonlinear response occurs in which the tendons stretch more than expected for a given load (the yield point). At loads that exceed the yield point, plastic deformation occurs and finally complete structural failure occurs [11]. The rupture of tendons' collagen fibers are usually involved at tendon damage. Inflammation, soreness, and an inability of the limb to function normally are the common symptoms.

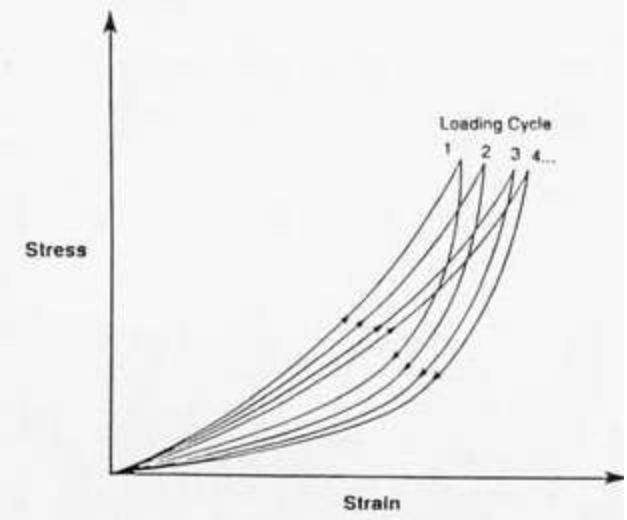

Figure 6 Hysteresis characteristics of tendons and ligaments [3]

All the three flexor tendons (SDFT, SL, and DDFT) h may be subject to injuries during horse racing events, however, it was perceived by Dr. C. A. Kirker-Head based on extensive clinical experience that, the tendon injuries tend to have predilection sites. For example, the SDFT in the mid to proximal metacarpal region of the front limb is the most frequently injured locus in racing thoroughbreds while the suspensory ligament (SL) is more frequently injured in racing standard breeds. Deep digital flexor tendon (DDFT) injury is most commonly encountered in jumping horses while hind limb proximal suspensory injury is more common in dressage horses [11].

2.3 Published studies on horse gait and horse leg motion in gait cycle

This section describes the previous studies on horse gait and horse movements. Parameters such as MCPJ moment, tendon tension forces and angels will be extracted and served as the inputs in the methodology section of the projects.

2.3.1 Reaction force and joint moment of horses at walking and trotting

The invese dynamic method and quasi-static method were utlized by Merritt et al. to calculate the major joint reaction force components in the MCPJ and coffin joints during walking and trotting in the horse. [12]. The forces exerted by wrapping of the tendons around both the proximal and distal sesamoid bones were taken into account when performing the joint reaction force calculations. The joint moments, forces and tension forces of the three major ligaments, namely, superficial digital flexor (SDF), deep digital flexor (DDF) and interosseus ligament (IL), were calculated with the kinetic and kinematic data of a forelimb model in 2D sagittal plane (Figure 7).In this study, the bone segments of the horse forelimb were considered rigid segments in the 2D model, short pastern and long pastern were considered as one segment since the proximal interphalangeal joint between these two pastern bones were described as approximately rigid in Merritt's previous paper [12].

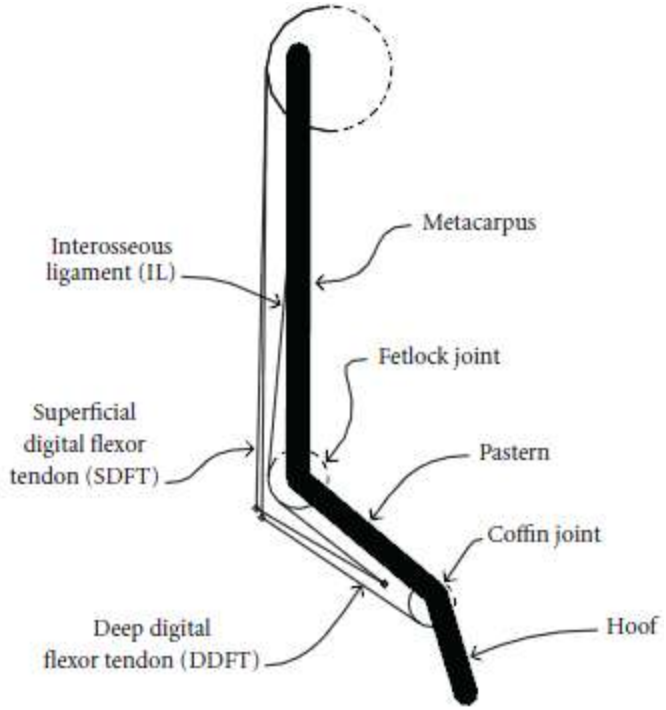

Figure 7 Two-dimensional sagittal plane model of the horse forelimb. The bone segments of the forelimb were considered rigid segments. In this study, the short pastern and long pastern were considered as one segment since the proximal interphalangeal joint between the two bones were described as approximately rigid in Merritt's previous paper [12].

Figure 8 presents the joint moments (torques) calculated at fetlock joint during walking and trotting in Merritt's study [12]. The coffin moment and fetlock moment are negative for the whole stance phase, that means the predominant muscle moment was on the palmar aspect. The change of the movement phase (felxion to extension) happened at 50% of the time phase, both in walk and trot. Appendix A summarizes the collected data to Merrit's research.

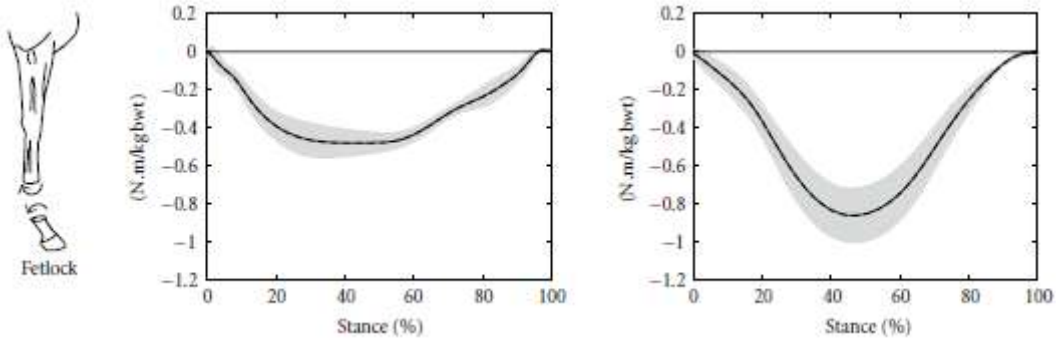

Figure 8- Joint moments (torques) calculated at fetlock during walking and trotting by Merritt [12]. At MCPJ, the change of the movement phase (felxion to extension) happened at 50% of the time phase, both in walk and trot.

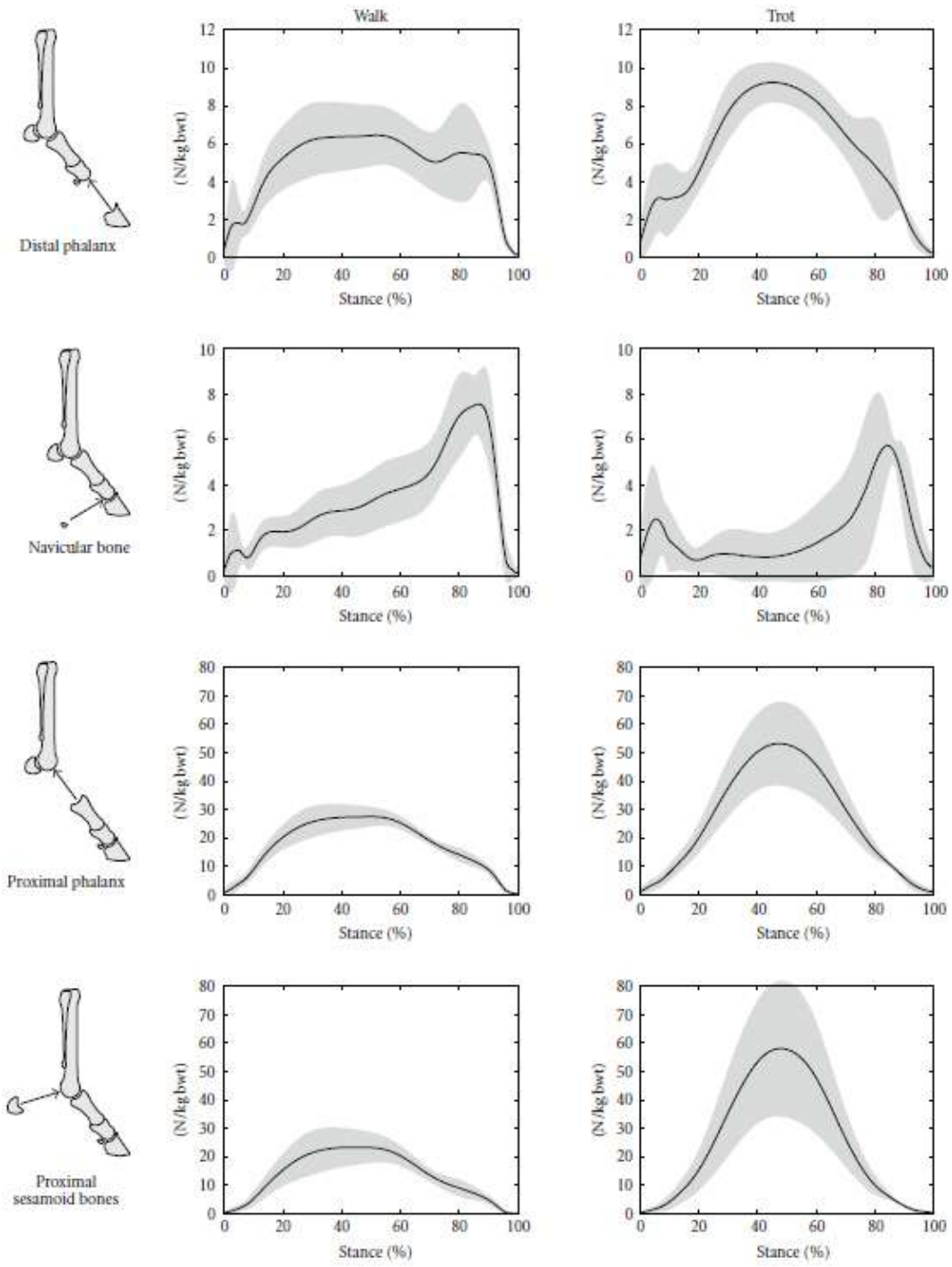

Figure 9 - Joint forces calculated at distal phalanx, navicular bone, proximal phalanx and proximal sesamoid bones by Merritt [12]. Schematics on the left are results for walk phase, while those on the right are for trot.

The joint forces at distal phalanx, navicular bone, proximal phalanx and proximal sesamoid bones were calculated over the full gate cycle (Figure 9). The pattern of the reaction force for each of the calculated joint (distal phalanx, navicular bone, proximal phalanx, and proximal sesamoid bones) are oppositive to that in the moment. The joint forces are positive in all joints during the whole phase. The force slowly rises at flexion stance from 0% to approximately 50%; after 50%, which is the change of

movement phase, the joint forces decrease (Figure 9). The limitations of the paper was concluded as followed: The 2D nature of the model limited it to considering only force components which could be projected onto the sagittal plane, as a result, all the calculated quantities may be affected [12].

2.3.2 Horse leg movement pattern of jumping horses

An inverse dynamic analysis was also utlized by Meershoek [13] to compute joint moments with collected kinematics and ground reaction forces from the leading and trailing forelimbs of six horses during jumping events. The limb was assumed as a chain of rigid segments that can rotate relative to each other. The researchers investigated whether 1) the joint moments during jumping landings exceeded those during trot, 2) moments are different betweeen leading and trailing limb and 3) if there was only flexor moments and no extensor moments during the stance phase.

The moments were the product of external forces and the distance between the tendon and the joints center of the rotation. Based on the results, it was concluded by Meershoek that, for the coffin joint, positive (extending) in the first half of the stance phase and negative (flexing) in the second half of the stance phase was observed in the forelimb, while negative (flexing) during the whole stance phase was observed in the trailing limb; for MCPJ, negative (flexing) during the whole stance for both limbs were observed; for carpal joint, negative (flexing) moments during most of the stance phase were observed in both limbs [13].

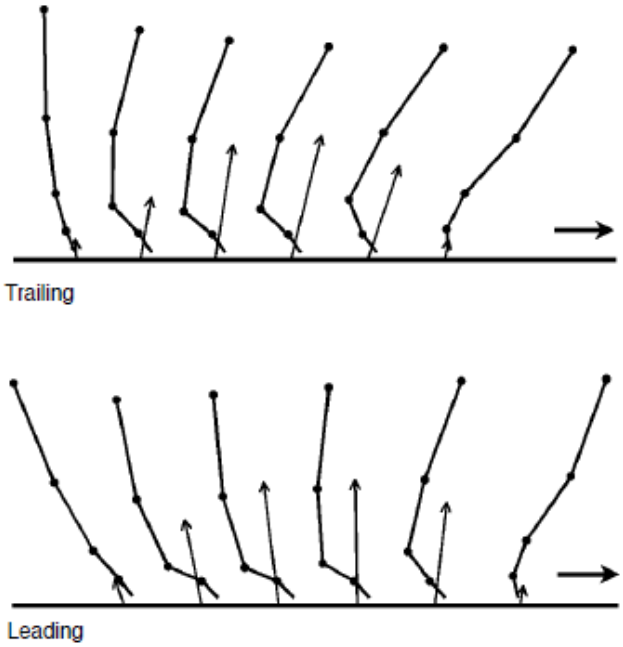

Figure 10 Stick figures showing the movement pattern of the trailing and leading limb of the jumping horses [13].

Figure 10 depicts the movement patterns of the lower leg of the horse forelimb, the stick figures were generated using the joint angles and ground reaction forces [13]. Cannon bone, pastern bones and coffin bones are shown as the thick sticks while the joints in between the bones are shown as the connected dots.

2.3.3 Tendon strain and joint angles of horse legs at gallop

Different from other researchers, a musculoskeletal model of the thoroughbred forelimb was developed in Swanstrom's research [14] to simulate the stance phase of high-speed gallop (speed: 18m/s, stride duration: 75ms) with a forward dynamic analysis. The joints of the model were also restricted to 2-D sagittal plane. A fetlock angle of −23° was produced by initially being placed 1.2 kN load to the model (25% of body weight).

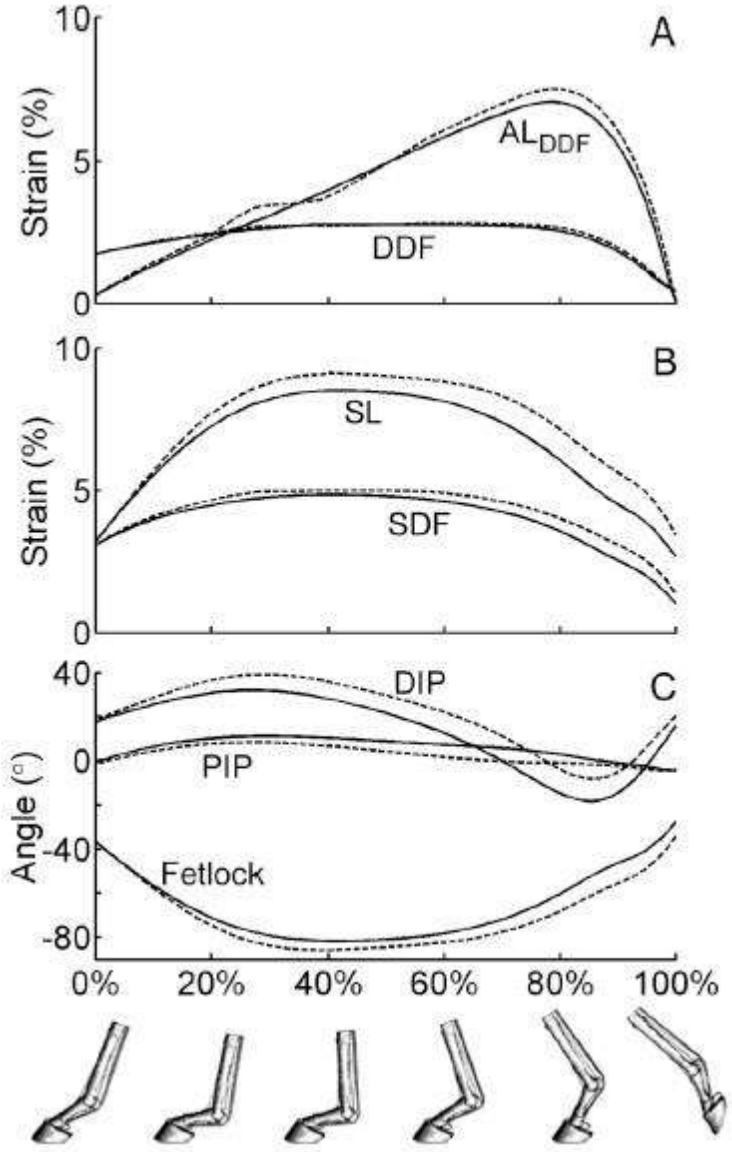

Figure 11 - Tendon strain and joint angles calculations by Swanstrom [14].

Figure 11 presents the movement pattern of the horse trailing and leading limb during the jumping test. It depicts that the joint angles showed similar patterns in both limbs. According the Meershoek, the MCPJ was hyperextended during the whole stance phase with peak amplitude at 55-65% of stance phase [13]. The tendon strains for each tendons were calculated. During the simulation, the peak strain observed for SDF tendon was 4.9% at 41% stance; for DDF tendon it was 2.8% at 55% stance; for

the AL(SDF) , 8.8% at 48% stance; for the AL (DDF), 7.1% at 79% stance; and for SL, 8.5% at 42% stance [14]. These peak stance all happened at the change of movement phase (flexion to extension as for MCPJ). The tendon strains were determined to be linearly proportional to the joint moment.

Table 1: The slacking/rest (L_0) and post-tensioned (L_{PT}) lengths of DDFT, SDFT and SL from Swanstrom'S Musculoskeletal Modeling Analysis are summarized. The strain of the ligaments are calculated.

Muscle	L_o (cm)	L_{PT} (cm)	ΔL (cm)	ε
DDFT	38.2	50.6	12.4	32.5%
SDFT	37.1	44.6	7.5	20.2%
SL	24.5	31.2	6.7	27.3%

The force-length behavior of DDFT, SDFT and SL was also studied by Swanstrom. The ligament lengths at isometric force provided by each ligament component were measured by incrementally stretching. Tabe 1 summarizes the rest and post-tensioned lengths of the three ligaments at maximum MCPJ extension of 81.2 °. The changes in lengths of DDFT, SDFT and SL are 12.4cm, 7.5cm and 6.7cm, respectively.

2.3.4 Three-dimensional joint moment calculation of horse forelimb at trot

In a 2011 study, Clayton et al. demonstrated the relationship between the torques and powers of the forelimb joints at trotting in a three dimensional musculoskeletal model by combining both kinetic and kinematic data of four sound horses (speed: 3.13 ±0.15m/s, stride duration: 706 ±16ms). In the model, each joint has six DOF, including three translations and three rotations. The cranial (+)/caudal (-) and abduction (+)/adduction (-) planes were chosen for the x-coordinates; the medial (+)/distal (-) and flexion (+)/ extension (-) planes formed the y-coordinate, while the z-coordinates included the proximal (+)/distal (-) and internal (+)/external (-) planes (Refer to Figure 12 for planes).

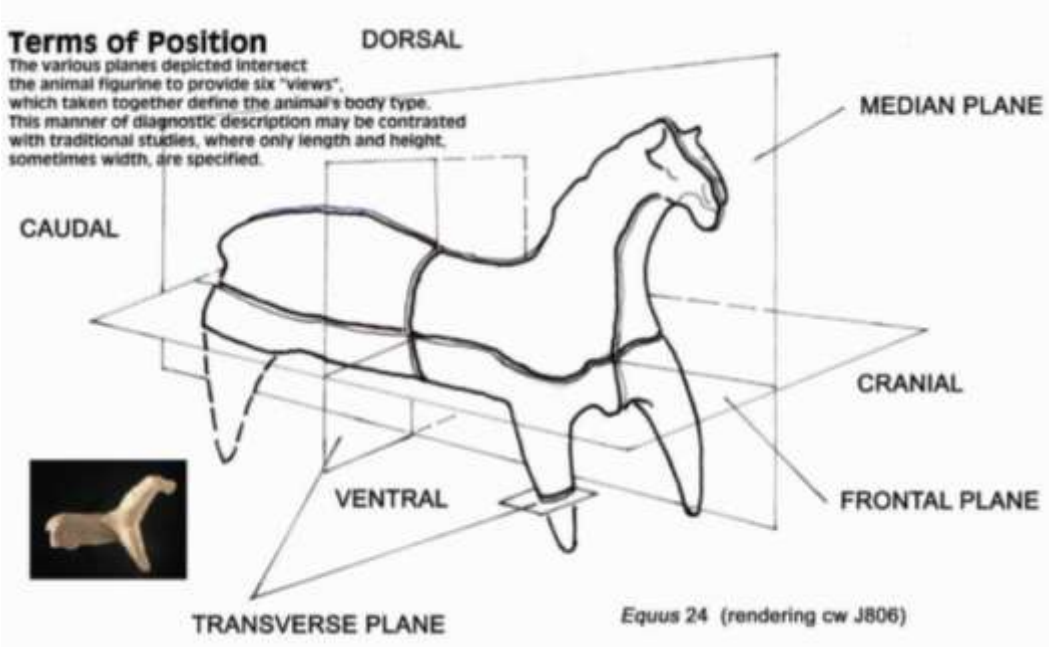

Figure 12 - The various planes depicted intersect the animal figurine to provide six views [15].

The joint torques and contact forces at trot (Figure 13) and at swing (Figure 14) were calculated with recursive Newton-Euler method by inputting the joint position, velocity, and acceleration and GRF data. The data (summarized in Appendix A) by Clayton et al. are not comparable to the previous data as the previous studies were presented in a 2D sagittal plane assumption and this is a full 3D kinetic analysis.

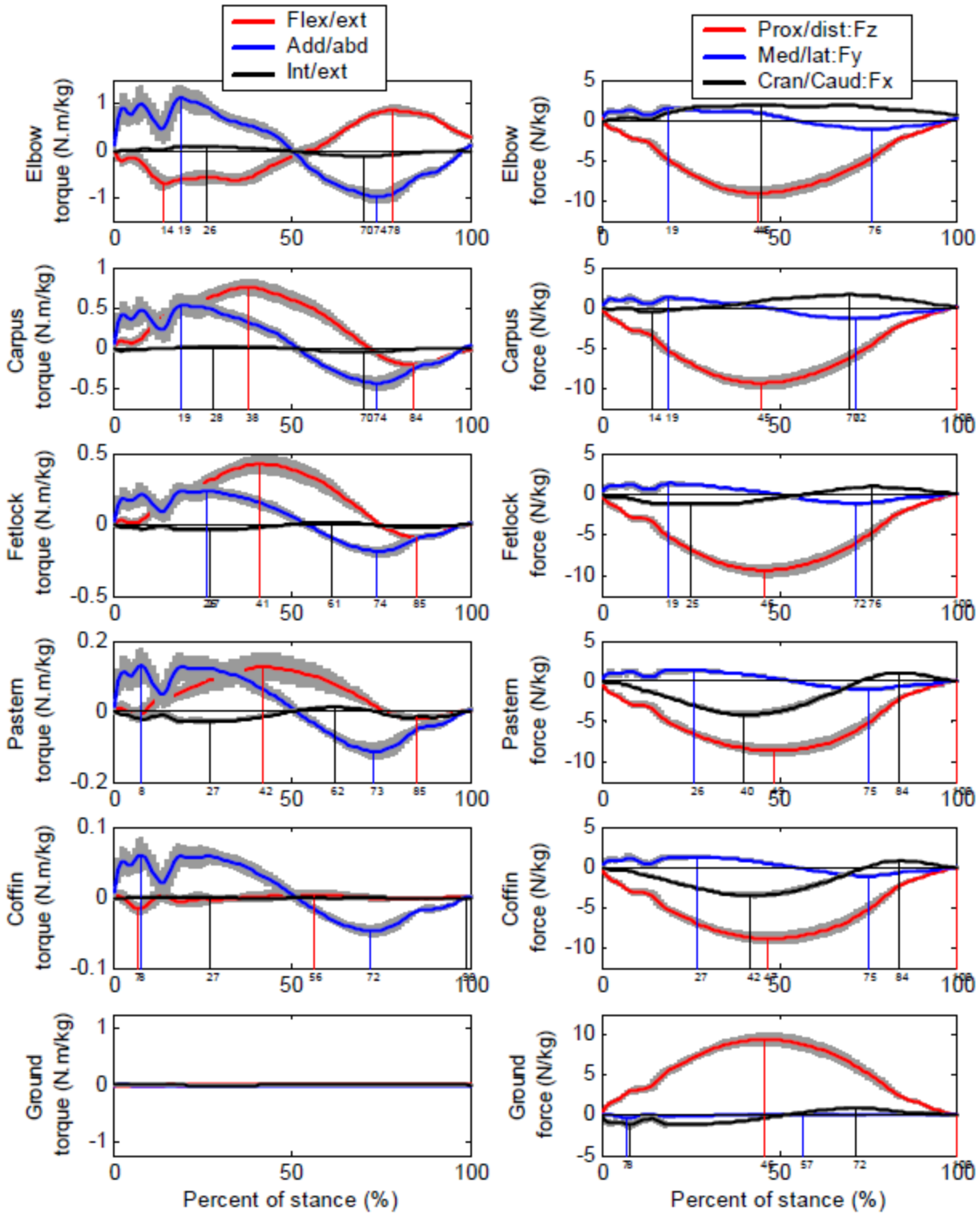

Figure 13 - Joint moments (torques) and contact forces at trot calculated by Clayton. Note the contact forces during stance include weights, inertial loads of segments and ground force [16].

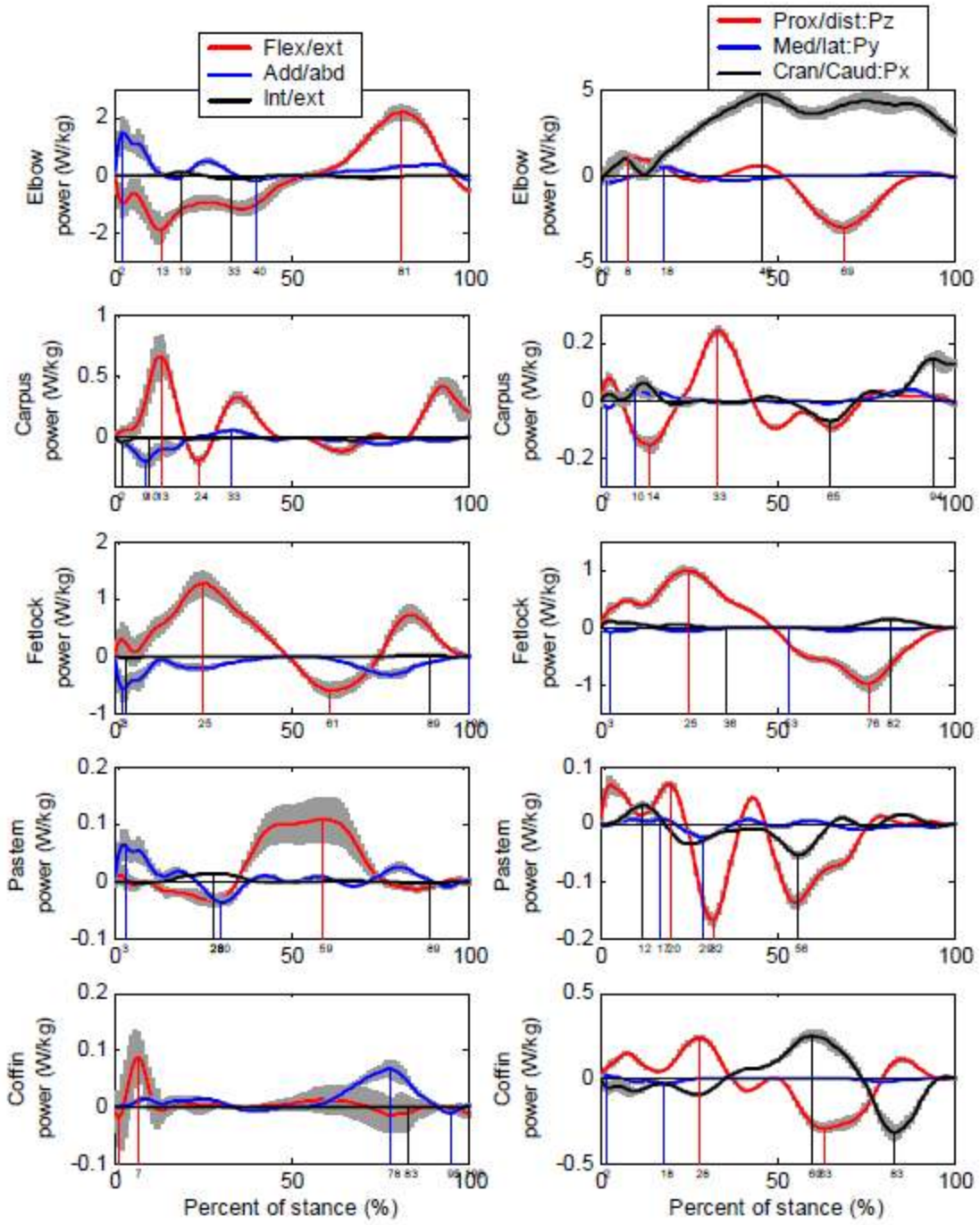

Figure 14 - Joint moments (torques) and contact forces at swing by Clayton [16].

Despite Clayton's data cannot be compared side by side to the previous 2D studies, it is still found that the moment pattern is similar. The change of stance phase is about 44.3 ±1.7% at MCPJ [16]. It was concluded that the kinetics outside the sagittal plane was significant large and could not be ignored compared with that within the sagittal plane. The results from this study will be a great asset to future

studies in the horse leg motion as it will provide a more acculturate evaluation on horse leg motion in a gait cycle.

2.4 Patents on existing horse leg protective devices

In early days, bandage wrapped boots were widely used to prevent injury of horse legs due to hyperextension. However, bandage wrapped boots had more disadvantages than advantages to the horse legs. For example, the bandage did not act as a shock absorber to dissipate energy. The bandage was very operator dependent to horses because it could be too loose or too tight. A too loose bandage would potentially tangle in the horse's leg and eventually cause injury. A too tight bandage would pull the horse leg tendons toward the bone and into an unnatural position, which did not provide good front support to the tendon [17]. As a protective device for horse leg, it should alleviate the tendon hyperextension problem, it should be light weight and easy to attach to the horse's leg by an amateur (instead of only by professionals), it should also be easily cleaned. Many inventions related to horse leg protective device were developed to achieve the goals stated above [17].

Most inventions related to horse leg protective device offered the same general design: a flexible dense plastic outside layer and a foamed-plastic inner layer. Energy dissipation was the primary function for the outer layer and Neoprene was a common material for the outer layer [18]. On the other hand, shock absorbing ability was the primary function for the inner layer; Rubatex was a common material for the inner cushion layer [18]. The following are examples in the market: Hampicke's invention (Patent Number: 4,140,116, Figure 15a), Hoyt, Jr.'s invention (Patent Number: 4,470,411, Figure 15b), Kostur's invention (Patent Number: 3,405,506, Figure 15c) and Armato's invention (Patent Number: 5,363,632, Figure 15d).

Despite the inventions shared the same general design, they had distinguishable differences such as the covered length and system advancement. Hampicke's invention (Figure 15a) was especially for jumping horses. The horse boot wrapped around the horse's shank to fetlock area (approximately ¾ around the cannon bone area) to afford protection and support of the tendons of the horse leg [19]. Hoyt, Jr.'s invention (Figure 15b) wrapped the whole cannon area of the horse leg [20]. Prior to the two inventions mentioned above, Kostur's invention (Figure 15c) consisted of a U-shaped bonded inner surface. The U-shaped bonded inner surface was designed for absorbing and uniformly distributing external impacts [17]. Similar to Hampicke's invention (Figure 15a), this protective device covered the shank to MCPJ area. Having incorporated the U-shaped bonded inner surface idea, Armato's invention (Figure 15d), patented on November 15, 1994, have added the inflatable function to the U-shape inner surface. Instead of only wrapping around the cannon bone, the device was designed to wrap around the lower leg of a horse above and below the MCPJ (between cannon bone and pastern bone). The lengthened device provided support and protection of the sesamoid bones in the horse leg. According to the patent information, the U-shaped inner surface would be filled resulting in substantially uniform pressure around the full circumference of the leg [21].

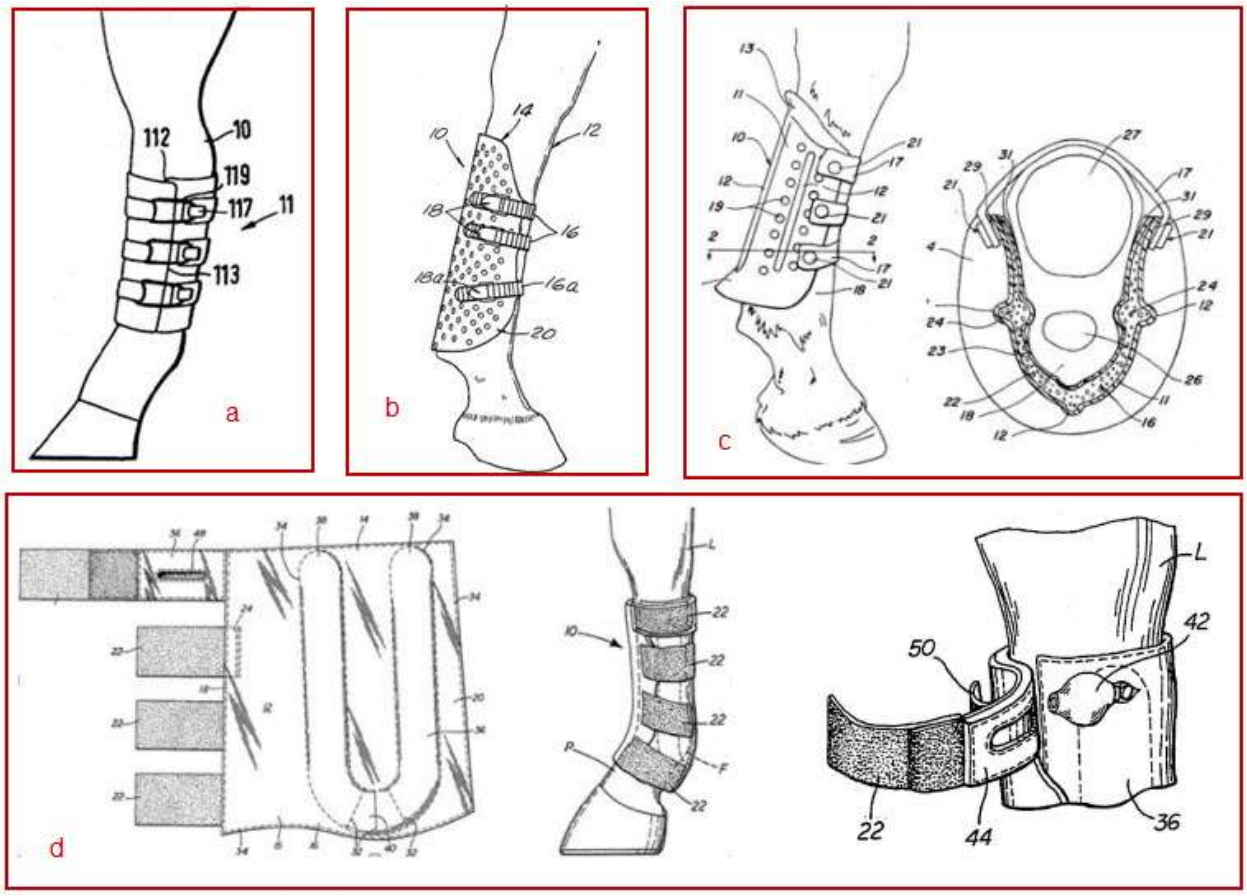

Figure 15 - Patented drawing of four horse leg protective devices other than bandage wrapped boots.

a - Patent Number: 4,140,116. Inventor: Willi Hampicke. Date of Patent: February 20, 1979.

b - Patent Number: 4,470,411. Inventor: Dolph G. Hoyt, Jr. Date of Patent: September 11, 1984.

c - Patent Number: 3,405,506. Inventor: R.E. Kostur. Date of Patent: October 15, 1968. Picture to the left shows side view of the invention mounted on the horse leg; picture to the right shows the top view of the invention.

d - Patent Number: 3,405,506. Inventor: Peter J. Armato, Date of Patent: November 15, 1994. Picture to the left shows the layout view of the patented invention (Patent Number: 5,363,632). Picture to the middle shows the side view of the invention mounted on a horse forelimb. Figure to the right shows the upper member of the Velcro strap includes an extension portion to extend over the pump to protect the pump and air pressure relief valve during use of the device.

The arrangement and structure of the fasting bands or straps was one of the main factors to determine whether the invention was a lasting solution or not. The fasting bands were designed to hold the outer layer and the inner layer in place. Slippage should be eliminated during the use of the device. A clamping device was longitudinally spaced at the end of the band or strap in Hampicke's invention (Figure 15a) and Hoyt, Jr.'s invention (Figure 15b) to engage the strap between these ridges and thus eliminate the possibility of slipping and loosening of the holding device for the boot [19, 20]. Kostur's invention (Figure 15c) buttons as the closure system. The locations of the buttons can be adjusted to get to three dimensional sizes of the protective device when wrapped. Armato's invention (Figure 15d) applied Velcro straps as the closure system. According to the patent information, the upper member of the Velcro strap included an extension portion to extend over the pump to protect the pump and air pressure relief valve during use of the device [21].

2.5 The proposed remedy to protect horse leg tendons

A simplified diagram of horse running gait (adapted from [22]) is shown in Figure 16. The timing of the labeled events during the gait cycle is approximate, as varies across individual horse and conditions. The horse gallop gait cycle is represented as starting (0%) and ending (100%) at the point of hoof strike (initial contact) on the same hoof, with hoof strike on the adjacent leg occurring at approximately 50% of gait cycle. At approximately 45-50% of the gait cycle, the joints of the horse forelimb undergo largest motion in extension.

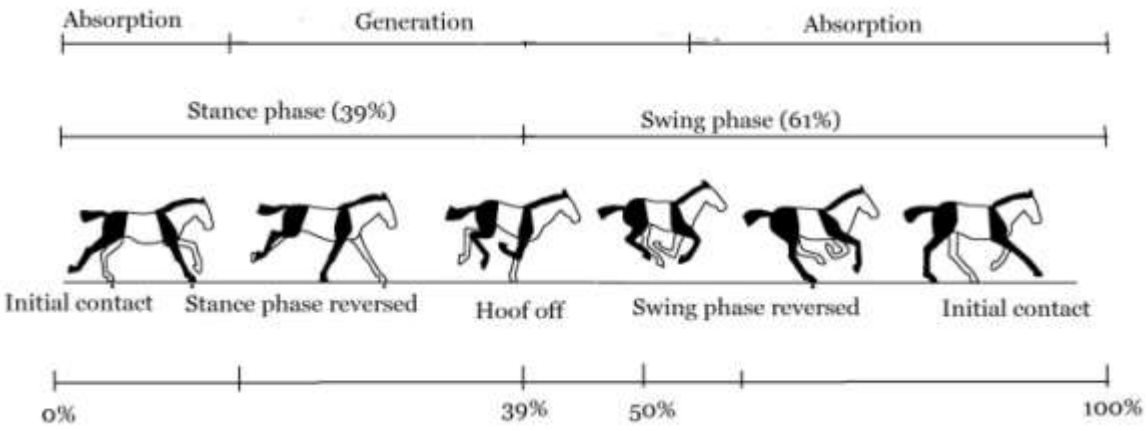

Figure 16 Horse running gait through one cycle, beginning and ending at hoof strike (initial contact). Percentages showing contact events are given at their approximate location in the cycle. Adapted from [22]

The approximate points when the forelimb transitions between phases of acceleration (stance) and deceleration (swing) were also indicated in Figure 16. These transitions happen with the forelimb first absorbing energy and then generating energy between the initial contact and hoof off. The generated energy accelerates the body during swing directly after hoof off until swing phase reversal, at which point the body begins to decelerate [2, 22].

It was first observed and concluded by Clayton et al. [23] that when the fetlock extends in early stance, energy is stored in the SL and flexor tendons (SDFT and DDFT); when the fetlock extends in late stance, energy is released in SL and flexor tendons recoil. Net joint power is the product of the joint moment and joint's angular velocity. Net joint moment is the torque produced primarily by the soft tissues (muscles, tendons and ligaments). Referring to Figure 17, horse MCPJ powers are positive when the net joint moment had the same polarity as the angular velocity, vice versa. When the horse is in early stance, negative work is done as the suspensory ligament and flexor tendons extend. As in the late stance, positive work is done as the suspensory ligament and flexor tendons recoil [23].

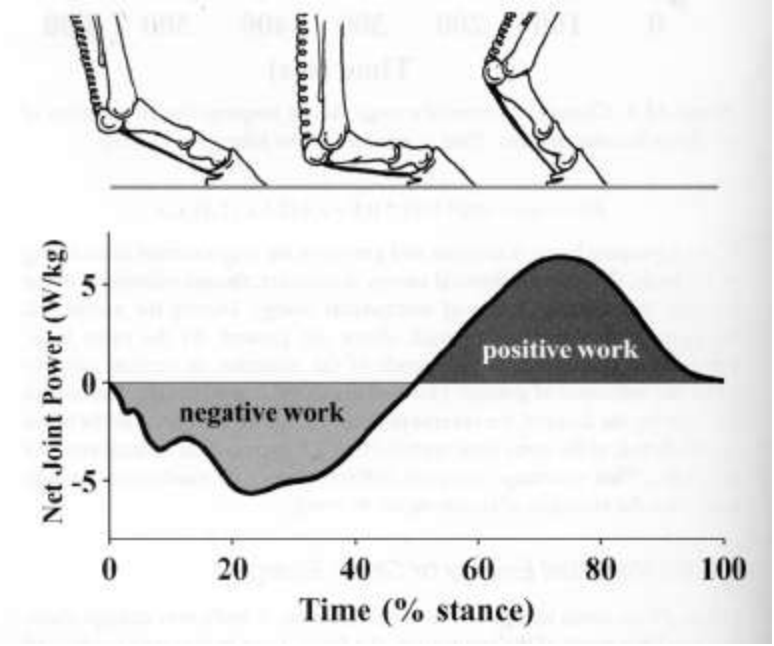

Figure 17 Net joint power at MCPJ during early stance to late stance. Joint powers are positive when the net joint moment had the same polarity as the angular velocity, vice versa. Negative work was produced in the early stance while positive work was produced in the late stance [23].

The horse forelimb must have the intrinsic stability and strength to resist the external forces. When a horse stands still, one of the forces exerted on the forelimb include the body weight, which is the force of gravity pushes downward on the entire body of the horse [24]. The bones in the forelimb are also subjected to a static load which are the internal forces to prevent the horse from falling to the ground. When the horse moves, the legs will withstand a dynamic load in order to support the horse in the dynamic situation. The majority of net joint moments are generated by the ligament tensions and ground reaction force. It is also suggested that kinematics regarding how the foot is placed on the ground may influence the net joint moment [25]. It was suggested by Kirker-Head to design a novel horse leg protective device that has means to modify MCPJ dynamics in a manner that will reduce extremes of motion and hence the likelihood of resultant flexor apparatus (SL, DDFT, and SDFT) injury [11].

The philosophy of the novel horse leg protective device is to influence the energy absorption of the horse leg tendons by reducing MCPJ moment through usage of a wrapped device on areas above and below the MCPJ [11]. A restrainer band is attached at the back of the novel horse leg protective device to provide counter tension force to horse leg tendon tension. As a result, the tension strain at the horse leg tendons decreases. Since the net joint moment is the torque produce primarily by the soft tissues (muscles, tendons and ligaments), as the tendon strain decreases, the tendon tensions decrease, eventually the MCPJ moment decreases [26].

The top level specification of the novel device is to reduce MCPJ moment by 10% without hurting the horse or significantly affecting the normal gait motion, in a market acceptable configuration. Up to 10% MCPJ moment reduction during installation of the device is suggested because the primary goal of the device is to maintain the speed at race while minimizing the subsequent use of energy. According to Kirker-Head, at a safe situation, The SDFT and DDFT are able to return elastic energy with

about 93% of energy stored, which means 10% MCPJ moment reduction is the reasonable specification [11]. A more explanation on the function and issue of the device is described in Chapter 3.

3.0. Problem Statement

This chapter describes the components and the function of the horse leg protective device by Manta Design Inc. The problem of the current restrainer band was also highlighted. In addition, the project goal and the task specifications were addressed.

3.1 Components and function of the device

A novel external forelimb wearable device is being developed at Tufts University Cummings School of Veterinary Medicine at Tufts University partnering with Manta Design Inc. The device supplements the natural behavior of the MCPJ and provides a linearly increasing torsional resistance through its range of motion (ROM) in extension from some rest position [11]. The prototype (Figure 18) is an aluminum linked based exoskeleton with rigid hinge (full pin joint). The device is comprised of the upper cuff and lower. These two components are connected by a pin joint connector, which represents the center of the MCPJ. There is a front layer and a back layer for each cuff. The horse leg protective device covers areas from ¾ of the cannon bone (with the upper cuff) to distal of the short pastern bone (with the lower cuff). This prototype is designed to fit in a horse leg with adjustable sizes.

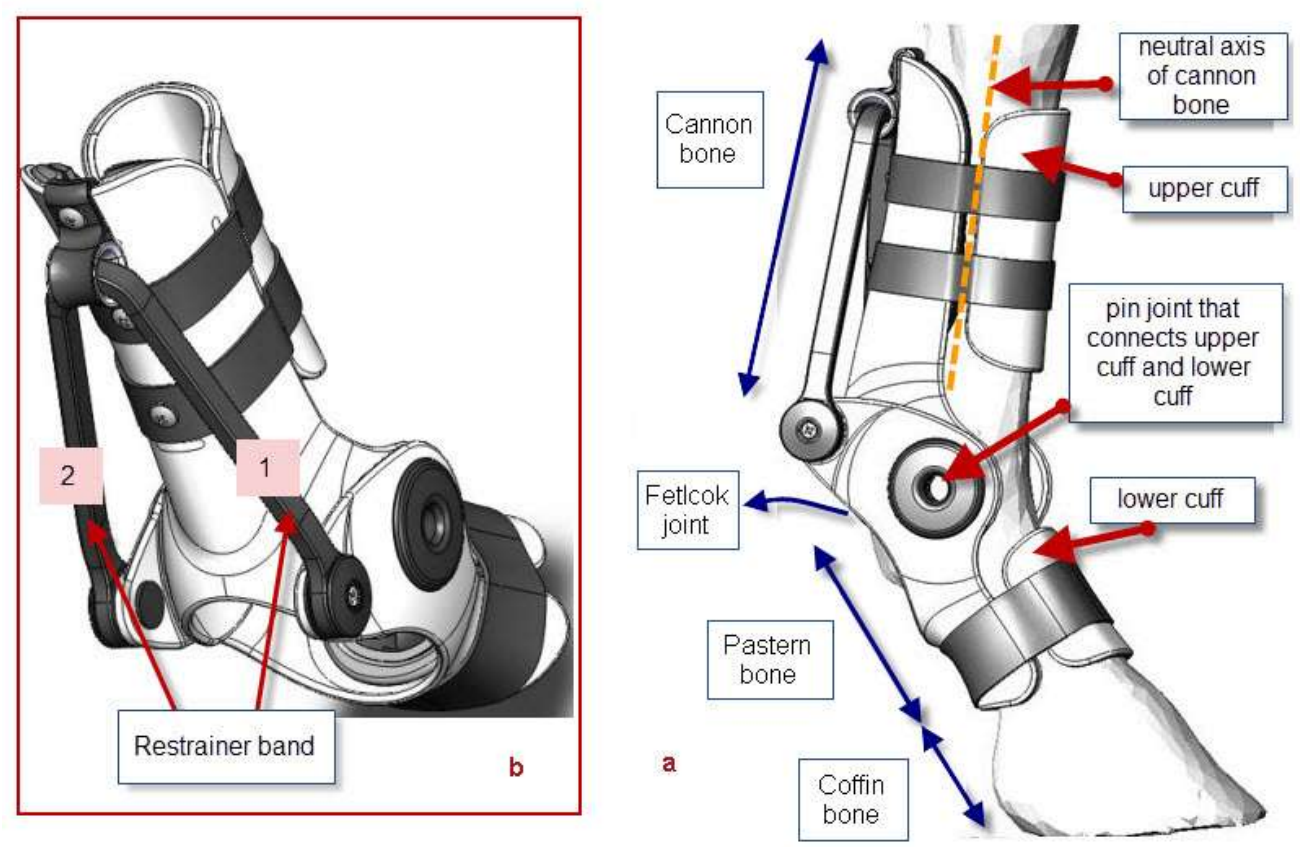

Figure 18 - Solidworks model of the prototype of protective device for horse leg with the restrainer band attached at the back of the device. Figure a depicts the side view of the assembly of the device and a horse forelimb, facing right. The horse leg device includes an upper cuff and a lower cuff with a pin joint connector and restrainer bands. Figure b is the back view of the device emphasizing the restrainer band connecting to the left and right side of the lower cuff.

Figure a- Lateral view of horse leg protective device with horses, right side

Figure a- Back view of horse leg protective device with horses. The restrainer band is connected in the back of the device and

A restrainer band is attached to the back of the horse leg protective device to mimic the tendon forces (SDFT, DDFT and SL). A hook is attached on the top of the upper cuff serving as a pulley to the restrainer band. The upper cuff is attached on the cannon bone of the forelimb, while the lower cuff covers the long and short pastern bones. The band extends as the lower cuff rotates forward.

3.2 Current issue of the restrainer band

The current restrainer band was designed by Sarcia et al. (Figure 19) from Manta Design Inc.. It was cut from a polyurethane sheet (3/8'' or 0.95cm thick, 95A Durometer, black) ordered from McMaster Carr (www.mcmaster.com) [27]. The part number is 8716K46 and the tensile strength was claimed to be 6500psi [28]. The total length of a restrainer band is 33.62cm, measured as the distance between the centers of the two holes. The width of the restrainer band is 0.5" (1.27cm) and the thickness is 3/8" (0.95cm).

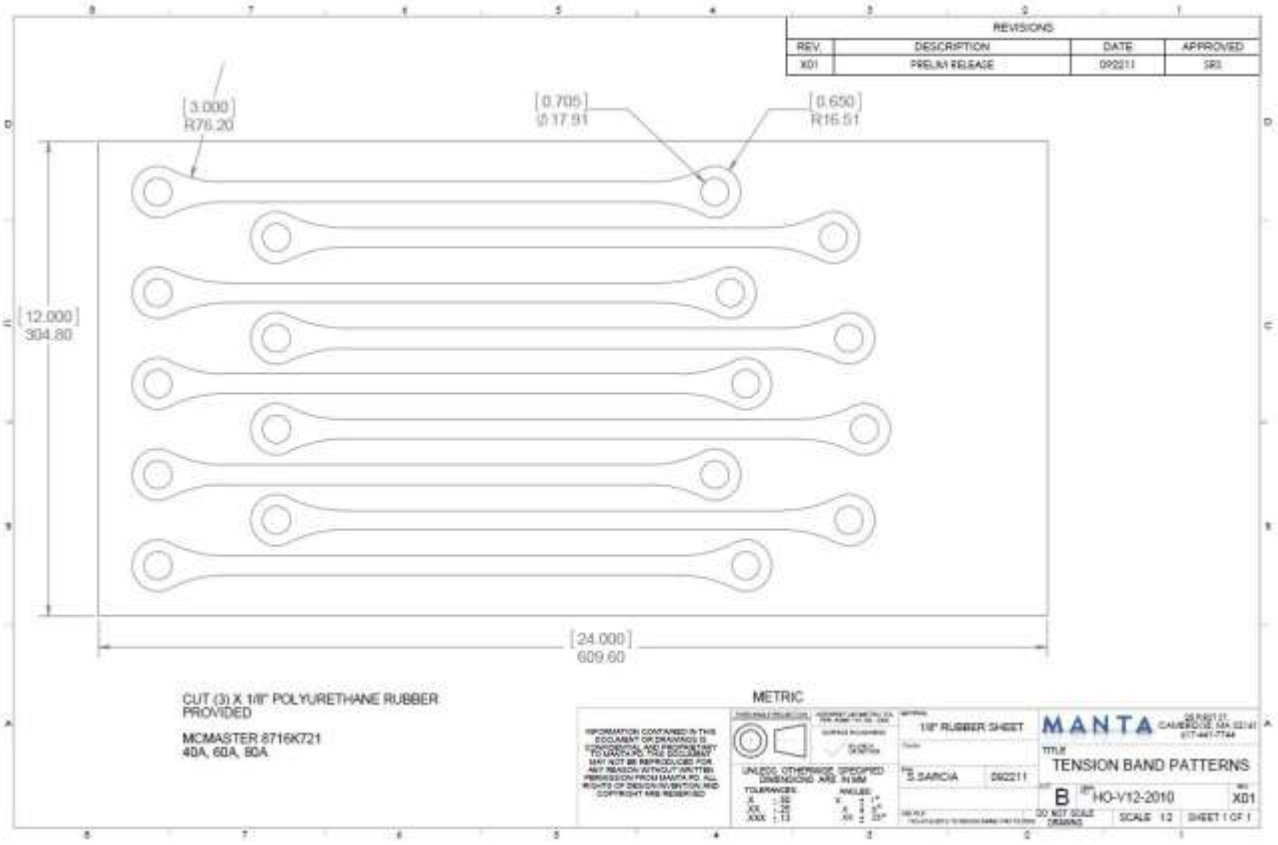

Figure 19-Solidworks drawing of restrainer band of the horse leg protective device (Figure 2) by Manta Inc. [29]

The restrainer band was designed to mimic the location of the flexor tendons (superficial digital flexor tendon and deep digital flexor tendon) and the suspensory ligament of horse forelimb [26]. It is the

essential sustaining element of the device, which applies the tension that is counter-acting the hyperextension of the fetlock.

Figure 20 – Demostration of the slack problem of restrainer band during flexion motion of horse forelimb.

The restrainer band is designed to be able respond to dynamic situations with a tension to stop the forelimb from overextending and reduce 10% of fetlock moment at maximum joint extension [26]. According to Clayton et al., a stance phase consists of the extension motion at the first half stance and flexion motion at the second half of stance [23]. The fetlock joint motion at maximum extension occurs at the change of motion from extension to flexion. The current design does not enable constant tension in the restrainer band (Figure 20-1) and therefore does not sufficiently protect the horse leg from injuries, in addition it will potentially causes a trip hazard to the horse.

3.3 Project goals and objective

The goal of this project was to estimate the restrainer band tension in a full gait cycle and improve the redesign process of the restrainer band in order to meet the restrainer band design specification of being able to reduce 10 percent of MCPJ moment. In order to fulfill the project goal, four objectives were identified: 1) the reaction force and resultant moment at the horse MCPJ at four gaits (walk, trot, gallop and fast gallop) were calculated based on the kinetic and kinematic data from the literatures; 2) the boundary conditions (rest and maximal extension) and tensions of restrainer band was determined; and 3) the reduced moment and the residual fetlock moment were computed and compared with the original fetlock moment.

4.0. Methodology

The purpose of the restrainer band of the device is to provide tension on the forelimb to restrict the range of motion of the fetlock join so as to reduce 10% of the MCPJ moment at maximum extension while maintaining the racing speed and minimizing the subsequent use of energy. The current design shows that the restrainer band slacks at flexion motion, and fails to provide tension to cancel out other forces acting on the forelimb tendons. It also generates a trip hazard to horse. The project goal is to study the mechanical behavior of a prototype restrainer band during a full gait cycle and thus improve the design for the restrainer band.

4.1 Model system and assumptions

To supplement the segmental data derived from the horse forelimb, Meershoek et al. [13] have used mathematical modeling procedures. With this approach, the horse forelimb is represented as a set of rigid sticks connected with dots (Figure 21). The advantage of this model is that only a few simple anthropometric measurements (e.g., segment lengths) are required to personalize the model and to calculate the joint moment and reaction force. However their assumptions typically used in modeling body segments limit the accuracy of the estimates: 1) segments are assumed to be rigid; 2) the boundaries between the segments are assumed to be distinct; and 3) segments are assumed to have a uniform density. In reality, there can be substantial displacement of the soft tissue during movement; the boundaries between segments are fuzzy; and the density varies within and between segments.

To determine the joint moment and reaction forces relate to MCPJ, the stick model system (Figure 21) is used, which divides the model system into three simple rigid segments of uniform density. The three simple rigid segments represent the metacarpus (cannon bone), (long and short) pastern and hoof. Based on Merritt, the proximal interphalangeal joint (the joint connecting long pastern and short pastern) was previously described as approximately rigid, so the long pastern and short pastern can be considered as one segment [12]. Since the horse leg movement is confined to be sagittal (x-y) plane, it is assumed that the left and right sides of the body are more or less performing the same movement. With these simplifications, the free body diagram can be reduced into a two- dimensional sagittal plane system.

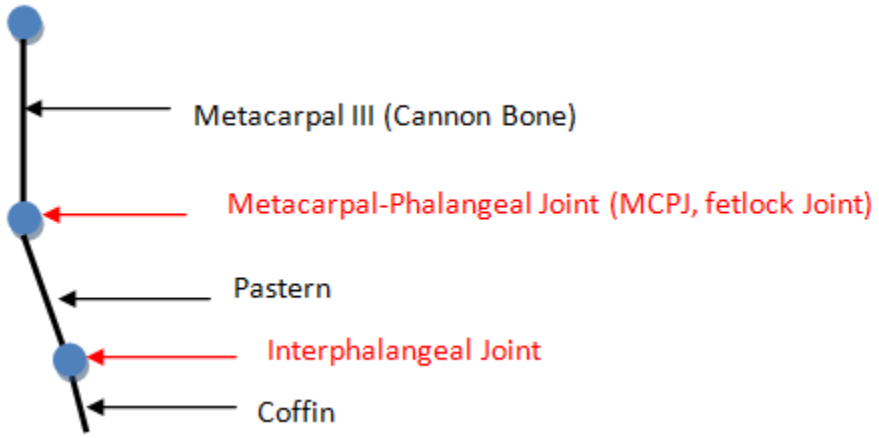

Figure 21 The schematic shows the locations of the bone segments of the horse forelimb. The bone segments are assumed to be rigid.

The horse leg protective device covers the cannon bone (upper cuff) and the pastern bone (lower cuff), while leaving the MCPJ area open. Referred to the horse forelimb with the device model in Figure 22, the restrainer band passes through the pulley on the upper cuff, and is fastened on both sides of the device. Because the restrainer band is not able to rotate around the pulley, the pulley is considered as a pin joint, which allows the restrainer band to translate through the pulley. No friction is taken into account when the restrainer band slides through the pulley.

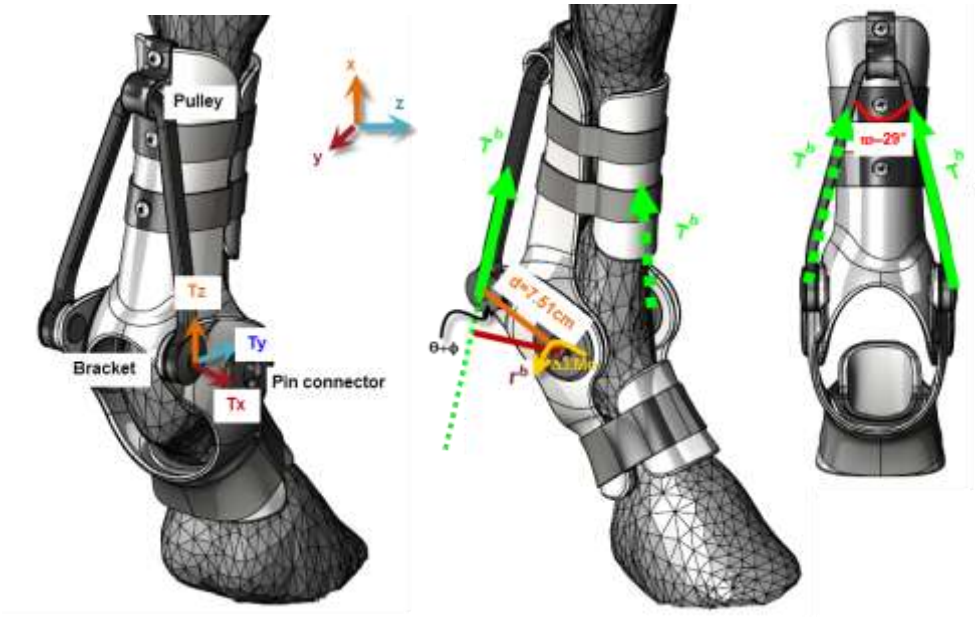

Figure 22: There are three components of the restrainer band tension, but Tx only contributes to the bending moment of the bracket, so the calculation of the restrainer band length and tension is modeled in a 2D system.

The two brackets which connect the restrainer band at both sides of the device are considered as hinge joints. Since the restrainer band is also hinged on the two brackets at both sides, the restrainer band can only stretch downward at horse forelimb extension motion. It is assumed that there is no friction when the restrainer band stretches.

The pin connector of upper and lower cuffs of the device mimics the location of the MCPJ. Therefore, the rotational axis of the pin connector is collinear to that of the horse MCPJ.

When the horse leg extends, the restrainer band stretches and results in tension in the band. Because of the 3D geometry of the restrainer band in the device, the elastic tension has three components (T_x, T_y and T_z) as referred to Figure 22. With the coordination system defined in Figure 22, T_x contributes to the bending moment of the bracket only. Since the reduced moment of the MCPJ is not partially generated by T_x, the calculation of the restrainer band lengths and tensions can be performed in a 2D model.

The assumptions of the project can be classified into two sections: horse forelimb biomechanics and restrainer band redesign.

Assumptions of horse forelimb biomechanics

- Bone segments are assumed to be rigid.
- Boundaries between the bone segments are assumed to be distinct.
- Bone segments are assumed to have a uniform density.
- The proximal interphalangeal joint is rigid and thus short pastern and long pastern is considered as one segment [12].
- The analysis is conducted in 2D sagittal plane: left and right side of the horse leg are performing same movement.
- There is no deformation of any tissue.
- Friction effects are neglected in the system.
- There is no acceleration at different gaits.
- Lines of action of all forces all oriented within the same plane.

Assumptions of restrainer band redesign

- No moment at the pulley of the upper cuff in the device.
- There is no friction in the pulley.
- There is no friction at the brackets on both sides of the device when the restrainer band stretches.
- The rotational axis of the pin connector is collinear to the rotational axis of the horse MCPJ.
- The calculation of the restrainer band lengths and tensions can be performed in a 2D system.

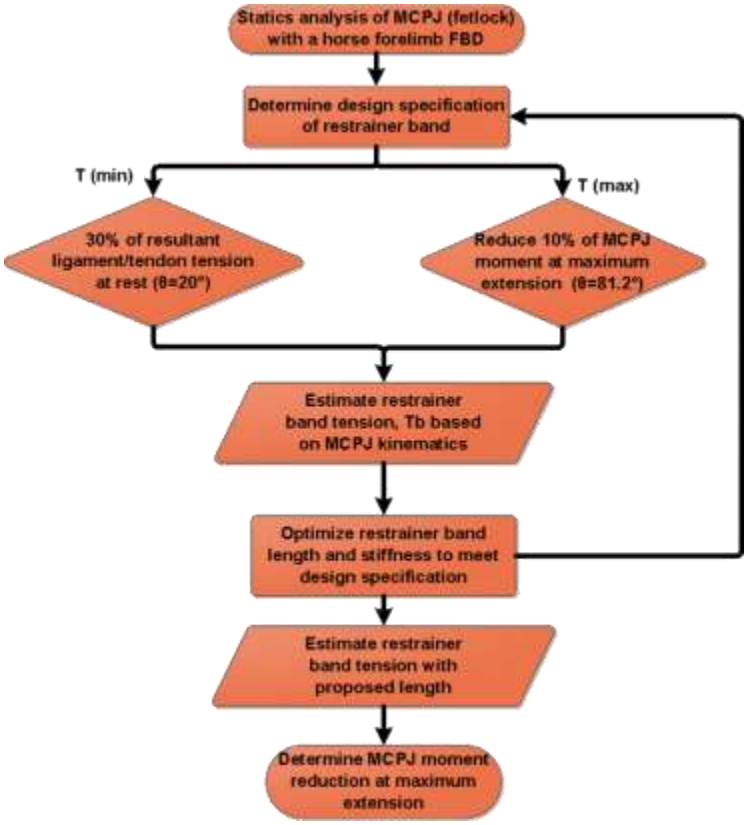

Figure 23: Flow chart illustrates the various steps in the analysis

Figure 23 depicts the methodology of the project in a flow chart. In the project, a static analysis associated with the horse forelimb free body diagram was performed to calculate the reaction force and joint moment generated at the MCPJ. Based on the design requirements, the design specifications of the restrainer band tensions were determined. The restrainer band tensions in a full gait cycle were then estimated with respect to the joint kinematics. Stiffness, length and area effects of the restrainer band were studied to improve the restrainer band design. The MCPJ moment reduction at maximum extension was eventually determined.

4.2 Static Analysis of MCPJ joint forces and moment

A study of the forces and moment applied to, and generated by the body is necessary to understand the mechanics of horse motion. With complexity of arrangements of bones in the lower forelimb throughout a full gait cycle, the tendon/ligament tensions would vary. Therefore, the analysis of biomechanics at the MCPJ would involve forces in different configurations. A simple static model of the horse lower forelimb was developed to obtain the reaction forces and moment in the MCPJ in related to its kinematics during four different horse gaits in an increasing order of speed (walk, trot, gallop and high speed gallop).

4.2.1 Forces applied to the lower forelimb

Fig. 24(b) describes the free body diagram of a horse lower forelimb at any gait configuration. The MCPJ moment is generated by the ground reaction force and the tendon tensions. Due to Newton's Third Law, a reaction force that is opposite to the resultant external load, acts at the MCPJ to keep the body segment balanced. The kinetic and kinematic data of Merritt's, Clayton's, Meershoek's and Swanstrom's studies [12, 16, 13, 14; Appendix A] were used for the analysis of fetlock loading during walking, trotting, galloping and fast galloping, respectively.

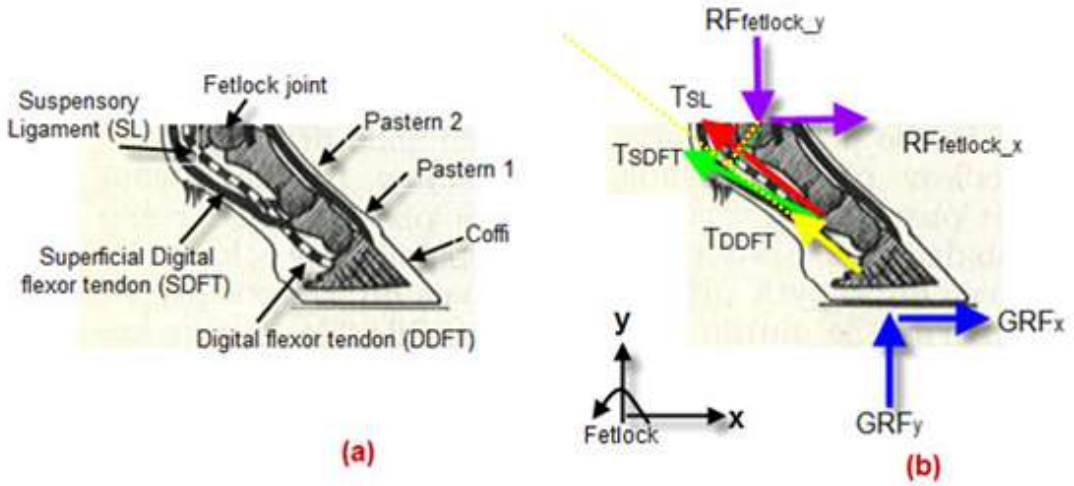

Figure 24: Anatomy and force free body diagram of MCPJ (for calculation of reaction force and resultant moment in MCPJ) (modified from [1]). The forces are indicated in solid arrowed lines and the corresponding moment arms of the tendons are indicated in the dashed lines.

To compute the reaction force and resultant moment at MCPJ, the magnitudes and directions of the external forces and the moment arms of the forces must be inquired. The initial orientation, magnitude and point of application with respect to the external forces were obtained by experiments from the past studies [12]. During normal joint rotation, both moment arms and tendon/ligament forces are constantly changing which results in the change of the force or moment curves. The orientations of the tendons (SDFT, DDFT and SL) at a full gait cycle were not measured in the studies. However, since the tendons spans the fetlock and joints (Figure 24(a)), the orientations of the tendons at any configuration can be computed relative to the joint angle.

Equation 1

$$\alpha = \alpha_0 - (\theta - \theta_0)$$

Equation 2

$$\beta = \beta_0 - (\theta - \theta_0)$$

Equation 3

$$\gamma = \gamma_0 - (\varphi - \varphi_0)$$

Notation	Reference
α	Angle of superficial digital flexor tendon (SDFT)
β	Angle of suspensory ligament (SL)
γ	Angle of digital flexor tendon (DDFT)
θ	Angle of MCPJ
φ	Angle of coffin joint
F,T	Force, Tension
M	Moment
l	Distance between tendon and joint center
R	Superscript, reaction force
r	Moment arm
G	Superscript, ground reaction force
0	Subscript, initial condition
1	Subscript, superficial digital flexor tendon (SDFT)
2	Subscript, suspensory ligament (SL)
3	Subscript, digital flexor tendon (DDFT)

The moment arms of each external force are the perpendicular distance from the point of application to the center of the MCPJ. The lengths and masses of the corresponding segments are summarized in Table 2. The moment arms can be calculated with respect to the tension directions and the distance from the tendon's line of action to the joint's center of rotation, as illustrated in Figure 24 (b). The moment arm lengths of each tendon can be calculated with Equation 4 to 6.

Equation 4

$$r_1^T = l_1 * sin\alpha$$

Equation 5

$$r_2^T = l_2 * sin\beta$$

Equation 6

$$r_3^T = l_3 * sin\gamma$$

Table 2: Length and Masses of selected Horse Forelimb Segments [23, 14]

Segments	Length (mm)	Mass (kg)
Long Pastern (P1)	56 ±10	0.329
Short Pastern (P2)	53 ±6	0.190
Coffin (P3)	80 ±5	0.343
Digital flexor tendon (DDFT)	382	
Superficial digital flexor tendon (SDF)	371	
Interosseous ligament (IL)	24.5	

4.2.2 Biomechanical analysis of the MCPJ

Referred to Figures 24(a) and 24(b), the drawings show a horse lower forelimb at rest. Fig. 24(a) shows the anatomical terms of the musculoskeletal forelimb, whilst Fig 24(b) represents a two dimensional free body diagram for the analysis of the MCPJ reaction forces and moment. Here, the loads at the MCPJ, F_x^R and F_y^R have the same magnitude and opposite directions to the resultant external loads. F_x^R and F_y^R can be calculated with Newton's Third Law of Motion, Equations 7 and 8.

Equation 7

$$\Sigma F_x = F_x^G - T_1 * \cos\alpha - T_2 * \cos\beta - T_3 * \cos\gamma + F_x^R = 0$$

Equation 8

$$\Sigma F_y = F_y^G + T_1 * \sin\alpha + T_2 * \sin\beta + T_3 * \sin\gamma - F_y^R = 0$$

The moments at the MCPJ, ΣM_O generated by the tendon tensions and the ground reaction force, can be calculated with Equation 9.

Equation 9

$$\Sigma M_O = F_x^G * r_x^G + F_y^G * r_y^G + T_1 * r_1^T + T_2 * r_2^T + T_3 * r_3^T$$

The fetlock moments at four different gaits would be calculated and compared.

4.3 Design specifications for restrainer band tension

The pre-stretched and maximum tension of the restrainer band are determined and provided as the targeted values of the restrainer band design. The pre-stretched restrainer band tension is determined to support at least 30% of the initial (at rest position) flexor tendon tensions. The fetlock moment is resulted in a 10% reduction at maximum extension and does not slack at flexion.

4.3.1 Restrainer band tension calculation at maximum extension (θ_{max}=81.2 °)

It was proposed that the restrainer band provides tension to restrict the hyperextension of the joint and results in 10% of resultant fetlock moment reduction, $\Delta\Sigma M_O^{max}$ [11]. Figure 25 shows the orientation of the device when the fetlock rotates to maximum extension angle (81.2 °).

As the MCPJ extends, the restrainer band provides tension to limit the hyperextension of the forelimb by stretching, which results in the increment of the length. Since the restrainer band is attached on both sides of the device symmetrically, the length of the restrainer band on either side is one half of the overall length. The pulley, the side attachment of the band and the pin forms the triangle ABO. Side AO or c is defined as the distance between the pin and the pulley; side BO or d is the distance between the pin and the attachment point. The fetlock angle, θ, ranges from the rest at 20° to the maximum extended angle at 81.2 °[14]. ϕ is the angle offset between side BO and the rotational axis of the lower cuff, which is 35 °. Note that 35 °is fixed in all time phase during the gait cycle and should be added to the calculation of total angle in all cases.

The reduced fetlock moment generated by the restrainer band can be obtained by Equations 10 and 11.

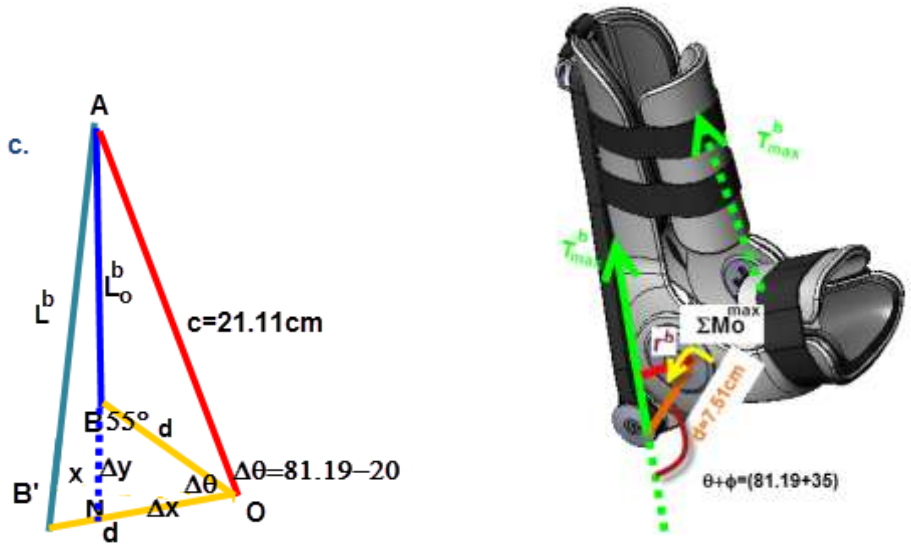

Figure 25 The orientation of device with restrainer band when the fetlock rotates to 81.2 °.

Equation 10

$$\Delta\Sigma M_O^{max} = \Sigma M_O^{max} * 10\%$$

Equation 11

$$r^b_{max} = d * \sin(180° - \phi - \theta_{\max}) = d * sin63.81°$$

Notation	Reference
θ_{max}	Maximum fetlock angle, 81.2 °
φ	Angular offset between rotational axis of MCPJ and side BO, 35 °
F,T	Force, Tension
$\Delta\Sigma M_O^{max}$	Maximum reduced fetlock moment at gallop (10% of original fetlock moment)
r^b_{max}	Moment arm length at maximum fetlock extension
T^b_{max}	Maximum restrainer band tension (θ=81.2°)
d	Distance between pin and attachment point of the band
b	Superscript, restrainer band

Since the restrainer band is distributed into two equal components in the calculation, the reduced fetlock moment generated by the restrainer band can also be obtained by Equation 12 and the maximum required tension of the restrainer band can be obtained easily.

Equation 12

$$\Delta\Sigma M_O^{max} = 2 * T^b_{max} * r^b_{max}$$

$$T^b_{max} = \frac{\Delta\Sigma M_O^{max}}{2 * r^b_{max}}$$

4.3.2 Restrainer band tension calculation at rest (θ_0=20 °)

To eliminate the slack at flexed movement, a force should be applied to the restrainer band at rest. This force is the minimum of the restrainer band tension in the redesign process. When the horse is at rest, the tensions of the tendon/ligaments are relatively small. The initial tension of the restrainer band was set to be 30% of the initial resultant tendon/ligament tension (Equation 13).

The value of 30% is based on a series of percentage of tension reduction preliminary calculations. The purpose of the calculations was to study to effect of the percentage of restrainer band tension to the fetlock moment reduction. The calculations were performed in 5% intervals, between 0% - 50% of tendon/ligament tensions as the band tension. It was observed that the MCPJ moment started to have a greater reduction when the restrainer band tension is 30% of the initial tendon/ligament tension. Thus the value of 30% is used as the minimum restrainer band tension requirement.

Equation 13

$$T_{min}^{b} = T_R * 30\% = \sqrt{T_1^2 + T_2^2 + T_3^2} * 0.3$$

Notation	Reference
T	Tension
T_{min}^{b}	Pre-stretched restrainer band tension (θ=20°)
T_R	Resultant tendon/ligament tension
1	Subscript, superficial digital flexor tendon (SDFT)
2	Subscript, suspensory ligament (SL)
3	Subscript, digital flexor tendon (DDFT)

4.4 Responses of restrainer band tension in a full gait cycle

It is necessary to improve the restrainer band length and stiffness in order to meet the restrainer band design specification (restrainer band tension at rest position and at maximum extension). In this section, the change in length of the restrainer band will be determined. Since the stiffness of the restrainer band was given, the restrainer band length in response to the design specifications can be determined using Hooke's Law.

4.4.1 Change in length of restrainer band

The restrainer band experiences a tension when its length is greater than the natural length due to the rotation of the MCPJ. Since the band is attached symmetrically on the front and back sides of the device, it stretches with an equal change in length on both sides. The change in length property of the restrainer band is important for computing the restrainer band tension. The methods to compute the original length, the stretched length and the change in length of the restrainer band are discussed in this section.

4.4.1.1 Calculating the original length of the restrainer band

The fetlock angle at rest position is 20 °[14]. Figure 26a shows the side view of the horse leg device, and L_0^b is original length of the restrainer band at either side before the forelimb extends. \Side AO or c is defined as the distance between the pin and the pulley; side BO or d is the distance between the pin and the attachment point. The fetlock angle, θ, ranges from the rest at 20 °to the maximum extended angle at 81.2 °[14]. ϕ is the angle between side BO and the rotational axis of the lower cuff, which is 35 °.

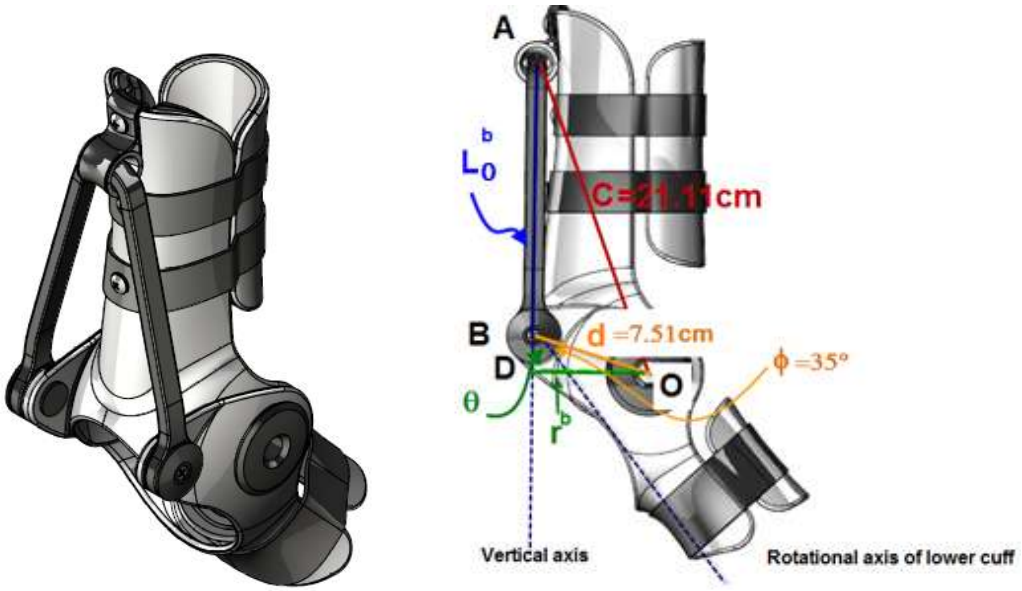

Figure 26: a. (the isometric view) the restrainer band is attached on both sides of the device symmetrically to the pulley. b. (the side view) the original length of the restrainer band at either side can be calculated with the mathematical representation with the Law of Cosine.

Since ΔABO is a secant triangle, the length of L_0^b would be inquired through the relationship between the lengths of the sides, which is the Law of Cosine (Equation 14). To be specific, the length of AO (c=21.11cm) is considered as a function of the magnitude of Angle ABO and the lengths of sides BO (d=7.51cm) and AB (L_0^b). Angle ABO is the collinear angle of $(\theta + \phi)$.

Equation 14

$$c^2 = (L_0^b)^2 + d^2 - 2 * L_0^b * d * \cos(180° - \theta - \phi)$$

Reduced from Equation 14, L_0^b can be obtained from a quadratic equation,

Equation 15

$$(L_0^b)^2 - 15.02 * L_0^b * \cos(145° - \theta) - 389.23 = 0,\ \theta = 20°$$

One positive and one negative answer would be obtained from Equation 15 for the length of L_0^b, but L_0^b is the positive value from the quadratic equation.

4.4.1.2 Calculating the elongation of the restrainer band

Figure 27b shows the orientation of the device when the fetlock rotates to 50 °. As the MCPJ extends, the restrainer band provides tension to limit the hyperextension of the forelimb by stretching, which results in the increment of the length. The position of the attachment point, B', moves as the lower cuff rotates. Figure 27c relates the orientation of the restrainer band at rest to its orientation at fetlock extension.

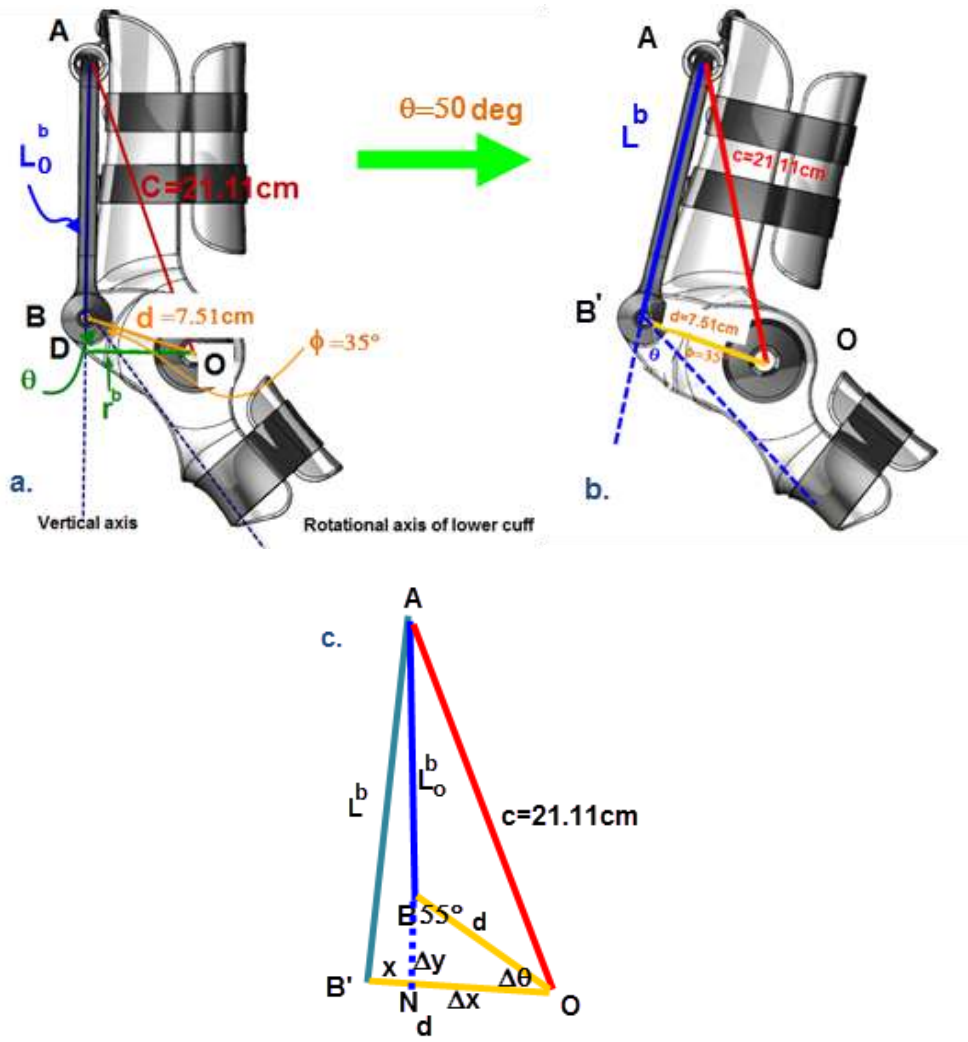

Figure 27: a. the original position of restrainer band when the horse is at rest; b. The restrainer band position at θ=50°. The restrainer band stretches as the fetlock angle increases; c. A mathematical representation is illustrated to calculate the stretched length of the restrainer band, L^b

The calculation of the stretched band length is derived from the mathematical representation shown in Figure 27c. The pulley, the pin, the band attachment point at rest and at fetlock extension are represented as points A, O, B and B' in the schematic. The orientation of the restrainer band at rest is referred to side AB in the obtuse triangle ABO, while the orientation of the band after stretched is referred to side AB' in the acute triangle AB'O. Although the device rotates according to the movement of the MCPJ, the distances from the pin to the pulley (OA) and to the band attachment point (OB' or OB) are fixed.

The stretched length of the restrainer band, AB' or L^b, can be calculated in ΔANB' the Law of Cosines. However, the lengths of side AN and B'N are still unknown yet but can be computed with the Law of Sine in ΔBNO.

Referred to ΔBNO in Figure 27c, line BN is the rotational axis of the upper cuff at rest and BO is the rotational axis of the lower cuff, therefore Angle NBO is 55 °(=20 °+ 35 °), which is the opposite angle of side ON (Δx). Angle BOB' or Δθ is the offset of the fetlock angle from the rest position (Equation 16), and it is the opposite angle of the vertical change in length, Δy. The lengths of Δx and Δy can be evaluated with Equations 17 and 18.

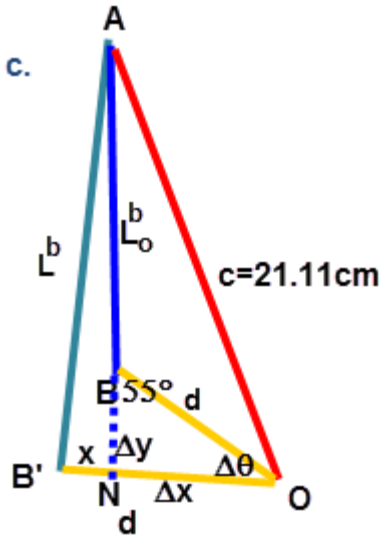

Equation 16

$$\Delta\theta = \theta - 20°$$

Equation 17

In triangle BNO,

$$\frac{d}{\sin(180° - (20° + 35°) - \Delta\theta)} = \frac{\Delta y}{\sin(\Delta\theta)}$$

$$\rightarrow \frac{7.51}{\sin(125° - \Delta\theta)} = \frac{\Delta y}{\sin(\Delta\theta)}$$

Equation 18

$$\frac{\Delta x}{\sin(20° + 35°)} = \frac{d}{\sin(180° - (20° + 35°) - \Delta\theta)}$$

$$\rightarrow \frac{\Delta x}{\sin(55°)} = \frac{d}{\sin(125° - \Delta\theta)}$$

The lengths of BN (x) and NA (y) in ΔB'NA can be calculated with respect to Δx and Δy (Equations 19 and 20). The angle between B'N and NA is the collinear angle of Angle BNO, so Angle B'NA is (55°+Δθ). Consequently, the stretched band length, AB' or L^b, can be computed with the Law of Cosines in Equation 21.

Equation 19

$$\text{NA} = y = L_0^b + \Delta y$$

Equation 20

$$\text{BN} = x = d - \Delta x$$

Equation 21

$$(L^b)^2 = x^2 + y^2 - 2 * x * y\cos(55° + \Delta\theta)$$

$$\rightarrow L^b = \sqrt{x^2 + y^2 - 2 * x * y\cos(55° + \Delta\theta)}$$

4.4.1.3 Calculating the change in length of the restrainer band at either side

The change in length of the restrainer band at either side, ΔL^b, is the distance of the stretched band from its original length. It can be calculated with Equation 22.

Equation 22

$$\Delta L^b = L^b - L_o^b$$

4.4.2 Responses of the restrainer band tension at a full gait cycle

The restrainer band material selected by Manta Design Inc. is polyurethane MP950 (Durometer 95A) [30]. The Durometer is the International Standard Instrument used to measure the hardness of rubber materials. Durometers measure hardness by the penetration of an indenter into the rubber sample. There are three types (shores) of durometers: Type A, which are the soft rubber and plastics; Type D: indicating the hard rubber and plastics and Type 00, which are sponge and foam. For shore A, the hardness of rubber can range from 5 to 100 with increment of 5 for each material hardness type [31].

The polyurethane material used in the restrainer band with durometer 95A is a high performance polyether based urethane formulated to tear and abrasion resistance and hardness stability. It is widely used in many applications including springs, rolls, shock absorbers, bumpers and belts etc [30].

MECHANICAL PROPERTY	ASTM Test	MP 300	MP 600	MP 750	MP 850	MP 900	MP 950	MP 160	MP 175
Durometer, Shore	D-2240	30A	60A	75A	85A	90A	95A	60D	75D
100% Modulus, psi	D-412	80	250	350	600	1,100	1,800	3,000	5,500
300% Modulus, psi	D-412	170	600	1,000	1,500	2,100	4,000	6,500	-
Tensile, psi	D-412	380	4,500	5,500	6,000	4,500	5,500	6,500	7,500
Elongation, %	D-412	515	500	500	500	450	320	300	225

Figure 28: The material used in the device restrainer band is polyurethane MP950. Its hardness of 95A durometer.

Mechanical Properties of polyurethanes in various durometers is shown in Figure 28. The Modulus (100%) of polyurethane with durometer 95A is 12.4MPa (1800psi). The tension of the stretched restrainer band can be calculated with respect to its change in length (from section 4.4.1) using Hooke's Law. Hooke's law provides the basis for calculation of deformation as long as the elasticity of the restrainer band does not exceed 100%.

Equation 23

$$\sigma = E\varepsilon = \frac{\Delta L^b}{L_0^b} E = \frac{T_b}{A_0}$$

Notation	Reference
E	Modulus of elasticity of restrainer band at maximum strain
ΔL^b	Change in length of the restrainer band on one side
L_0^b	Initial restrainer band length on one side (θ=20°)
A_0	Initial cross-sectional area of the restrainer band
w_0	Initial width of restrainer band
t_0	Initial thickness of restrainer band

Reduced from Equation 23, the tensions of the restrainer band can be calculated with Equation 23.

$$T_b = \frac{\Delta L^b}{L_0^b} * E * A_0$$

Where

$$A_0 = w_0 * t_0$$

w_0 is the original restrainer band width 0.5" (1.27cm); t_0 is the original restrainer band thickness 3/8" (0.95cm).

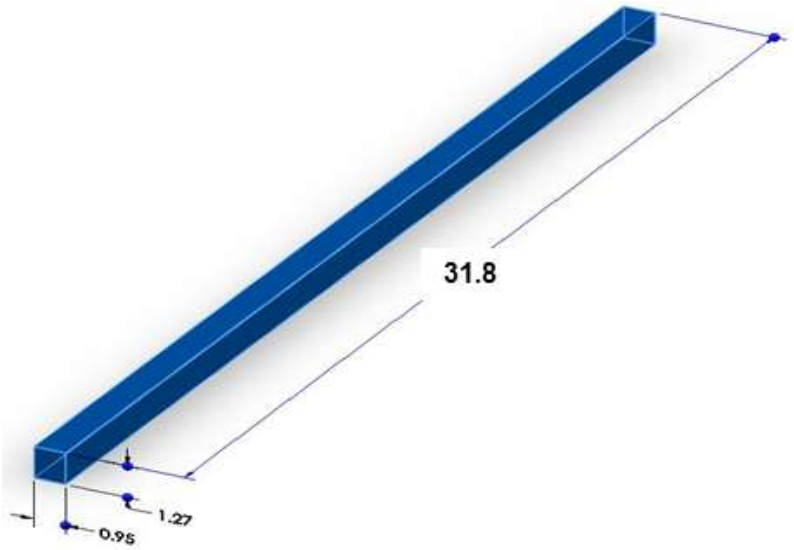

Figure 29: the original design of the restrainer band is made of polyurethane MP950. The length, width and thickness of the die-cut band are 31.8cm, 1.27cm and 0.95cm, respectively.

4.5 Calculations of reduced moments generated by the restrainer band

Since the restrainer band is attached symmetrically on both sides of the device as illustrated in Figure 30,

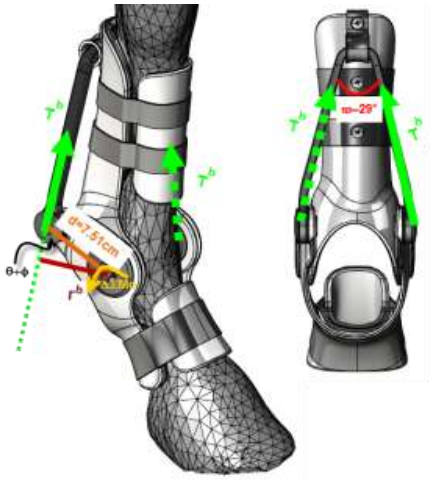

Figure 30: The reduced fetlock moment is generated by two equal restrainer band tensions.

two restrainer band tensions with equal magnitudes generate the reduced moment at the pin. Therefore, the reduced fetlock moment can be computed with Equation 24.

Equation 24

$$\Delta \Sigma M_O = 2 * T^b * r^b$$

Where T^b is the proposed tension of the restrainer band, and r^b is the moment arm of the tension with respect to the fetlock angles.

Equation 25

$$r^b = d * \sin(\theta + \phi)$$

Notation	Reference
T^b	proposed tension of the restrainer band
r^b	the moment arm of the tension with respect to the fetlock angles
d	Distance between pin connector and band attachment point
θ	Fetlock angle
ϕ	Angular offset between rotational axis of lower cuff and pin

5.0. Results and Discussion

The restrainer band redesign is based on the meta-carpophalangeal joint (MCPJ or fetlock) static analysis, moment reduction requirement and the band elongation property. The reaction force and moment acted on the MCPJ at different gaits were calculated with the kinematic and kinetic data from the previous studies. The design requirements of the restrainer band were determined based on the statics data. The elongations as well as the tensions of the restrainer band were estimated as the MCPJ angle varies. Suggestions of the restrainer band redesign were provided to meet the design specifications. This chapter highlights the results on the MCPJ statics, the band elongation and tension.

5.1 Statics analysis at the MCPJ/fetlock joint

The internal forces and moment generated in the MCPJ were not determined in the previous published studies [12, 13, 14, 16]. A static analysis of the horse MCPJ at four different gaits was evaluated with the empirical equations based on the kinematic and kinetic data from the literature. The values of the MCPJ reaction force components, F_x^R, F_y^R and the MCPJ moment, ΣM_O, were determined associated with the free body diagram in Figure 31, with respect to walk (v=1.78m/s), trot (v=3.36m/s) , and fast gallop (v=18m/s). The initial joint reaction force at rest is 377N. At maximum MCPJ extension, the joint reaction force is estimated to be 4850N, 5680N, 7560N and 7870N during walking, trotting, galloping and fast galloping. The MCPJ moment at gallop (v=12.5m/s) was directly obtained from Swanstrom's study. Note the average speeds of walk, trot and fast gallop were recorded in the study of Harris et al [32].

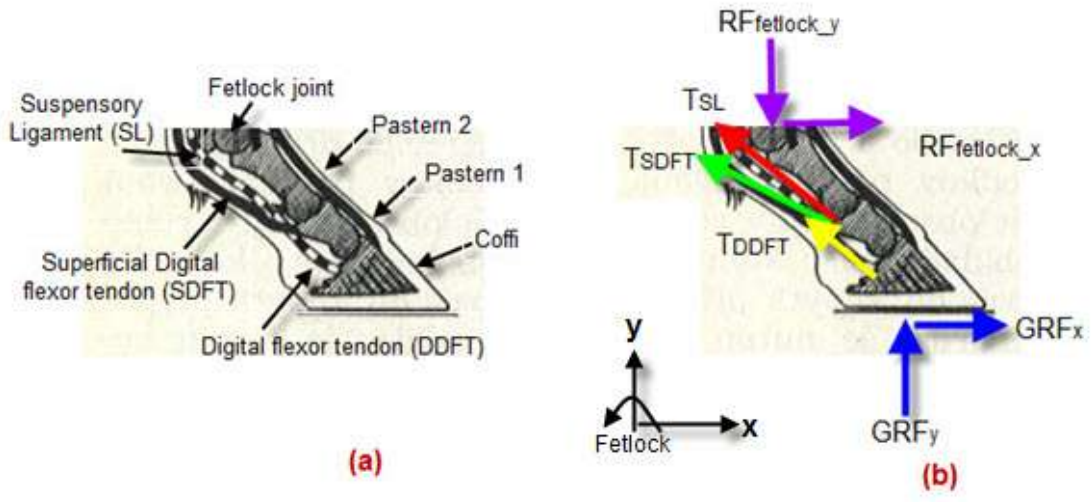

Figure 31: Anatomy and force free body diagram of fetlock joint (for calculation of reaction force and resultant moment in fetlock joint) (modified from [1])

5.1.1 Comparisons of fetlock moments at different gaits

The resultant MCPJ moment is the sum of individual moments produced by the ground reaction force and muscle and soft tissue forces that produce the moment. The analysis of the loading and moment was assumed to be centered directly over the fetlock joint of rotation in the sagittal plane. With the Cartesian coordinate system defined in Figure 31, the resultant MCPJ moments are generated in a clockwise direction, so the values are negative. All the calculations were based on a horse with the mass

of 500kg. The net joint moments in the sagittal plane across the meta-carpophalangeal joint during walk, trot, gallop and fast gallops are plotted and compared in Figure 32.

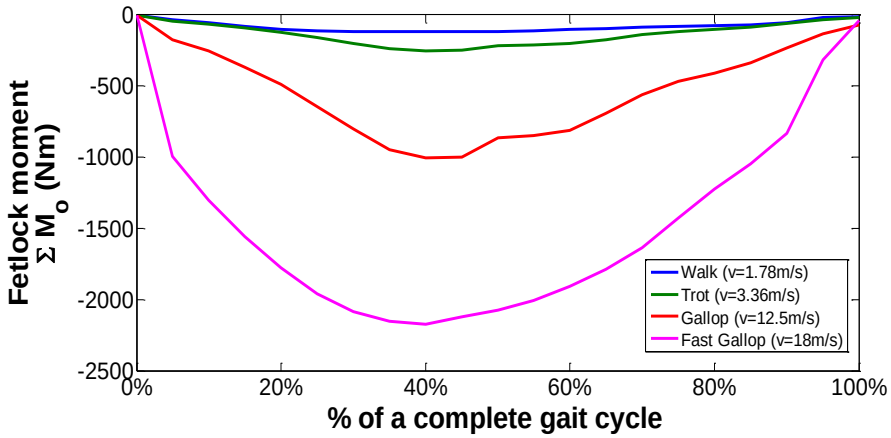

Figure 32: Calculated resultant moment [Nm/kg] of fetlock joint at four different gait cycles, in a increasing order of speeds. The resultant moment increases.

The resultant MCPJ moment curves in walk, trot, gallop and fast gallop were illustrated as parabolas in Figure 32. The minimums in the curves indicate the peak value of the moments at different gaits. The peak moments are also the pivot points from flexion to extension, which occurred at 40% to 60% stride phase. Table 3 summarizes the peak calculated resultant MCPJ moments in walk, trot, gallop and fast gallop stance phase.

Table 3: Peak resultant moments at MCPJ at different strikes

	MCPJ Joint Moment (Nm)
Walking (v=1.78m/s)	118
Trotting (v=3.36m/s)	252
Galloping (v=12.5m/s)	1005
Fast Galloping (v=18m/s)	2175

5.1.2 Relationship between tendon/ligament tension and MCPJ moment

Reduced from the statics data at MCPJ, the relationship between the tendon/ligament tensions and the MCPJ moment at fast gallop are described in Figure 33.

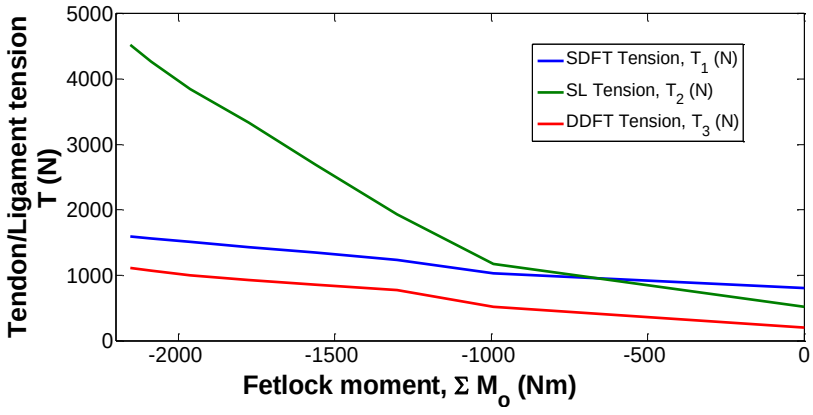

Figure 33: Relationships of tendon/ligament tensions and the calculated fetlock (MCPJ) moment at fast gallops. The suspensory ligament generates the most moment at the fetlock joint.

From Figure 33, the suspensory ligament tension increases linearly with a greater slope while the other two ligament tensions increase. It is concluded that the SL contributes the most the generated MCPJ moment.

5.1.3 Relationship between MCPJ moment and fetlock angle during extension movement at gallop

The relationship of the MCPJ moments versus MCPJ angles during the extension movement at gallop is also studied. Table 4 summarizes the resultant MCPJ moment as a function of MCPJ angle.

Table 4: The fetlock moments at MCPJ extension movement during gallop [14] increase as the fetlock angle increases.

θ (°)	MCPJ moment, Σ Mo (Nm)
27.2	-40
36.8	-571
46.4	-832
47.1	-993
52.7	-1045
56.6	-1301
64.7	-1560
71.3	-1775
75.5	-1790
76.0	-1961
79.4	-2087
81.2	-2154
81.2	-2173

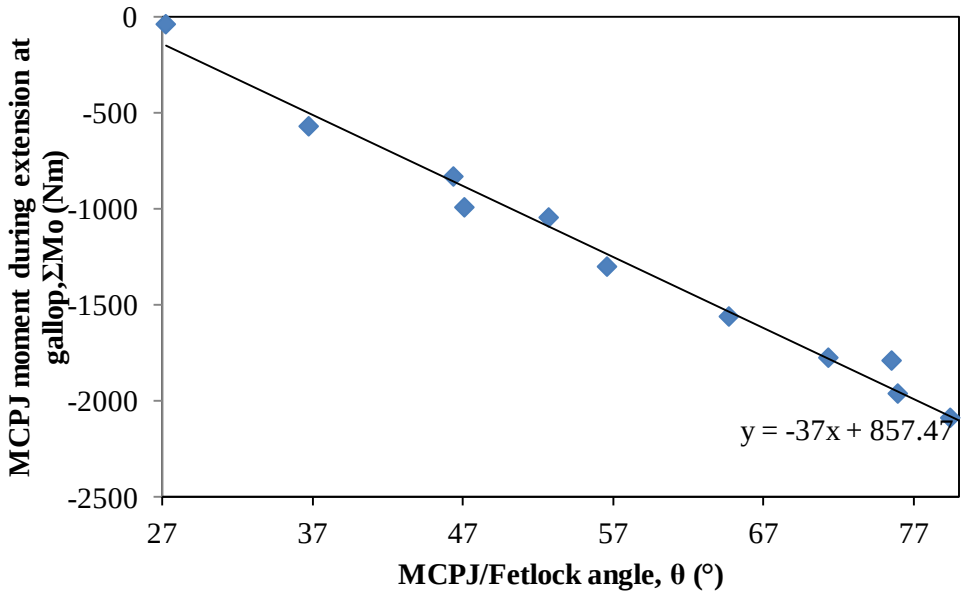

Figure 34: The curve describes the MCPJ moment during extension at gallop increases linearly with a slope of -37Nm/deg. The range of motion of the horse forelimb can be proportionally reduced with supplemental support of joint moment.

The resultant moments according to the linear regression of the plotted data in Figure 34, the MCPJ moment increases with a slope of -37Nm/deg as the joint extends from the rest position. Therefore, the range of motion of the horse forelimb can be proportionally reduced with supplemental support of joint moment.

5.1.4 Summary of MCPJ static analysis

The reaction force and moment acted on the MCPJ/fetlock joint during walking, trotting, galloping and fast galloping were calculated with a 2D free body diagram and compared. The MCPJ moment is generated by the tensions of the tendons and ligament, as well as the ground reaction force. Since the tendons and ligaments are principally responsible for enabling the locomotion by providing propulsive forces and storing energy, the speeds increase as the forces increase. Therefore, the resultant moment at fast gallop was generated the most. It is also observed that the MCPJ moment is affected mostly by the suspensory ligament tension. In addition, the MCPJ moment increases as the fetlock angle increases. In conclusion, reducing the suspensory ligament tension enables the MCPJ moment reduction, and the range of motion of the horse forelimb can be proportionally reduced with supplemental support of joint moment.

5.2 Design specifications of restrainer band

The design specifications of the restrainer band are required to provide guideline on the development of the band. The section discusses the determinations of the design specifications including the minimum and maximum tensions of the restrainer band throughout a full gait cycle.

5.2.1 Requirement of maximum restrainer band tension

The maximum tension of the restrainer band occurs at the maximum MCPJ extension (θ = 81.2 °). From Figure 35, the restrainer band provides counting tensions as the joint rotates, thus the motion of the forelimb is restricted by the counting tension and eventually reduces the joint moment. In addition, the reduced MCPJ moment ($\Delta\Sigma M_o$) is the product of the restrainer band tension (T^b) and the tension moment arm (r^b).

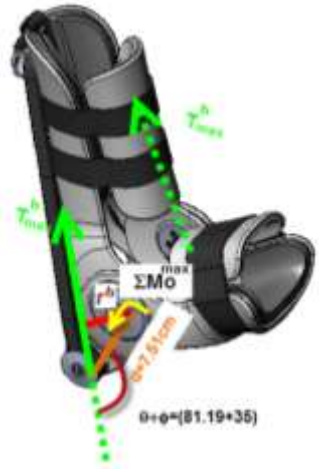

Figure 35: The restrainer band provides counting tensions at both side of the device, consequently reduces the MCPJ moment.

The restrainer band is proposed to reduce 10% MCPJ moment at maximum extension at fast gallop, so the maximum reduced moment can be obtained from Equation 19.

$$\Delta\Sigma M_O^{max} = \Sigma M_O^{max} * 10\% = 2175 * 0.1 = 218\text{Nm}.$$

From the geometry in Figure 35, the moment arm is the perpendicular distance from the pin connector. Thus,

$$r_{max}^b = d * \sin(180° - \phi - \theta_{\max}) = d * \sin(180° - 35° - 81.2°) = d * sin63.81°$$
$$= 7.51cm * sin63.81 = 6.74cm = 6.74 * 10^{-2}m$$

The reduced MCPJ moment is contributed by two restrainer band tensions with equal values act on both sides of the device (Equation 21),

$$\Delta\Sigma M_O^{max} = 2 * T_{max}^b * r_{max}^b$$

$$\rightarrow T_{max}^b = \frac{\Delta\Sigma M_O^{max}}{2 * r_{max}^b} = \frac{217.5Nm}{2 * (6.74 * 10^{-2}m)} = 1620\ N$$

The maximum tension needed by the restrainer band when the fetlock angle is 81.2 °is **1620N.**

5.2.2 Pre-stretched tension needed in the restrainer band at rest (θ=20°)

The MCPJ is positioned at is 20 °[14] when the horse is at rest. The amount of pre-stretched resistance needed for the restrainer band must be determined to prevent the band from slacking during flexion movement. In other words, the band installed in the device would need to have a certain amount of stretched tension in it even before starting the movement, so that the target tension of 1620N can be met at maximum extension

It is also clear to see that little change of MCPJ moment is produced at walk in Figure 32. The minimum restrainer band tension is set to be 30% of the resultant tension of the tendon/ligament acting on the forelimb at rest. The individual tensions of the ligament/tendons at rest are tabulated in Table 5.

Table 5: Individual tensions of the SDFT, SL and DDFT at rest (θ=20°)

Tendon	Tension (N)	Angle (°)
SDFT	0	33
SL	64	46.1
DDFT	225	49.2

The y-component, T_y^R of the resultant ligament tension is:

$$T_y^R = 0N * \cos(30°) + 64N * \cos(46.1°) + 225N * \cos(49.2°) = 191N$$

The x-component, T_x^R of the resultant ligament tension is:

$$T_x^R = 0N * \sin(30°) + 64N * \sin(46.1°) + 225N * \sin(49.2°) = 217N$$

Thus, the net resultant ligament tension is:

The y-component, T_y^R of the resultant ligament tension is:

$$T_R = \sqrt{(191N)^2 + (217N)^2} = 289N$$

Thus, the pre-stretched tension needed in the restrainer band at rest is:

$$T_0^b = 0.3 * 289 = 87N$$

5.2.3 Summary

In summary, the design specifications of the restrainer band tensions at rest and at maximum extension were determined and tabulated in Table 6. The pre-stretched band provides at least 87N at rest stance. The maximum band tension should be limited within 1620N at maximum extension.

Table 6: The fetlock joint angles, the reduced restrainer band moments, the moment arms perpendicular to the tensions and the limits of the restrainer band tensions for a horse with a body mass of 500kg

Boundary conditions	Fetlock angle, $\theta_{fetlock}$ (°)	Moment arm, r (m)	Reduced Fetlock Moment, $\Delta\Sigma M_{fetlock}$ (Nm/kg), normalized to mass	Reduced Fetlock Moment, $\Delta\Sigma M_{fetlock}$ (Nm)	Restrainer band tension, T_{band} (N)
Rest	20	/	/	/	87
Max. Extension	81.2	0.0742	1.449	217	1620

5.3 Changes in length of restrainer band in a full gait cycle

The restrainer band tension is caused by the change of the band length, due to the change of the fetlock angles. This section begins with the calculation of the original restrainer band length at rest and shows a sample calculation of the stretched band length when the fetlock angle is 50 °. The relationship of restrainer band length and the fetlock angle is then studied with respect to the change of the device orientation.

5.3.1 Calculation of the original restrainer band length at rest, L_0^b

Referred to Figure 36, when the horse forelimb is at rest stance position, the fetlock angle θ is 20°. The other known variables are c=21.11cm, d=7.51cm, and ϕ=35 °,

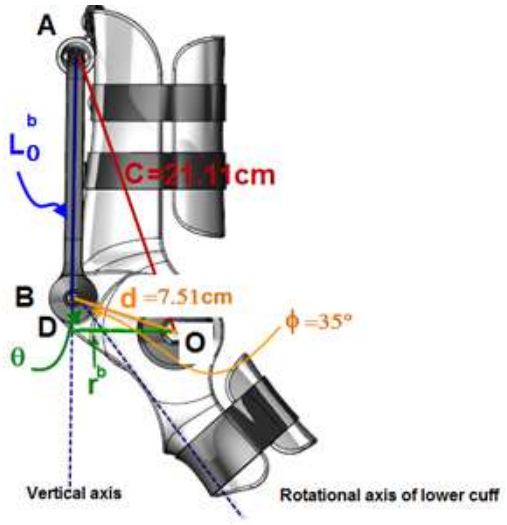

Figure 36: A mathematical schematic describes the calculation of the original restrainer band length at rest (θ=20°).

L_n^b can be obtained by the Law of Cosine using Equation 2

$$21.11^2 = (L_0^b)^2 + 7.51^2 - 2 * L_0^b * 7.51 * \cos(180° - 20° - 35°)$$

$\rightarrow \ (L_0^b)^2 - 15.02 * L_0^b * \cos(125°) - 389.23 = 0$

$\rightarrow \ L_0^b = -24.3cm \ or \ 15.9cm$

Since L_0^b must be greater than zero, the length of L_0^b when the fetlock rotates at 20 °is 15.9cm, which is the restrainer band length at rest.

5.3.2 Calculation the stretched length of the restrainer band when θ=50°

Referred to Figure 37, the MCPJ angle, θ, rotates to 50 °from rest position. At this point, the other known variables include c=21.11cm, d=7.51cm, and ϕ=35 °,

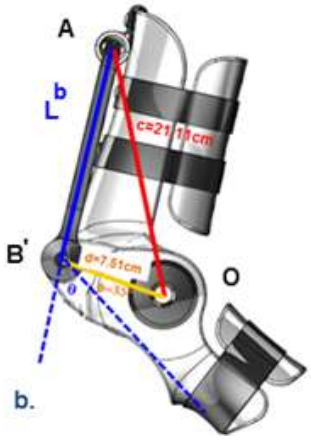

Figure 37: A mathematical schematic describes the calculation of the change in length restrainer band length at rest (θ=50°).

Using Equation 12, the changes of the MCPJ angle is $\Delta\theta = \theta - 20° = 50° - 20° = 30°$

In triangle BNO in Figure 38, the vertical change, Δy, from Point B (bracket position when θ=20°) to Point B' (bracket position when θ=50°) can be determined using Equation 13,

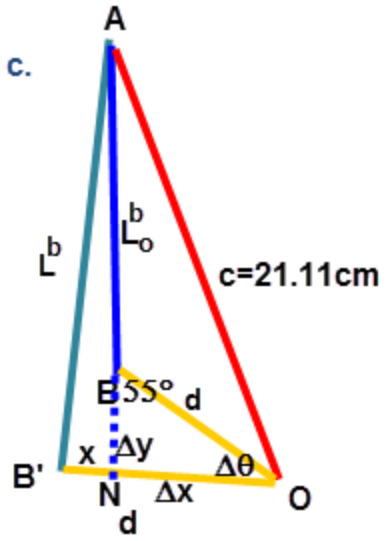

Figure 38: A mathematical representation is used to calculate the stretched length of the restrainer band, L^b

$$\frac{d}{\sin(180° - (20° + 35°) - \Delta\theta)} = \frac{\Delta y}{\sin(\Delta\theta)}$$

$$\rightarrow \frac{7.51}{\sin(125° - \Delta\theta)} = \frac{\Delta y}{\sin(\Delta\theta)}$$

$$\rightarrow \frac{7.51}{\sin(95°)} = \frac{\Delta y}{\sin(30°)}$$

$$\rightarrow \Delta y = 3.77cm$$

The horizontal change from B to B' can be determined by the difference of B'O and NO (Δx). B'O is distance from the bracket to the pin connector (d=7.51cm). Δx can be determined using Equation 14,

$$\frac{\Delta x}{\sin(20° + 35°)} = \frac{d}{\sin(180° - (20° + 35°) - \Delta\theta)}$$

$$\rightarrow \frac{\Delta x}{\sin(20° + 35°)} = \frac{7.51cm}{\sin(180° - (20° + 35°) - 30°)}$$

$$\rightarrow \Delta x = 6.18cm$$

BN= $x = d - \Delta x$ = 7.51cm – 6.18cm = 1.33cm

Since $L_0^b = 15.88cm$ $(calculated\ from\ Part\ 1\ of\ this\ section)$. Using Equation 15,

NA = $y = L_0^b + \Delta y$ = 15.88cm + 3.77cm = 19.65cm, BN=1.33cm

The stretched length of the restrainer band can be determined with the Law of Cosine in Equation 17,

$$(L^b)^2 = x^2 + y^2 - 2 * x * ycos(55° + \Delta\theta)$$

$$\rightarrow L^b = \sqrt{x^2 + y^2 - 2 * x * ycos(55° + \Delta\theta)}$$

$$= \sqrt{1.33^2 + 19.65^2 - 2 * 1.33 * 19.65 * cos(55° + 30°)}$$

$$= 19.58cm$$

Thus, when the MCPJ rotates to 50 °, the restrainer band elongates by:

$$\Delta L^b = L^b - L_o^b = 19.58cm - 15.88cm = 3.70cm$$

5.3.3 Relationship between changes in length of restrainer band and fetlock angles

The stretched length of the restrainer band, L^b, as the MCPJ angles extends from 20 °can be calculated based on the method described in Chapter 5.3.2. The results of the stretched length, changes in length and the strain of the restrainer band when MCPJ angle varies from 20 °to 81.2 ° with a 5 °interval are tabulated in Table 7.

Table 7: The results of the normal projected length, the overall length and the overall change in length of the restrainer band when fetlock angle is from 20 °to 81.2 °[15]

Fetlock, θ (°)	Δθ (°)	Δx (cm)	Δy (cm)	x (cm)	y (cm)	AB, L^b (cm)	ΔL^b (cm)	ε
20	0	7.51	0.00	0.00	15.9	15.9	0.00	0.00%
25	5	7.10	0.76	0.41	16.6	16.4	0.56	3.50%
30	10	6.79	1.44	0.72	17.3	17.0	1.15	7.22%
35	15	6.55	2.07	0.96	18.0	17.6	1.76	11.1%
40	20	6.37	2.66	1.14	18.5	18.3	2.40	15.1%
45	25	6.25	3.22	1.26	19.1	18.9	3.04	19.2%
50	30	6.18	3.77	1.33	19.7	19.6	3.70	23.3%
55	35	6.15	4.31	1.36	20.2	20.3	4.35	27.4%
60	40	6.18	4.85	1.33	20.7	20.9	5.00	31.5%
65	45	6.25	5.39	1.26	21.3	21.5	5.65	35.6%
70	50	6.37	5.96	1.14	21.8	22.2	6.28	39.5%
75	55	6.55	6.55	0.96	22.4	22.7	6.89	43.4%
80	60	6.79	7.18	0.72	23.1	23.4	7.49	47.2%

When the MCPJ joint rotates to 80 °, the restrainer band with a rest length of 31.9cm is estimated to elongate by 7.49cm, resulting in a 47.2% tensile strain (Table 7). Compared with the stretched ligament lengths in Swanstrom's musculoskeletal modeling analysis [14] (Table 1), the changes in length of DDFT, SDFT and SL at maximum MCPJ extension (θ=81.2°) are 12.4cm, 7.5cm and 6.7cm, respectively. The

strains of the ligaments at maximum extension are 32.5%, 20.2% and 27.3%. The maximum length increments of the restrainer band lies within the range of the maximum ligament increments. Thus, the restrainer band changes in length which provided by the tension, are reasonable.

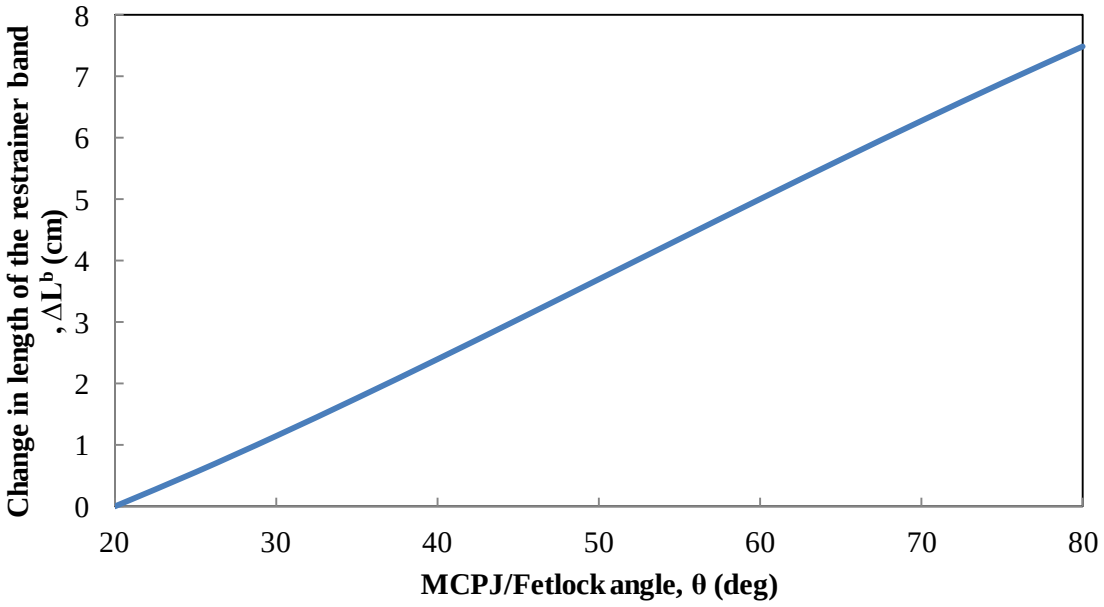

Figure 39: The overall change in lengths of the restrainer band increases as the MCPJ angle increases.

The restrainer band length increments calculated from the mathematical representation are also plotted in Figure 39. Since the rest restrainer band length was designed to be identical to the distance of the device pulley and the bracket, there is no change in length when the forelimb is at rest. As the MCPJ angle increases, the restrainer band change in length increases accordingly. Figure 39 illustrates that the changes in length of the restrainer band approaches to a quasi-linear relationship with the MCPJ angle.

5.3.4 Summary of restrainer band length calculation

The original length of the restrainer band at either side of the device is 15.9cm (total length is 31.8cm), and it is assumed to be fit perfectly from the bracket to the pulley without producing any pre-stretched tension at rest. The stretched lengths of the restrainer band are obtained with the relationship of the changes from that at the rest position. The calculated elongation of the restrainer band shows a quasi-linear relationship with the variation of the fetlock angle. The elongation property provides useful information on determining the tension requirement of the restrainer band.

5.4 Calculations and optimization of restrainer band tensions

The restrainer band tensions were calculated with respect to the changes in length in a full gait cycle. Results were compared with the design specifications. The effects of stiffness, cross-sectional area and length on the restrainer band tensions were also studied. The pre-stretched length of the restrainer band was adjusted to modify the stiffness, consequently approach the design specifications of the restrainer band.

5.4.1 Restrainer band tension in a full gait cycle

The initial design of the restrainer band is assumed to fit perfectly on the pulley and the bracket when the horse is at rest, so the original length of the restrainer band is equal to the distance from the pulley to the bracket at rest. The original length, L_0^b of the restrainer band at either side of the device was found to be $15.9*10^{-2}$m.

The tension of the stretched restrainer band, T^b, with respect to its change in length can be determined by Hook's Law. Equation 22 shows the elaborated calculation of the stress of the restrainer band:

$$\sigma = E\varepsilon = \frac{\Delta L^b}{L_0^b} E = \frac{T_b}{A_0}$$

$$T_b = \frac{\Delta L^b}{L_0^b} * E * A_0$$

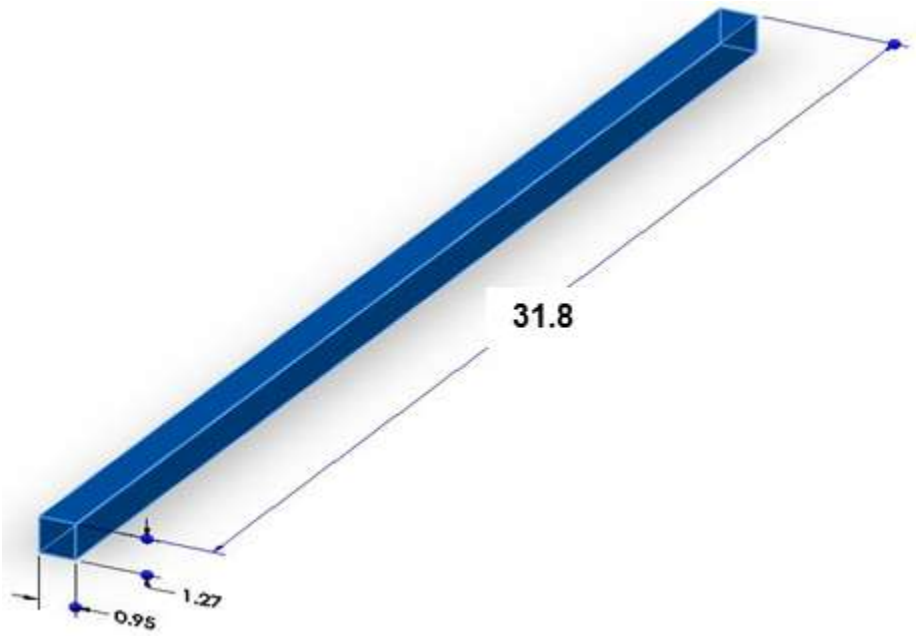

Figure 40: The original design of the restrainer band is made of polyurethane MP950. The length, width and thickness of the die-cut band are 31.8cm, 1.27cm and 0.95cm, respectively.

A_o is the cross-sectional area of the restrainer band. Referred to Figure 40, the cross-sectional area

$$A_0 = w_0 * t_0 = 0.95cm * 1.27cm = 1.21 * 10^{-4} m^2$$

MECHANICAL PROPERTY	ASTM Test	MP 300	MP 600	MP 750	MP 850	MP 900	MP 950	MP 160	MP 175
Durometer, Shore	D-2240	30A	60A	75A	85A	90A	95A	60D	75D
100% Modulus, psi	D-412	80	250	350	600	1,100	1,800	3,000	5,500
300% Modulus, psi	D-412	170	600	1,000	1,500	2,100	4,000	6,500	-
Tensile, psi	D-412	380	4,500	5,500	6,000	4,500	5,500	6,500	7,500
Elongation, %	D-412	515	500	500	500	450	320	300	225

Figure 41 The mechanical properties of various polyurethane sheets by McMaster Carr. The selected sheet material by the design group was MP950.

The selected material by Manta Design Inc. was Polyurethane with durometer 95A (MP950). Figure 41 illustrates the mechanical properties of the available polyurethane sheets in McMaster Carr (www.mcmaster.com) [27]. Since the strain of the restrainer band is 47% at maximum extension of the horse fetlock joint and it is within 100% of the elongation, the Elasticity Modulus, E, to be used in the future calculation of the restrainer band tension should be 1800psi (or 12.4 MPa)

The length of change of the restrainer band, ΔL^b were calculated and tabulated in Table 7. The values of T_b were then determined with Hooke's Law and tabulated in Table 8. It shows the responses of the restrainer band tension at a full gait cycle.

Table 8 Calculated restrainer band tension T_b as a function of MCPJ angle

Fetlock angle (°)	T_b (N)
20	0.0
25	52.4
30	108.0
35	166.1
40	225.9
45	286.9
50	348.6
55	410.3
60	471.7
65	532.3
70	591.8
75	649.8
80	706.0

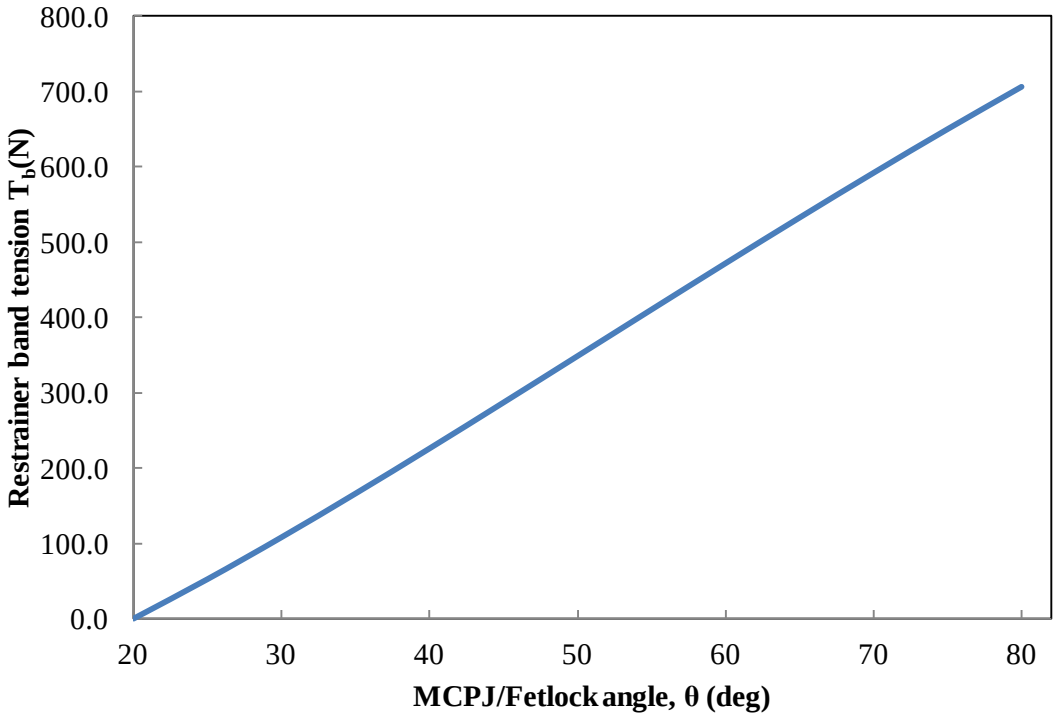

Figure 42 The restrainer band tension (L_0^b=31.8cm) is associated with the change in length of the restrainer band. The tension increases linearly as the MCPJ angle increases.

Since there is no length increment of the restrainer band at rest due to its design, no pre-stretched tension is observed when horse forelimb is at rest. However, the proposed required restrainer band tension at rest is at least 87N from the design specification. In addition, the restrainer band tension at maximum extension is only half of the maximum tension requirement. Therefore, adjustments of the restrainer band, such as the stiffness, area and length, should be made to meet the design specifications.

5.4.2 Stiffness effect on the restrainer band

The maximum restrainer band tension in Figure 42 is calculated to be 706N, which is less than half of the maximum tension requirement. A much greater tension is needed to approach 1620N at maximum extension with the same change in length of the band. Thus, the restrainer band should be made of a stiffer material. In other words, the spring constant of the restrainer band should be greater.

Current spring constant (stiffness) of the restrainer band is

$$k_{950} = \frac{A_0}{L_0^b} * E_{950} = \frac{1.21 * 10^{-4} * 1.24 * 10^7}{31.9 * 10^{-2}} = 4710 N/m$$

The stiffness of the other polyurethane materials with different durometers (MP 300, 600, 750, 900, 160 and 175, Figure 43) are compared to the original design (MP 950) without changing the dimensions of the design. Since the strain of the restrainer band is 47% at maximum extension of the horse fetlock joint and it is within 100% of the elongation, the Elasticity Modulus, E, to be used in the tension calculations of MP 160 and MP 175 would be the value of 100% modulus.

MECHANICAL PROPERTY	ASTM Test	MP 300	MP 600	MP 750	MP 850	MP 900	MP 950	MP 160	MP 175
Durometer, Shore	D-2240	30A	60A	75A	85A	90A	95A	60D	75D
100% Modulus, psi	D-412	80	250	350	600	1,100	1,800	3,000	5,500
300% Modulus, psi	D-412	170	600	1,000	1,500	2,100	4,000	6,500	-
Tensile, psi	D-412	380	4,500	5,500	6,000	4,500	5,500	6,500	7,500
Elongation, %	D-412	515	500	500	500	450	320	300	225

Figure 43: The mechanical properties of various polyurethane sheets by McMaster Carr. The stiffness of the other polyurethane materials is compared to that of MP 950. [28]

For MP 300, E_{300}=80psi=0.55MPa,

$$k_{300} = \frac{A_0}{L_0^b} * E_{300} = \frac{1.21 * 10^{-4} * 5.5 * 10^5}{31.9 * 10^{-2}} = 209 N/m$$

For MP 750, E_{750}=250psi=1.72MPa

$$k_{750} = \frac{A_0}{L_0^b} * E_{750} = \frac{1.21 * 10^{-4} * 1.72 * 10^6}{31.9 * 10^{-2}} = 652 N/m$$

For MP 850, E_{850}=600psi=4.14MPa,

$$k_{850} = \frac{A_0}{L_0^b} * E_{850} = \frac{1.21 * 10^{-4} * 4.14 * 10^6}{31.9 * 10^{-2}} = 1570 N/m$$

For MP 900, E_{900}=1100psi=7.58MPa

$$k_{900} = \frac{A_0}{L_0^b} * E_{900} = \frac{1.21 * 10^{-4} * 7.58 * 10^6}{31.9 * 10^{-2}} = 2880 N/m$$

For MP 160, E_{160}=3000psi=20.7MPa,

$$k_{160} = \frac{A_0}{L_0^b} * E_{160} = \frac{1.21 * 10^{-4} * 2.07 * 10^7}{31.9 * 10^{-2}} = 7850 N/m$$

For MP 175, E_{175}=5500psi=37.9MPa

$$k_{175} = \frac{A_0}{L_0^b} * E_{175} = \frac{1.21 * 10^{-4} * 3.79 * 10^7}{31.9 * 10^{-2}} = 1.44 * 10^4 N/m$$

Since the change in length of the restrainer band, ΔL^b, of all the restrainer band materials with respect to the joint angle is the same, the tension at maximum extension (θ=81.2 °) for different polyurethane materials can be easily calculated by the product of the stiffness and the change in length.

Since the reduced MCPJ moment is generated by two equal tensions at both sides of the device, so the required tension of the restrainer band is doubled.

At maximum MCPJ extension, the tension of the restrainer band with Polyurethane MP 950,

$$T_{950}^{b}=2*\ k_{950}*L_{max}^{b}=2*4710*7.49*10^{-2}=706N$$

For Polyurethane MP 300, $T_{300}^{b}=2*\ k_{300}*L_{max}^{b}=2*209*7.49*10^{-2}=31.3N$

For Polyurethane MP 750, $T_{750}^{b}=2*\ k_{750}*L_{max}^{b}=2*652*7.49*10^{-2}=97.7N$

For Polyurethane MP 850, $T_{850}^{b}=2*\ k_{850}*L_{max}^{b}=2*1570*7.49*10^{-2}=235N$

For Polyurethane MP 900, $T_{900}^{b}=2*\ k_{900}*L_{max}^{b}=2*2880*7.49*10^{-2}=431N$

For Polyurethane MP 160, $T_{160}^{b}=2*\ k_{160}*L_{max}^{b}=2*7850*7.49*10^{-2}=1180N$

For Polyurethane MP 175, $T_{175}^{b}=2*\ k_{175}*L_{max}^{b}=2*1.44*10^{4}*7.49*10^{-2}=2150N$

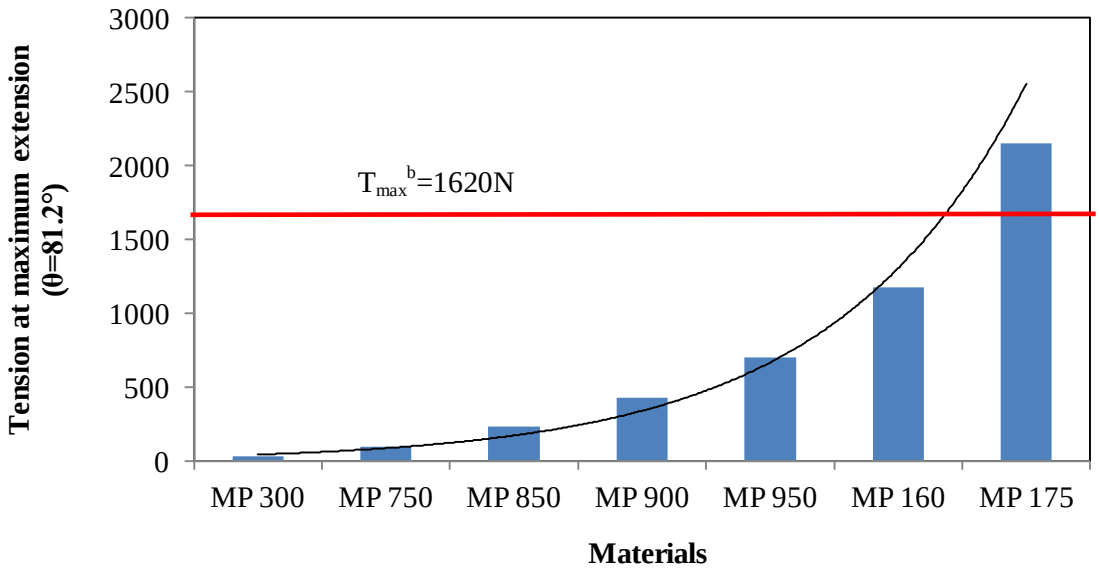

Figure 44: Comparisons of the tensions at maximum MCPJ extension with the polyurethane materials provided by sheets by McMaster Carr. The dimensions (rest length and cross-sectional area) remained the same in the comparison study. The stiffness of the restrainer band is calculated by varying the elastic modulus. The band length increment at maximum joint extension is 7.49cm and the band tensions are obtained with Hooke's Law. The red horizontal line indicates the maximum required tension in the design specification (T_{max}^{b}=1620N).

With controlled dimensions of the neutral restrainer band, the stiffness of the restrainer band with different polyurethane materials is calculated. The restrainer band tensions with different materials are calculated with Hooke's Law and compared in Figure 44. The restrainer band made of MP 160 and MP175 are stiffer compared to the rest of materials with the same dimensions, so more tensions are required to result in the same length increment of the restrainer band with MP 160 and MP 175. In addition, MP 160 and MP 175 are usually used in impact strength applications such as bearing pads, material handling equipment, rolls due to their exceptionally high tensile and tear strengths. Polyurethane

MP 300 is used for hot melt adhesive. The materials such as polyurethane MP 750, 850, 900 and 950 can be selected for applications including springs, restraint components, shock absorbers and many more. Cross-sectional area and length effects of these four selected materials will be studied.

5.4.3 Cross-sectional area effect of restrainer band

Polyurethane MP 750, 850, 900 and 950 are used for restraint components. They are selected for a cross-sectional area effect of restrainer band to achieve 1620N at maximum MCPJ extension (θ=81.2 °). The rest lengths of the restrainer band with four different materials are identical to the original design, L_o^b=31.9cm. The band length increment at maximum extension is 7.49cm. The required cross-sectional areas of the restrainer band to achieve 1620N at maximum extension from 87N pre-stretched tension can be calculated by:

$$A_0 = \frac{T_b * L_0^b}{\Delta L^b * E}$$

For MP 750, A_{750}^b=(1620-87)*0.0749/ (0.319*1.72E6) = $2.21*10^{-4}m^2$

For MP 850, A_{850}^b=(1620-87)*0.0749/ (0.319*4.14E6) = $9.19*10^{-5}m^2$

For MP 900, A_{900}^b=(1620-87)*0.0749/ (0.319*7.58E6) = $5.02*10^{-5}m^2$

For MP 900, A_{900}^b=(1620-87)*0.0749 /(0.319*1.24E7) = $3.07*10^{-5}m^2$

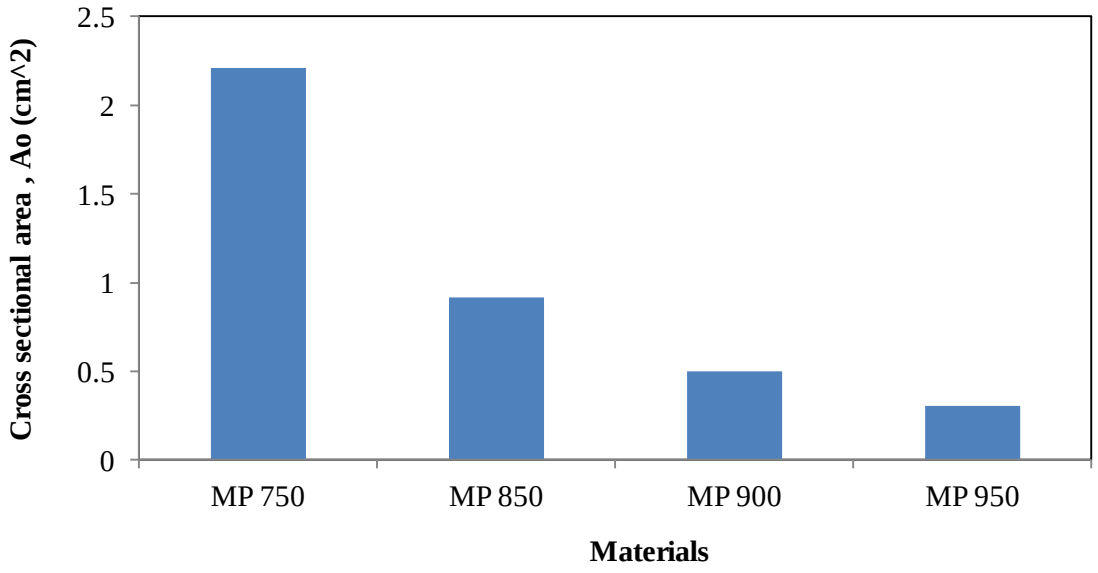

Figure 45: Comparisons of required cross-sectional area, A_0, of the restrainer band with the polyurethane materials provided by sheets by McMaster Carr. The rest length of the band remained the same (L_o=31.9cm) in the comparison study. The band length increment at maximum joint extension is 7.49cm.

The required cross-sectional areas of the restrainer band with different polyurethane materials are compared in Figure 45. With constant restrainer band length, the cross-sectional area is inversely proportional to the elastic modulus of the material. MP 750 requires the greatest cross-sectional area of the restrainer band to achieve 1620N at maximum extension from 87N pre-stretched tension, and the area is doubled the cross-sectional area of the original restrainer band design with MP 950 (A_o=1.21cm^2). The

cross-sectional area for MP 950 must be reduced to about ¼ of that of the original design, which implies that the dimensions of width and thickness should be reduced by a half.

5.4.4 Calculations of restrainer band length adjustments

The restrainer band length must be reduced to produce pre-stretched tension at rest. The restrainer band cross-sectional area remains to be the cross-sectional area of the original design in study of restrainer band length effects.

$$L = \frac{T}{\Delta L * E * Ao}$$

Where T=required maximum tension-band tension at maximum extension with L_0=0.319m=1620-T_o^b

ΔL=length increment of the restrainer in new length=ΔL_{max}^b+L_0^b-L=0.0749+0.319-L

A_o=1.21*$10^{-4}$$m^2$

When fetlock angle θ = 81.2 º, the difference between the proposed restrainer band tension 1620N and the current restrainer band tension 706N is T = 1620N-706N = 914N. The new original length of the restrainer band can be calculated

For MP 750

$$T = \frac{\Delta L * E * Ao}{L}$$

$$\rightarrow (1620 - 97.7)N = \frac{(0.0749m + 0.319 - L) * 1.72 * \frac{10^6 N}{m^2} * 1.21 * 10^{-4} m^2}{L}$$

$$\rightarrow \frac{0.394 - L}{L} = 7.314$$

$$\rightarrow L = 0.0474m$$

Therefore, the initial restrainer band length should be reduced by:

ΔL_0 = 0.319m-0.0474m= 0.272m

For MP 850

$$T = \frac{\Delta L * E * Ao}{L}$$

$$\rightarrow (1620 - 235)N = \frac{(0.0749m + 0.319 - L) * 4.14 * \frac{10^6 N}{m^2} * 1.21 * 10^{-4} m^2}{L}$$

$$\rightarrow \frac{0.394 - L}{L} = 2.76$$

$$\rightarrow L = 0.104m$$

Therefore, the initial restrainer band length should be reduced by:

ΔL_0 = 0.319m-0.104m= 0.215m

For MP 900

$$T = \frac{\Delta L * E * Ao}{L}$$

$$\rightarrow (1620 - 431)N = \frac{(0.0749m + 0.319 - L) * 7.58 * \frac{10^6 N}{m^2} * 1.21 * 10^{-4} m^2}{L}$$

$$\rightarrow \frac{0.394 - L}{L} = 1.30$$

$$\rightarrow L = 0.171m$$

Therefore, the initial restrainer band length should be reduced by:

ΔL_0 = 0.319m-0.171m= 0.148m

For MP 950

$$T = \frac{\Delta L * E * Ao}{L}$$

$$\rightarrow (1620 - 706)N = \frac{(0.0749m + 0.319 - L) * 1.24 * \frac{10^7 N}{m^2} * 1.21 * 10^{-4} m^2}{L}$$

$$\rightarrow \frac{0.394 - L}{L} = 0.609$$

$$\rightarrow L = 0.246m$$

Therefore, the rest restrainer band length should be reduced by:

ΔL_0 = 0.319m-0.246m= 0.073m

Since the neutral length of the restrainer band, L, is shortened from 0.319m, a pre-stretched tension is produced at rest position. The tensions provided the improved restrainer band with different materials can be calculated with Hooke's Law, $T = \frac{\Delta L}{L} * E * Ao$, and summarized in Table 9.

Table 9: The tensions provided the improved restrainer band with different polyurethane materials are calculated with Hooke's Law. The stiffness of the restrainer band with different material is adjusted with the specific length. A pre-stretched tension is produced at rest position with the shortened restrainer band length.

	T^b (N)			
Fetlock angle, θ (°)	MP 750	MP 850	MP 900	MP 950
20	1.19E+03	1.04E+03	7.94E+02	4.56E+02
25	1.24E+03	1.09E+03	8.54E+02	5.26E+02
30	1.30E+03	1.15E+03	9.17E+02	6.00E+02
35	1.35E+03	1.21E+03	9.83E+02	6.76E+02
40	1.41E+03	1.27E+03	1.05E+03	7.56E+02
45	1.46E+03	1.33E+03	1.12E+03	8.36E+02
50	1.52E+03	1.39E+03	1.19E+03	9.18E+02
55	1.58E+03	1.45E+03	1.26E+03	1.00E+03
60	1.63E+03	1.52E+03	1.33E+03	1.08E+03
65	1.69E+03	1.58E+03	1.40E+03	1.16E+03
70	1.75E+03	1.64E+03	1.47E+03	1.24E+03
75	1.80E+03	1.70E+03	1.53E+03	1.32E+03
80	1.85E+03	1.76E+03	1.60E+03	1.39E+03

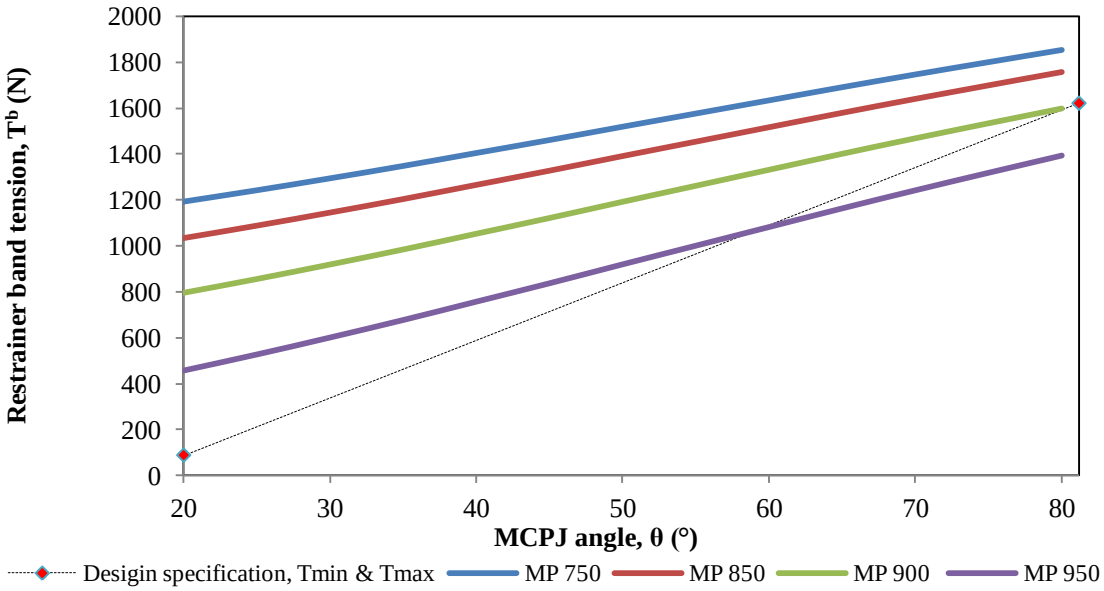

Figure 46: The original restrainer band length is adjusted in order to provide a pre-stretched tension to the band as well as to target the maximum band tension. The color straight lines indicate the restrainer band tensions of different polyurethane materials after length adjustments. The red diamonds indicate the design specifications of the restrainer band tensions. The required minimum tension is 87N when θ=20° and the maximum tensions is 1620N when θ=81.2°. The dotted straight line is the linear regression of the design specifications.

The rest restrainer band length is reduced to desired length with cross-sectional area of $1.21*10^{-4}$ m^2 to provide a pre-stretched tension to the band as well as to target the maximum band tension. The restrainer band pre-stretched tensions summarized in Table 9 are 1190N, 1040N, 794N and 456N for MP 750, 850, 900 and 950, respectively. The restrainer band tensions at maximum extension are 1850N, 1760N, 1600N and 1390N for MP 750, 850, 900 and 950, respectively.

The tensions produced by restrainer band with different materials are compared in Figure 46. The color straight lines indicate the restrainer band tensions of different polyurethane materials after length adjustments. The restrainer band tensions at maximum MCPJ extension are over 1620N for MP 750 and MP 850. The restrainer band tension for MP 900 at maximum joint extension is the closet to 1620N. The required minimum restrainer band tension is 87N, which is 30% of the resultant tendon tension. The pre-stretched tensions of each restrainer band are greater than the resultant tendon/ligament tension (288N), but it can help reduce the vibration from ground reaction force before any movement. However, the initial MCPJ reaction force is 377 according to the static analysis in Chapter 5.1. It is better not to obtain a pre-stretched tension over the initial joint reaction force. Therefore, if the cross-sectional area remains the same, the restrainer band should be made of polyurethane MP 950 and its slacking/rest length should be 0.246m. A pre-stretched tension of 456N is generated as the band is extended to fit the band brackets of the device. The maximum tension of the proposed band is 1390N, which is smaller than the maximum targeted tension, 1620N, but it is within the range of the restrainer band limits.

5.4.5 Summary

The tensions of the original restrainer band design were calculated with respect to the changes in length in a full gait cycle. The effects of stiffness, cross-sectional area and length on the restrainer band tensions of different polyurethane materials were studied with controlled parameters. It was concluded that polyurethane MP 750, 800, 900, and 950 can be selected for restraint components. Cross-sectional area effects of these four selected materials indicate an inversely proportional relationship with the elastic modulus but it cannot provide enough suggestion on the restrainer band design. The rest restrainer band length is reduced to desired length with the identical cross-sectional area of the original design to provide a pre-stretched tension to the band as well as to target the maximum band tension. The pre-stretched tensions provided by MP 750, 850 and 900 are greater than the initial joint reaction force. Based on the comparisons of restrainer band design parameters, it is suggested that the restrainer band should be made of polyurethane 950A with cross-sectional area of $1.21*10^{-4}m^2$ and 0.246m. The restrainer band provides 456N pre-stretched tension at rest and 1390N at maximum joint extension. The moment reduction will be estimated in the next section.

5.5 Reduced moment generated by the restrainer band tension in a full gait cycle

The original fetlock joint moment results at fast gallop phase and the calculated reduced fetlock joint moment results during use of horse leg protective device were compared and illustrated in Figure 47. The reduced fetlock joint moment results were the supported fetlock joint moment by the improved restrainer band tension, $T_{b,}$ which was calculated previously. The moment arm and proposed restrainer band tension of the restrainer band tension was calculated as

$$r_b = d * \sin(\theta + \phi)$$

Where θ is the fetlock angle of the horse leg and ϕ is the angle between side BO and the rotational axis of the lower cuff, which is 35 °.

The reduced fetlock joint moment was generated by the counter tensions at both sides of the device and could be calculated using: $\Delta\Sigma M = 2 * T_b * r_b$

The residual joint moment is the difference between the resultant MCPJ moment without device and the reduced joint moment.

$$\Sigma M_o^b = \Sigma M_o - \Delta\Sigma M$$

A comparison of the original fetlock moment during extension movement at gallop and the reduced moments generated by the restrainer band is summarized in Table 10. At maximum joint extension, the band provides 1390N counter tension and reduces 189Nm joint moment. The joint moment reduction at maximum extension is 8.4%.

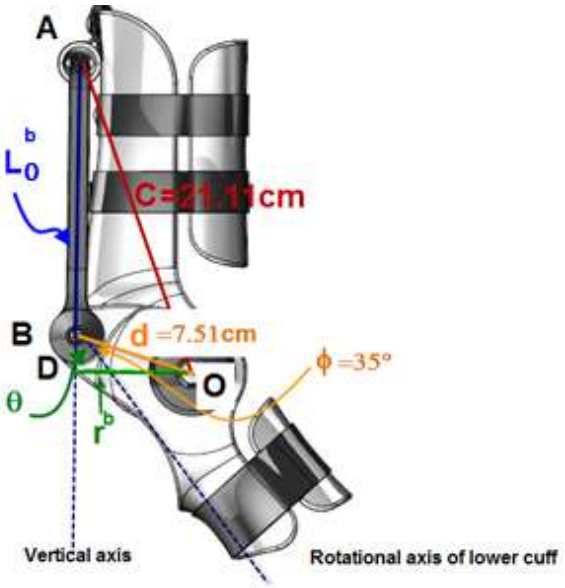

Table 10: The restrainer band tensions are calculated with respect to the change in length. The reduced fetlock moment is generated by two equal tensions at both sides of the device. The restrainer band reduces 8.4% MCPJ moment at maximum joint extension.

Fetlock angle, θ (°)	ΔL^b (m)	T^b (N)	Moment arm, r^b (m)	Reduced Fetlock Moment, $\Delta\Sigma M_o$ (Nm)	$\Sigma M_o{}^b$ (Nm)	Reduction %
20	0.036	456	0.0615	56.1	-25.1	11.20%
25	0.041	526	0.0650	68.4	-92	6.09%
30	0.047	600	0.0680	81.7	-156	7.25%
35	0.053	676	0.0705	95.1	-331	5.90%
40	0.06	756	0.0725	110	-512	7.70%
45	0.066	836	0.0739	124	-721	8.50%
50	0.073	918	0.0748	137	-851	6.90%
55	0.079	1000	0.0751	150	-1060	7.28%
60	0.086	1080	0.0748	162	-1210	8.90%
65	0.092	1160	0.0739	172	-1350	6.20%
70	0.099	1240	0.0725	180	-1550	10.40%
75	0.105	1320	0.0705	186	-1730	7.30%
80	0.111	1390	0.0680	189	-1920	8.40%

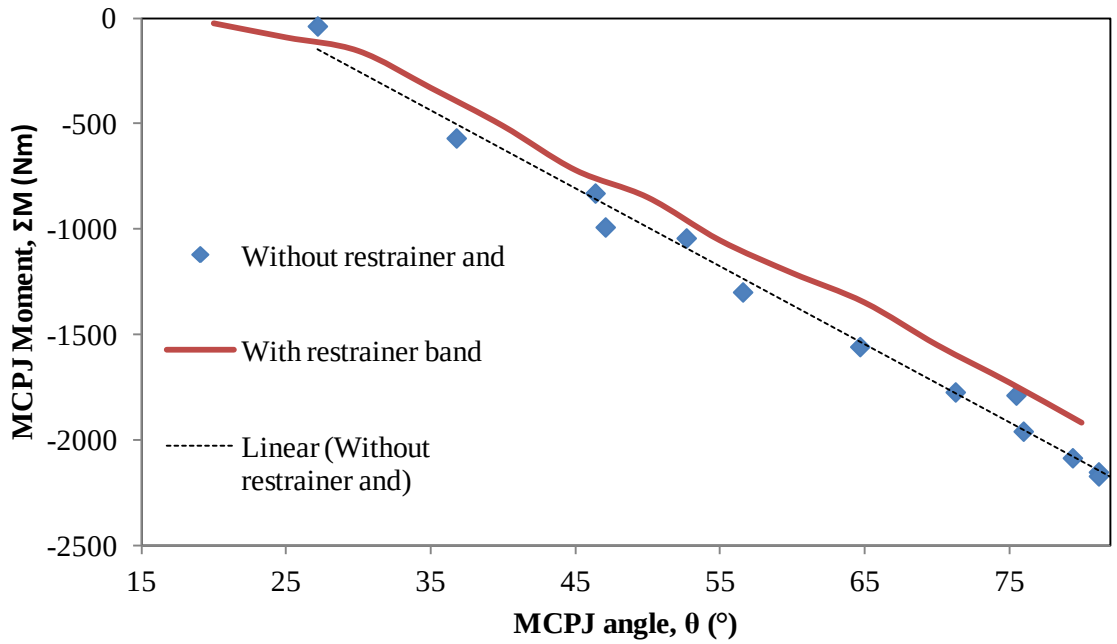

Figure 47 Comparison between original fetlock joint moment results and residual moment contributed by the restrainer band tension.

The restrainer band provides consistent counter tension to the horse forelimb, and thus the range of motion of the horse forelimb can be proportionally reduced with supplemental support of joint moment. Figure 47 shows the original MCPJ moment and the residual moment employing the restrainer band with respect to the joint angles. The resultant MCPJ moments and the residual moments are generated in a clockwise direction, so the values are negative. The red line in Figure 47 indicates that the fetlock moment is reduced synchronously with the same slope. However, However, the moment reduction percentage of the fetlock joint at 80 degrees is $\frac{189}{2184} * 100\% = 8.4\%$, which is close to 10%. Therefore, the device with a 0.246m-long restrainer band can reduced about 10% of fetlock moment at maximum extension.

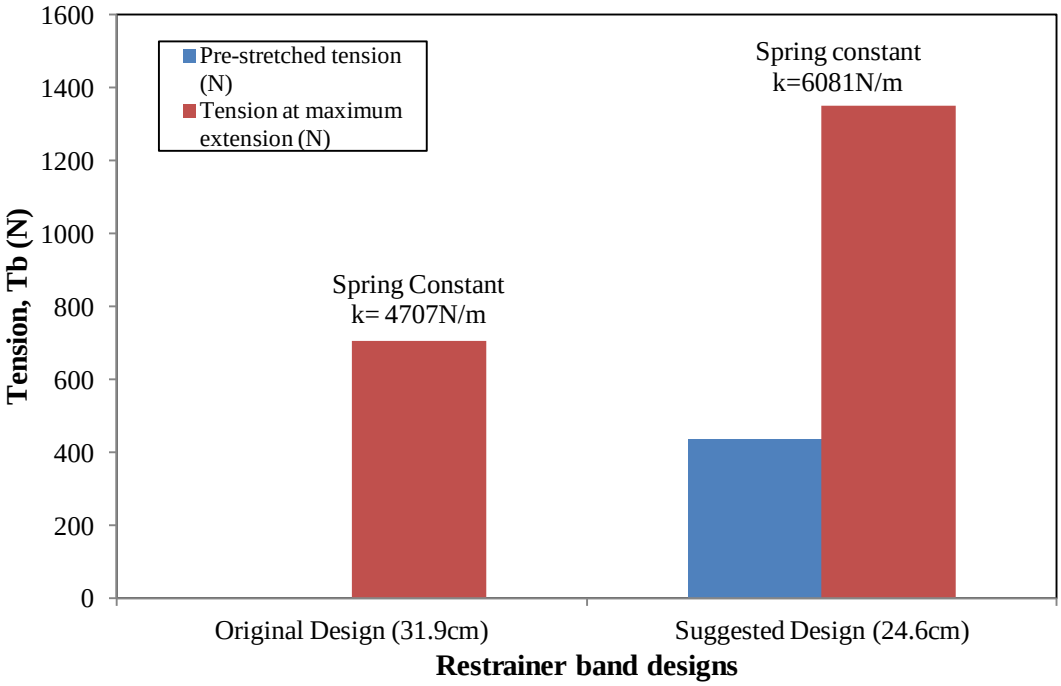

Figure 48: Comparisons of restrainer band tensions, stiffness and lengths of the original and improved designs.

Figure 48 describes the comparisons of the original and improved designs of the restrainer band in rest length, stiffness, pre-stretched tension and the tension at maximum extension. The minimum and maximum restrainer band tension is designed to be 87N and 1620N. Based on the comparisons of restrainer band design parameters, it is suggested that the restrainer band should be made of polyurethane 950A with cross-sectional area of $1.21*10^{-4}m^2$. The slacking restrainer band length is suggested to reduce to 24.6cm from 31.9cm. Since the original prototyped restrainer band was designed to fit in the pulley and bracket perfectly at rest without changing the dimensions, no pre-stretched tension is observed at rest and the tension at maximum extension is 707N, which is near a half of the required tension. The improved restrainer band provides 456N pre-stretched tension at rest and 1390N at maximum joint extension. The restrainer band is also stiffer with shortened length. This device with a 0.246m-long restrainer band can reduced about 8.4% of fetlock moment at maximum extension.

6.0. Conclusion

The reaction force and moment acted on the MCPJ/fetlock joint during walking, trotting, galloping and fast galloping were calculated with horse lower limb free body diagram in a 2D saggital plane. The MCPJ moments were generated by the tensions of the tendons and ligament, as well as the ground reaction force. The peak moments occurred at 40% to 60% stride phase, which were at the movement alternation from extension to flexion, or at the maximum extension position. It was also observed that the MCPJ moment was affected mostly by the suspensory ligament tension. In addition, the MCPJ moment increased as the fetlock angle increased. Reducing the suspensory ligament tension would enable the MCPJ moment reduction, and the range of motion of the horse forelimb could be proportionally reduced with supplemental support of joint moment.

Based on the static analysis, the design specifications of the restrainer band tensions at rest and at maximum extension were determined. The restrainer band was proposed to account for at least 30% of resultant flexor tendons and suspensory ligament tension at rest position, and to achieve by a 10% fetlock moment reduction at maximum extension. The restrainer band was calculated to provide at least 87N pre-stretched tension at rest stance and achieve up to 1620N tension at maximum extension. A mathematic model of the protective device was developed to study the elongation of the restrainer band with respect to the fetlock angles in a full gait cycle. The calculated elongation of the restrainer band showed a quasi-linear relationship with the variation of the fetlock angle. The elongation property provided useful information on adjusting the restrainer band tension properties.

The prototyped restrainer band was made of polyurethane MP950. The original length of the restrainer band at either side of the device was 15.9cm (total length is 31.8cm), and it was assumed to be fit perfectly from the bracket to the pulley without producing any pre-stretched tension at rest. The original restrainer band length was recommended to adjust to 0.123m at each side (total length of the band is 0.246m) in order to provide a pre-stretched tension to the band as well as to target the maximum band tension. A pre-stretched tension of 437N was generated as the band extended to fit the band brackets of the device. The calculated pre-stretched tension of the restrainer band was greater than the resultant tendon/ligament tension (288N), but it could help reduce the vibration from ground reaction force before any movement. The maximum tension of the proposed band was 1350N, which was within the maximum targeted tension limit, 1620N.

The device would not able to reduce the fetlock moment synchronously with the same slope. However, the moment reduction percentage of the fetlock joint at 80 degrees was calculated to be $\frac{184}{2184} * 100\% = 8.42\%$, which was close to 10%. Therefore, the device with a length change on the existing restrainer band was estimate to provide the desired conditions.

7.0. Future Work Recommendations

Although the improved restrainer band is able to supplement 8.4% MCPJ moment at maximum extension, further studies are suggested to optimize the design of the restrainer band. The study addressed a two-dimensional systematic approach in the sagittal plane and calculated joint force and moment at MCPJ of horse forelimb. The restrainer band tension requirements were determined according to the static analysis. The force component which generates the device bending moment is ignored. However, neglect of the force components in internal rotation may cause a change in the static analysis and tension calculation. Different designs of the restrainer band (shapes or additional embellishment as a shock absorber) are recommended. Future studies are suggested to involve a three-dimensional finite-element modeling of the mechanical interactions at the device components for better understanding the restrainer band function and dysfunction in a full gait cycle. It is also suggested to compare the simulated results with experimental data.

This study assumed a frictionless interface in the device. However, the frictional force will alter in the system if there are any minor changes, ex. sands or rocks slip into the device components. Besides the material optimization of the restrainer band, the material used for internal protection inside the cuffs is not trivial. The tissues of the horse forelimb will become necrotic if there is too much skin pressure from the brace. It is suggested to study the pressure necrosis of the skin and muscle in horse and conduct a research on the materials selection and the skin pressure.

The calculated joint reaction force and joint moment at MCPJ, as well as the improved design of the restrainer band can be used as references for further device optimization to the Tufts Cumming School of Veterinary Medicine.

8.0. Bibliography

[1] K.-D. Budras, W. O. Sack and S. Rock, "Thoracic Limb," in *Anatomy of the Horse: An Illustrated Text,* Iowa State Press, 2001, pp. 4-14.

[2] H. S. Thomas, The Horse Conformation Handbook, Storey Publishing, LLC, 2005.

[3] J. Ahmat, "Tendon Injuries," 2005. [Online]. Available: http://www.athletic-animals.com/tendon.htm. [Accessed 19 October 2011].

[4] J. S. Sanders, "Effect of Two Bandage Protocols on Equine Fetlock Kinematics," Auburn, 2009.

[5] L. Sellnow, "On the Forehand," TheHorse, 2006.

[6] B. R. Pony, "Forever Horses," [Online]. Available: http://foreverhorses.blogspot.com/2009/11/anatomy-of-equine-forleg.html. [Accessed 14 March 2012].

[7] G. Ferraro, S. Stover and M. B. Whitcomb, "Suspensory Ligament Injuries in Horses," *UC Davis Center for Equine Health,* 2007.

[8] C. Carballo, *A diagram of Soft Tissue Unit of Equine Forelimb,* Grafton, 2011.

[9] M. H. Ratzlaff, "Quantitative Methods for the Analysis of Equine Locomotion and Their Applications to Other Species1," *American Zoologist,* vol. 29, no. 1, pp. 267-285, 1989.

[10] P. Harrison, "Joint Stresses in the Performance Horse," 2001. [Online]. Available: http://www.horseit.com/en/Health2001/articles/TRMjointstresses190707.htm. [Accessed 18 October 2011].

[11] C. A. Kirker-Head, "AER Device Design Specifications," Grafton, 2011.

[12] J. S. Merritt, H. M. Davies, C. Burvill and M. G. Pandy, "Influence of Muscle-TendonWrapping on Calculations of Joint Reaction Forces in the Equine Distal Forelimb," *Journal of Biomedicine and Biotechnology,* p. 9, 2008.

[13] L. S. Meershoek, L. Roepstorff, H. C. Schamhardt, C. Johnston and M. F. Bobbert, "Joint moments in the distal forelimbs of jumping horses during landing," *Equine Veterinary Journal,* pp. 410-415, 2001.

[14] M. D. Swanstrom, L. Zarucco, M. Hubbard, S. M. Stover and D. A. Hawkins, "Musculoskeletal Modeling and Dynamic Simulation of the Thoroughbred Equine Forelimb During Stance Phase of the Gallop," *Journal of Biomechanical Engineering,* pp. 318-328, 2005.

[15] R. Hauser, "The Urkesh system - Measuring figurines," 2003. [Online]. Available: http://www.urkesh.org/urkeshpublic/352n%20revised.htm. [Accessed 15 March 2012].

[16] D. S. a. D. M. H.M. Clayton, "Three-dimensional Torques and Power of Horse Forelimb Joints at Trot," 2011.

[17] R.E.Kostur, "Protective Device for the Leg of a Horse". Patent 3,405,506 , 15 October 1968.

[18] D. Scott, "Leg Support Wrap for Horses". Spring Valley, California, USA Patent 5,115,627, 26 May 1992.

[19] W. Hampicke, "Leg or Foot Bandages, Especially for Horses". Germany Patent 4,140,116 , 20 February 1979.

[20] D. G. H. Jr., "Protective Boot for Leg of Horse". Los Angeles, California, USA Patent 4,470,411 , 11 September 1984.

[21] P. J. Armato, "Equine Athletic Boot with Inflatable U-shaped Bladder". Mt. Sterling, Ky Patent 5,363,632 , 15 November 1994.

[22] J. E. Bertram and A. Gutmann, "Motions of the running horse and cheetah revisited: fundamental mechanics of the transverse and rotary gallop," vol. 328, 2008.

[23] H. M. Clayton, J. L. Lanovaz, H. C. Schamhardt, M. A. Willemen and G. R. Colborne, "Net joint moments and powers in the equine forelimb in the stance phase of the trot," *Equine Veterinary,* pp. 384-389, 1998.

[24] S. M. Kerr, J. G. Jacobson and N. E. Almstrom, "Horse Gait Analysis," Worcester Polytechnic Insitute, Worcester, 2000.

[25] E. Simonsen, P. Dyhre-Poulsen, M. Voigt, P. Aagaard and N. Fallentin, "Mechanisms contributing to different joint moments observed during human walking.," *Scand J Med Sci Sports,* pp. 1-13, 1997.

[26] S. Sarcia, Interviewee, *Restrainer band conference interview at WPI.* [Interview]. 6 Oct 2011.

[27] C. Morse, Interviewee, *Engineer at Manta, Inc.*. [Interview]. 12 March 2012.

[28] McMaster Carr, "McMaster-Polyurathane (Part Number: 8716K46)," [Online]. Available: http://www.mcmaster.com/#8716k46/=gnwiv6. [Accessed 14 March 2012].

[29] S. Sarcia, *Solidworks drawing of restrainer band of the horse leg protective device designed by Manta Inc.*, Boston, MA: Manta Inc., 2011.

[30] Harkness Industries, 2000. [Online]. Available: http://www.harknessindustries.com/pdfs/MP950.pdf.

[31] RubberMill, "Hardness of Rubber: Durometer," RubberMill.

[32] S. Harris, Horse Gait, Balance, and Movement, New York: Howell Book House, 1993.

[33] M. Hildebrand, "Motions of the Running Cheetah and Horse," *Journal of Mammalogy,* vol. 40, no. 4, pp. 481-495, 1959.

[34] H. M. Clayton, J. L. Lanovaz, H. C. Schamhardt, M. A. Willemen and G. L. Colborne, "net joint moments and joint powers in horses with superficial digital flexor tendinities," *American Journal of Veterinary Research ,* pp. 197-201, 2000.

[35] M. T. K. L. G. a. D. L. S. Paul DeVita, "A Functional Knee Brace Alters Joint Torque and Power Patterns During Walking and Running," vol. 29, 1996.

[36] A. M. Dollar and H. Herr, "Lower-Extremity Exoskeletons and Active Orthoses Challenges and State of the Art," vol. 24, no. 1, 2008.

[37] T. Sandin, "Useful Equipment for Protection of Horse Leg," 2005. [Online]. Available: http://www.sustainabledressage.net/tack/other_equipment.php. [Accessed 29 February 2012].

[38] B. D. Robertson and G. Sawicki, "Influence of Parallel Spring-Loaded Exoskeleton on Ankle Muscle-Tendon Dynamics During Simulated Human Hopping," Chapel Hill, 2011.

[39] G. L. Ferraro, S. M. Stover and M. B. Whitcomb, "Suspensory Ligament Injuries in Horses," Center for Equine Health, Davis, 2009.

[40] Stokesley Science, "Stiffness," Stokesley Science, 2009. [Online]. Available: http://www.stokesleyscience.org/A%20level%20Physics/Materials/stiffness.htm. [Accessed 1 March 2012].

[41] A. A. Biewener, "Muscle-tendon stresses and elastic energy storage during locomotion in the horse," vol. 98, no. 24, 1999.

[42] Joint Healing, "Knee Braces for Sports," Joint Healing, 2000. [Online]. Available: www.jointhealing.com. [Accessed 27 Feb 2012].

[43] Christine M. Kleinert Institute for Hand and Micro Surgery, "The Wonders of the Hand and Upper Limb," 2009. [Online]. Available: http://www.cmki.org/about/hwachapter.cfm. [Accessed 12 December 2011].

[44] A. Lefley, "Deep Knee Bends: Measuring Knee Stress with a Mechanical Model," 2007. [Online]. Available: http://www.sciencebuddies.org/science-fair-projects/project_ideas/HumBio_p006.shtml . [Accessed 2 March 2012].

[45] CES EduPack, "Flexural modulus," 2011.

[46] Dechra Veterinary Products, "Dechra Veterinary Products-Equine Pain Matters," Dechra Veterinary Products, [Online]. Available: http://www.equinepainmatters.com/downloads/anatomy-charts.php. [Accessed 14 March 2012].

Appendix

Appendix A: Data extracted by previous published articles

Results by Meershoek et al [13].

	carpal joint moment	fetlock joint moment	coffin joint moment	carpal joint angle	fetlock joint angle	coffin joint angle	GRF Verticle	GRF Force - after
	Nm/kg	Nm/kg	Nm/kg	deg	deg	deg	N/kg	N/kg
0%	-0.46	-0.20	0.00	6.25	12.56	-2.65	0.38	-0.10
5%	-0.13	-0.24	0.17	5.15	28.63	-16.64	0.58	-0.30
10%	-1.04	-0.58	0.24	10.74	33.74	-21.53	0.84	-0.32
15%	-1.60	-0.94	0.26	13.87	39.39	-24.98	1.08	-0.22
20%	-2.04	-1.19	0.24	13.87	41.05	-24.98	1.24	-0.24
25%	-2.32	-1.42	0.26	13.19	44.52	-26.63	1.44	-0.28
30%	-2.58	-1.61	0.29	12.46	47.99	-26.63	1.60	-0.26
35%	-2.74	-1.79	0.24	11.13	49.82	-27.04	1.68	-0.22
40%	-2.83	-1.93	0.17	11.13	51.36	-26.08	1.78	-0.18
45%	-2.85	-2.05	0.07	11.13	52.32	-24.42	1.80	-0.14
50%	-2.83	-2.16	0.00	11.13	53.23	-22.81	1.80	-0.10
55%	-2.74	-2.24	-0.10	11.13	54.50	-21.05	1.78	-0.04
60%	-2.58	-2.28	-0.20	10.74	55.37	-18.84	1.72	0.00
65%	-2.37	-2.28	-0.26	10.16	56.10	-15.34	1.72	0.04
70%	-2.04	-2.21	-0.34	9.19	54.84	-10.45	1.64	0.08
75%	-1.69	-2.08	-0.42	8.87	53.23	-4.75	1.54	0.12
80%	-1.36	-1.87	-0.48	7.49	50.29	3.76	1.38	0.18
85%	-0.84	-1.52	-0.48	5.62	44.11	14.32	1.24	0.20
90%	-0.30	-0.94	-0.44	3.10	34.24	28.48	0.94	0.18
95%	0.13	-0.44	-0.40	-3.22	21.77	40.22	0.58	0.12
100%	0.30	0.00	-0.13	-14.04	13.53	35.01	0.26	0.04

Figure 49 Joint moment and joint angles at carpal joint, MCPJ and coffin joint, as well as ground reaction forces in a full gait from 0% to 100% with 5% increment, data extracted from article by Meershoek et al.

Results by Merritt et al [12].

Walk	Coffin	Fetlock	Carpus
	N.m/kg bwt	N.m/kg bwt	N.m/kg bwt
0%	0.000	0.000	0.000
5%	-0.028	-0.095	-0.130
10%	-0.030	-0.180	-0.249
15%	-0.058	-0.312	-0.370
20%	-0.063	-0.400	-0.418
25%	-0.069	-0.444	-0.412
30%	-0.076	-0.472	-0.370
35%	-0.079	-0.481	-0.330
40%	-0.077	-0.485	-0.300
45%	-0.078	-0.485	-0.276
50%	-0.078	-0.477	-0.239
55%	-0.080	-0.489	-0.180
60%	-0.077	-0.438	-0.133
65%	-0.075	-0.396	-0.085
70%	-0.075	-0.332	-0.045
75%	-0.088	-0.289	-0.027
80%	-0.101	-0.238	0.000
85%	-0.100	0.020	-0.035
90%	-0.085	-0.132	0.090
95%	-0.022	-0.043	0.088
100%	0.005	0.000	0.012

Figure 50 Joint moment at carpal joint, MCPJ and coffin joint of the walking horse at a full gait cycle from 0% to 100% with 5% increment, data extracted from article by Merritt et al.

Trot	Coffin	Fetlock	Carpus
	N.m/kg bwt	N.m/kg bwt	N.m/kg bwt
0%	-0.015	0.000	-0.010
5%	-0.033	-0.085	-0.090
10%	-0.050	-0.161	-0.164
15%	-0.018	-0.250	-0.289
20%	-0.018	-0.390	-0.424
25%	-0.027	-0.547	-0.543
30%	-0.030	-0.690	-0.615
35%	-0.028	-0.800	-0.675
40%	-0.025	-0.888	-0.703
45%	-0.025	-0.920	-0.710
50%	-0.027	-0.900	-0.684
55%	-0.030	-0.870	-0.700
60%	-0.033	-0.789	-0.502
65%	-0.033	-0.680	-0.393
70%	-0.035	-0.565	-0.252
75%	-0.041	-0.417	-0.142
80%	-0.048	-0.260	-0.023
85%	-0.045	-0.175	-0.031
90%	-0.028	-0.085	-0.065
95%	-0.013	-0.027	-0.062
100%	0.000	0.000	0.000

Figure 51 Joint moment at carpal joint, MCPJ and coffin joint of the trotting horse at a full gait cycle from 0% to 100% with 5% increment, data extracted from article by Merritt et al.

Walk	P3-P2	Navicular bone	P1-cannon	Proximal Sesamoid
	N/kg bwt	N/kg bwt	N/kg bwt	N/kg bwt
0%	0.75	0.75	0.15	0.00
5%	1.99	1.33	2.92	1.61
10%	2.76	1.36	8.29	5.00
15%	4.40	1.97	1.43	10.32
20%	5.13	2.00	1.98	15.00
25%	5.75	2.10	2.29	18.71
30%	6.11	2.42	2.52	20.97
35%	6.21	2.67	2.64	22.58
40%	6.30	2.74	2.68	23.06
45%	6.30	2.80	2.70	23.06
50%	6.32	3.06	2.68	23.06
55%	6.30	3.31	2.68	22.26
60%	6.05	3.51	2.49	20.16
65%	5.52	3.67	2.20	16.94
70%	5.09	4.05	1.89	13.23
75%	5.13	4.98	1.59	10.65
80%	5.45	6.04	1.35	8.71
85%	5.41	6.39	1.14	6.94
90%	4.95	5.94	8.45	4.68
95%	1.44	2.03	2.59	0.48
100%	0.39	0.56	0.00	0.00

Figure 52 Joint forces at carpal joint, MCPJ and coffin joint of the walking horse at a full gait cycle from 0% to 100% with 5% increment, data extracted from article by Merritt et al.

Trot	P3-P2	Navicular bone	P1-cannon	Proximal Sesamoid
	N/kg bwt	N/kg bwt	N/kg bwt	N/kg bwt
0%	1.00	0.80	1.00	0.00
5%	3.10	2.39	3.85	1.17
10%	3.17	1.65	7.97	4.00
15%	3.36	1.06	13.35	8.83
20%	4.54	0.78	20.00	15.83
25%	6.24	1.00	28.71	25.50
30%	7.68	1.02	37.58	36.50
35%	8.55	0.98	44.54	47.00
40%	9.00	0.90	49.61	54.67
45%	9.17	0.90	52.14	59.33
50%	9.07	1.00	51.98	59.50
55%	8.74	1.22	49.29	55.83
60%	8.20	1.52	44.70	49.17
65%	7.44	1.85	37.26	37.83
70%	6.48	2.37	29.18	26.33
75%	5.65	3.32	21.27	16.67
80%	4.85	4.88	17.00	10.00
85%	3.97	5.69	10.03	5.67
90%	2.51	3.81	5.28	2.17
95%	1.02	1.32	2.11	0.67
100%	0.41	0.49	1.16	0.00

Figure 53 Joint forces at carpal joint, MCPJ and coffin joint of the trotting horse at a full gait cycle from 0% to 100% with 5% increment, data extracted from article by Merritt et al.

Walk	Interrosseous Ligament (IL)	Deep digital flexor tendon (DDFT)	Superficial digital flexor tendon (SDFT)
	N/kg bwt	N/kg bwt	N/kg bwt
0%	0.43	1.50	0.00
5%	0.43	2.31	2.84
10%	2.50	2.44	7.32
15%	4.94	3.64	11.43
20%	6.69	3.90	15.00
25%	8.48	4.20	17.10
30%	9.49	4.59	17.65
35%	10.23	4.71	17.56
40%	10.60	4.67	17.47
45%	10.83	4.67	17.29
50%	10.78	4.71	16.83
55%	10.64	4.80	15.82
60%	10.00	4.76	13.63
65%	8.90	4.67	10.70
70%	7.42	4.76	7.41
75%	6.14	5.49	4.02
80%	4.76	6.26	1.83
85%	3.60	6.30	0.73
90%	2.22	5.79	0.00
95%	0.80	2.36	0.00
100%	0.43	1.24	0.00

Figure 54 Tendon tension forces at interosseous ligament, deep digital flexor tendon and superficial flexor tendon of the alking horse at a full gait cycle from 0% to 100% with 5% increment, data extracted from article by Merritt et al.

Trot	Interrosseous Ligament (IL)	Deep digital flexor tendon (DDFT)	Superficial digital flexor tendon (SDFT)
	N/kg bwt	N/kg bwt	N/kg bwt
0%	0.40	1.00	0.00
5%	0.44	2.52	0.28
10%	2.50	1.99	1.37
15%	6.66	1.46	2.93
20%	9.50	1.38	6.39
25%	12.50	1.95	10.55
30%	15.40	2.33	15.00
35%	17.69	2.41	20.16
40%	18.92	2.37	24.09
45%	19.89	2.37	25.98
50%	19.93	2.45	25.84
55%	19.52	2.56	23.80
60%	18.88	2.60	19.35
65%	16.04	2.56	14.72
70%	13.02	2.60	9.51
75%	9.27	2.98	4.87
80%	7.26	3.74	1.04
85%	3.14	3.78	0.19
90%	1.49	2.41	0.05
95%	0.90	1.00	0.00
100%	0.90	0.58	0.00

Figure 55 Tendon tension forces at interosseous ligament, deep digital flexor tendon and superficial flexor tendon of the trotting horse at a full gait cycle from 0% to 100% with 5% increment, data extracted from article by Merritt et al.

Results by Swanstrom [14]

	GRF Y	GRF X	Fetlock Angle	DIP Angle	PIP Angle	DDF Force	SDF Force	SL Force	DDF Strain	SDF Strain	SL Strain
	N/kg	N/kg	deg	deg	deg	N/kg	N/kg	N/kg	%	%	%
0%	4.93	-1.66	36.75	17.18	0.00	1.34	5.37	3.44	1.74	3.10	3.25
5%	9.33	1.70	47.11	22.30	3.46	3.48	6.87	7.83	1.95	3.56	4.38
10%	11.93	2.46	56.60	26.15	6.63	5.13	8.25	12.89	2.17	3.96	5.51
15%	14.57	2.96	64.71	29.14	8.96	5.69	9.01	17.96	2.30	4.26	6.46
20%	16.86	2.96	71.33	31.08	10.65	6.21	9.55	22.26	2.43	4.47	7.21
25%	18.90	2.46	75.95	32.38	11.35	6.67	10.09	25.65	2.53	4.64	7.80
30%	20.10	1.34	79.44	32.14	11.35	7.13	10.39	28.43	2.64	4.77	8.17
35%	20.54	0.18	81.19	30.73	11.35	7.41	10.63	30.15	2.72	4.83	8.41
40%	20.34	-1.02	81.19	28.39	10.65	7.61	10.63	30.83	2.77	4.83	8.48
45%	19.76	-0.16	81.19	25.35	10.14	7.41	10.63	30.83	2.77	4.83	8.48
50%	18.72	-3.14	81.19	21.92	8.96	7.23	10.39	30.15	2.77	4.77	8.77
55%	17.58	-3.98	79.44	17.54	8.36	7.13	9.91	29.33	2.77	4.72	8.31
60%	16.30	-4.78	78.23	12.82	7.56	6.93	9.41	27.89	2.77	4.64	8.10
65%	14.76	-5.39	75.54	7.05	7.05	6.67	8.83	25.97	2.77	4.47	7.80
70%	13.01	-5.79	71.85	0.00	6.02	6.51	7.95	23.22	2.72	4.26	7.36
75%	10.77	-6.13	66.60	-7.53	4.77	5.97	6.87	19.92	2.67	3.96	6.79
80%	9.33	-5.39	60.01	-14.58	3.46	4.99	5.59	15.88	2.53	3.56	6.09
85%	8.47	-4.97	52.72	-18.10	1.16	3.90	4.12	11.65	2.30	3.10	5.24
90%	7.17	-4.18	46.38	-14.13	1.11	2.46	2.92	8.23	1.85	2.57	4.53
95%	2.04	-1.26	39.99	-1.73	2.69	0.64	1.78	5.63	1.15	2.01	3.90
100%	0.00	0.00	27.24	16.09	4.50	0.00	0.00	2.26	0.47	1.03	2.70

Figure 56 Ground reaction forces, joint angles (at fetlock, coffin to short pastern and short pastern to long pastern), Tendon tension forces and tendon strain at suspensory ligament, deep digital flexor tendon and superficial flexor tendon of the jumping horse at a full gait cycle from 0% to 100% with 5% increment, data extracted from article by Swanstrom et al.

Results by Clayton (2011) [16]

	Carpus			Fetlock			Pastern			Coffin		
	Flex/ext	Add/abd	Int/ext	Flex/ext	Add/abd	Int/ext	Flex/ext	Add/abd	Int/ext	Flex/ext	Add/abd	Int/ext
	deg	deg	deg	deg	deg	deg	deg	deg	deg	deg	deg	deg
0%	-4.3	0.0	-4.5	10.0	1.8	-1.9	5.0	-0.2	0.6	5.6	-0.2	-1.3
5%	-7.4	0.0	-4.0	-2.3	-1.4	-3.3	4.4	0.6	0.2	18.9	2.1	0.4
10%	-6.8	-5.0	-2.5	-11.2	-3.3	-3.3	5.1	0.9	1.3	23.5	2.1	0.4
15%	-8.0	-5.0	-2.0	-15.9	-4.2	-3.7	5.7	0.2	2.2	25.8	1.5	-1.3
20%	-8.3	-5.0	-2.0	-17.5	-4.2	-3.7	3.7	0.6	1.5	22.9	2.7	0.4
25%	-7.4	-5.0	-2.0	-14.6	-3.7	-3.7	1.7	0.4	1.7	17.1	1.5	2.1
30%	-7.4	0.0	-3.0	-8.0	-2.3	-4.2	-1.4	0.2	1.3	21.2	-0.8	5.0
35%	-7.1	0.0	-3.0	5.3	2.2	-2.8	-2.7	-0.3	0.9	-22.7	-4.8	7.3
40%	-3.4	0.0	-3.5	16.6	3.6	-1.4	-3.4	-1.5	0.4	-33.7	-0.8	6.2
45%	10.9	2.0	-4.0	27.4	6.3	-0.5	2.4	0.9	0.2	-6.5	1.0	1.5
50%	25.1	3.0	-1.5	44.7	10.0	1.3	7.5	-7.0	0.9	5.6	1.0	-0.2
55%	44.3	6.0	1.0	43.5	9.1	0.4	5.7	0.6	-0.2	4.4	1.0	0.4
60%	58.2	9.0	2.5	39.4	8.6	-0.5	6.2	0.4	-0.3	7.9	1.0	-0.8
65%	63.5	10.0	3.5	44.4	9.5	1.3	7.1	0.4	-0.2	11.4	2.7	-1.3
70%	62.5	9.5	3.5	50.4	10.5	1.8	7.3	0.4	-0.7	11.9	2.7	0.4
75%	55.7	8.5	3.5	51.7	11.4	1.8	7.3	0.4	-0.7	10.2	2.7	0.4
80%	44.0	6.5	0.5	48.5	10.9	0.9	6.2	0.8	-0.7	12.5	2.7	0.4
85%	26.7	1.0	-4.0	35.9	7.3	-1.0	7.0	0.9	-0.2	15.4	2.1	0.4
90%	9.9	0.0	-5.0	25.8	5.0	-2.3	7.1	1.1	-0.2	10.8	3.3	0.4
95%	3.1	-1.0	-6.0	20.1	4.5	-2.3	6.2	0.4	0.0	5.6	3.3	0.4
100%	-3.7	-1.0	-5.0	12.5	2.7	-3.7	4.8	-0.3	0.4	10.2	2.7	0.4

Figure 57 Tendon angles of the carpus, fetlock, pastern and coffin bone of a trotting horse at a full gait cycle from 0% to 100% with 5% increment, data extracted from article by Clayton et al.

	Carpus			Fetlock			Pastern			Coffin		
	Pro/dis	Med/lat	Cra/Cau	Pro/dis	Med/lat	Cra/Cau	Pro/dis	Med/lat	Cra/Cau	Pro/dis	Med/lat	Cra/Cau
	m	m	m	m	m	m	m	m	m	m	m	m
0%	0.0000	0.0000	0.0000	0.0060	0.0003	-0.0065	0.0000	0.0000	0.0005	-0.0026	-0.0005	0.0000
5%	0.0000	0.0040	-0.0022	0.0000	-0.0010	-0.0118	-0.0007	0.0007	-0.0002	-0.0018	-0.0010	0.0065
10%	0.0000	0.0040	-0.0017	-0.0050	-0.0020	-0.0133	-0.0003	0.0007	0.0000	-0.0028	-0.0015	0.0077
15%	0.0000	0.0040	0.0000	-0.0083	-0.0028	-0.0133	0.0007	0.0007	0.0003	-0.0036	-0.0010	0.0082
20%	0.0000	0.0040	-0.0044	-0.0095	-0.0033	-0.0133	0.0003	0.0005	0.0002	-0.0031	-0.0013	0.0075
25%	0.0000	0.0050	-0.0011	-0.0075	-0.0030	-0.0135	0.0013	0.0002	0.0007	-0.0026	-0.0013	0.0053
30%	0.0000	0.0050	-0.0028	-0.0048	-0.0018	-0.0135	0.0013	0.0007	0.0003	-0.0010	-0.0018	-0.0009
35%	-1.0000	0.0030	-0.0033	0.0035	-0.0008	-0.0085	0.0017	-0.0002	0.0002	-0.0018	-0.0010	-0.0130
40%	-3.0000	0.0020	0.0017	0.0825	0.0000	-0.0043	0.0013	0.0007	0.0008	-0.0023	-0.0010	-0.0202
45%	-0.0080	0.0000	0.0178	0.0115	-0.0005	0.0025	0.0000	0.0008	0.0003	-0.0005	-0.0021	-0.0116
50%	-0.0150	-0.0050	0.0333	0.0148	-0.0015	0.0120	-0.0003	0.0005	-0.0002	0.0005	-0.0005	-0.0032
55%	-0.0320	-0.0100	0.0461	0.0158	-0.0013	0.0118	0.0007	0.0008	0.0003	0.0010	-0.0013	-0.0019
60%	-0.0470	-0.0080	0.0550	0.0153	-0.0005	0.0095	0.0000	0.0010	-0.0003	0.0003	-0.0013	-0.0019
65%	-0.0510	-0.0080	0.0572	0.0153	-0.0013	0.0120	0.0000	0.0008	-0.0003	-0.0003	-0.0008	0.0002
70%	-0.0470	-0.0080	0.0567	0.0153	-0.0013	0.0163	0.0000	0.0010	0.0003	0.0000	-0.0005	0.0009
75%	-0.0360	-0.0080	0.0511	0.0153	-0.0023	0.0178	-0.0003	0.0007	-0.0003	0.0000	-0.0010	0.0009
80%	-0.0240	-0.0070	0.0444	0.0150	-0.0015	0.0153	0.0007	0.0007	-0.0002	0.0000	-0.0005	0.0018
85%	-0.0130	-0.0010	0.0311	0.0140	-0.0010	0.0065	-0.0010	0.0008	0.0000	0.0003	0.0005	0.0025
90%	-0.0050	0.0030	0.0189	0.0115	-0.0010	0.0008	-0.0002	0.0007	-0.0008	-0.0003	0.0000	0.0033
95%	-0.0030	0.0030	0.0089	0.0095	-0.0010	-0.0025	0.0000	0.0013	-0.0008	0.0000	0.0000	0.0004
100%	0.0000	0.0020	0.0011	0.0055	0.0000	-0.0065	0.0000	0.0007	-0.0005	0.0000	0.0000	0.0039

Figure 58 - Joint translations [m] of the carpus, fetlock, pastern and coffin bone of a trotting horse at a full gait cycle from 0% to 100% with 5% increment, data extracted from article by Clayton et al.

	Carpus			Fetlock			Pastern			Coffin		
	Flex/ext	Add/abd	Int/ext	Flex/ext	Add/abd	Int/ext	Flex/ext	Add/abd	Int/ext	Flex/ext	Add/abd	Int/ext
	Nm/kg	Nm/kg	Nm/kg	Nm/kg	Nm/kg	Nm/kg	Nm/kg	Nm/kg	Nm/kg	Nm/kg	Nm/kg	Nm/kg
0%	0.050	0.000	0.000	0.000	0.000	0.000	0.000	0.000	0.000	0.000	0.000	0.000
5%	0.069	0.370	0.014	0.016	0.186	-0.023	0.001	0.102	-0.014	-0.010	0.048	0.000
10%	0.240	0.399	0.009	0.080	0.170	-0.023	0.014	0.103	-0.019	-0.008	0.047	0.000
15%	0.429	0.306	0.000	0.170	0.142	-0.008	0.039	0.067	-0.013	0.001	0.030	0.000
20%	0.566	0.555	-0.018	0.242	0.235	-0.038	0.056	0.128	-0.027	-0.005	0.059	0.000
25%	0.608	0.526	-0.018	0.287	0.240	-0.050	0.080	0.122	-0.028	-0.002	0.060	0.000
30%	0.679	0.438	-0.018	0.356	0.229	-0.046	0.095	0.115	-0.026	-0.003	0.057	0.000
35%	0.755	0.384	-0.018	0.390	0.202	-0.046	0.111	0.102	-0.026	0.000	0.050	0.000
40%	0.755	0.306	-0.018	0.426	0.164	-0.035	0.124	0.074	-0.021	0.002	0.036	0.000
45%	0.679	0.204	-0.018	0.420	0.115	-0.023	0.121	0.046	-0.012	0.005	0.024	0.000
50%	0.600	0.048	0.000	0.388	0.061	-0.004	0.115	0.012	0.000	0.002	0.005	0.001
55%	0.514	-0.118	0.018	0.338	-0.016	0.018	0.103	-0.027	0.008	0.004	-0.012	0.001
60%	0.386	-0.255	0.036	0.279	-0.075	0.018	0.086	-0.057	0.011	0.005	-0.029	-0.001
65%	0.216	-0.362	0.041	0.178	-0.135	0.015	0.063	-0.088	0.009	0.003	-0.040	0.001
70%	0.060	-0.431	0.045	0.091	-0.179	0.003	0.038	-0.105	0.003	0.002	-0.047	0.000
75%	-0.101	-0.445	0.036	-0.003	-0.190	-0.016	0.007	-0.111	-0.007	0.001	-0.045	0.001
80%	-0.176	-0.367	0.009	-0.061	-0.163	-0.023	-0.008	-0.089	-0.014	0.001	-0.034	0.000
85%	-0.191	-0.235	0.005	-0.088	-0.092	-0.031	-0.019	-0.050	-0.014	0.001	-0.018	0.000
90%	-0.148	-0.187	-0.005	-0.069	-0.065	-0.020	-0.014	-0.038	-0.019	0.000	-0.015	0.000
95%	-0.068	-0.084	-0.005	-0.024	-0.026	-0.016	-0.002	-0.019	-0.012	0.003	-0.009	-0.001
100%	-0.025	0.000	0.000	0.000	0.000	0.000	0.000	0.000	0.000	0.000	0.000	0.000

Figure 59 - Joint moment of the carpus, fetlock, pastern and coffin bone of a trotting horse at a full gait cycle from 0% to 100% with 5% increment, data extracted from article by Clayton et al.

	Carpus			Fetlock			Pastern			Coffin		
	Flex/ext	Add/abd	Int/ext	Flex/ext	Add/abd	Int/ext	Flex/ext	Add/abd	Int/ext	Flex/ext	Add/abd	Int/ext
	Nm/kg	Nm/kg	Nm/kg	Nm/kg	Nm/kg	Nm/kg	Nm/kg	Nm/kg	Nm/kg	Nm/kg	Nm/kg	Nm/kg
0%	-0.050	0.038	-0.007	0.003	0.007	0.000	0.002	0.003	0.000	0.001	0.000	0.000
5%	-0.029	0.039	0.008	-0.003	0.007	0.001	-0.002	0.003	0.001	-0.001	0.000	0.001
10%	-0.029	-0.019	0.006	-0.010	-0.003	0.001	-0.006	-0.002	0.001	-0.002	0.001	0.001
15%	-0.012	0.007	0.001	0.005	-0.001	0.000	-0.003	0.000	0.000	-0.001	0.000	0.000
20%	-0.007	0.016	-0.007	0.000	0.005	0.000	0.000	0.002	0.000	0.000	0.000	0.000
25%	-0.008	0.011	-0.003	0.000	0.003	0.000	0.000	0.001	0.000	0.000	0.000	0.000
30%	-0.002	0.004	0.001	0.002	0.001	0.000	0.001	0.001	0.000	0.000	0.000	0.000
35%	0.000	-0.017	0.006	0.002	-0.003	0.001	0.001	-0.001	0.000	0.000	0.000	0.000
40%	-0.012	-0.008	0.005	-0.001	-0.002	0.000	-0.001	-0.001	0.000	-0.001	0.000	0.000
45%	-0.007	0.001	0.001	0.001	0.000	0.000	-0.001	0.000	0.000	-0.001	0.000	0.000
50%	-0.008	0.008	-0.001	0.001	0.002	0.000	0.000	0.001	0.000	0.000	0.000	0.000
55%	0.005	0.005	-0.002	0.002	0.001	0.000	0.000	0.000	0.000	0.000	0.000	0.000
60%	0.013	-0.016	0.003	0.002	-0.002	0.000	0.001	0.000	0.000	0.000	0.000	0.000
65%	0.026	0.002	0.001	0.004	0.000	0.000	0.002	0.000	0.000	0.000	0.000	0.000
70%	0.042	0.029	0.042	0.009	0.003	0.000	0.004	0.001	0.000	0.000	0.000	0.000
75%	0.067	0.020	0.032	0.017	0.002	0.000	0.007	0.001	0.000	0.001	0.000	0.000
80%	0.065	-0.023	-0.031	0.017	-0.004	0.000	0.005	-0.002	0.000	0.001	0.000	0.000
85%	0.025	-0.019	-0.028	0.005	-0.004	0.001	0.001	-0.002	0.000	0.000	0.000	0.000
90%	0.029	0.019	0.030	0.006	0.003	0.000	0.004	0.001	0.000	0.001	0.000	0.000
95%	0.065	0.010	0.017	0.016	0.002	0.000	0.007	0.001	-0.001	0.001	0.000	0.000
100%	0.025	0.000	0.001	0.007	0.000	0.000	0.003	0.000	0.000	0.001	0.000	0.000

Figure 60 - Joint moment of the carpus, fetlock, pastern and coffin bone of a horse during swing at a full gait cycle from 0% to 100% with 5% increment, data extracted from article by Clayton et al.

	Prox/dist: Fz	Med/lat: Fy	Cran/Caud: Fx	Prox/dist: Fz	Med/lat: Fy	Cran/Caud: Fx
	N/kg	N/kg	N/kg	N/kg	N/kg	N/kg
0%	-0.46	0.15	-0.22	-0.25	0.36	-0.13
5%	-1.94	0.83	-0.15	-1.68	0.92	-0.38
10%	-2.87	0.83	-0.40	-2.91	0.98	-0.69
15%	-3.86	0.59	-0.56	-3.53	0.55	-1.18
20%	-5.65	1.27	-0.34	-5.38	1.29	-1.18
25%	-6.82	1.02	-0.22	-6.68	1.17	-1.18
30%	-7.99	0.65	0.03	-7.73	0.98	-1.18
35%	-8.73	0.52	0.22	-8.59	0.80	-1.18
40%	-9.10	0.40	0.40	-9.09	0.55	-0.93
45%	-9.35	0.03	0.77	-9.33	0.24	-0.75
50%	-9.10	-0.28	1.02	-9.15	-0.01	-0.44
55%	-8.67	-0.77	1.20	-8.78	-0.38	-0.19
60%	-8.12	-1.14	1.27	-8.22	-0.81	0.18
65%	-7.25	-1.33	1.39	-7.42	-1.00	0.36
70%	-6.20	-1.33	1.62	-6.43	-1.12	0.80
75%	-4.91	-1.14	1.39	-5.13	-1.12	0.86
80%	-3.30	-1.08	1.20	-3.47	-0.81	0.80
85%	-2.07	-0.71	0.96	-2.11	-0.56	0.73
90%	-1.33	-0.52	0.59	-1.24	-0.38	0.61
95%	-0.65	-0.40	0.22	-0.56	-0.19	0.18
100%	0.11	-0.03	-0.03	0.19	0.00	-0.01

Figure 61 joint forces of the carpus, fetlock, pastern and coffin bone of a horse during trotting at a full gait cycle from 0% to 100% with 5% increment, data extracted from article by Clayton et al. (Part 1)

Prox/dist: Fz	Med/lat: Fy	Cran/Caud: Fx	Prox/dist: Fz	Med/lat: Fy	Cran/Caud: Fx	Prox/dist: Fz	Med/lat: Fy	Cran/Caud: Fx
N/kg	N/kg	N/kg	N/kg	N/kg	N/kg	N/kg	N/kg	N/kg
-0.47	0.35	-0.15	-0.44	0.00	0.00	0.26	0.14	-0.31
-2.22	0.97	-0.34	-1.85	0.96	-0.25	2.04	-0.12	-0.88
-3.03	0.79	-0.90	-3.13	1.02	-0.57	3.11	-0.12	-0.88
-3.97	0.66	-1.59	-3.64	0.70	-1.08	3.93	0.07	-0.50
-5.47	1.35	-2.28	-5.42	1.34	-1.79	5.90	-0.12	-1.00
-6.29	1.41	-2.97	-6.44	1.34	-2.30	6.97	-0.12	-1.00
-7.23	1.23	-3.53	-7.47	1.34	-2.81	8.05	-0.12	-1.00
-7.85	1.04	-3.97	-8.17	1.22	-3.25	8.87	0.07	-0.88
-8.23	0.85	-4.16	-8.61	1.02	-3.44	9.25	0.07	-0.62
-8.54	0.60	-4.03	-8.93	0.70	-3.44	9.50	0.14	-0.37
-8.48	0.22	-3.78	-8.93	0.39	-3.44	9.44	0.14	-0.24
-8.48	-0.04	-3.22	-8.68	0.00	-3.25	9.06	0.14	0.33
-8.10	-0.40	-2.47	-8.17	-0.38	-2.81	8.43	0.14	0.58
-7.66	-0.65	-1.59	-7.47	-0.57	-2.23	7.73	0.14	0.71
-6.66	-0.97	-0.72	-6.51	-0.89	-1.47	6.53	0.14	0.90
-5.41	-0.97	0.22	-5.23	-1.02	-0.57	5.20	0.14	0.90
-3.72	-0.90	0.97	-3.38	-0.83	-0.19	3.62	0.14	0.58
-2.16	-0.59	1.04	-1.98	-0.44	-0.77	2.16	0.14	0.52
-1.22	-0.43	0.85	-1.15	-0.44	-0.83	1.47	0.14	0.26
-0.59	-0.21	0.47	-0.51	-0.13	-0.70	0.64	0.14	0.26
-0.03	-0.09	0.04	-0.06	0.07	0.00	0.20	0.14	0.14

Figure 62 joint forces of the carpus, fetlock, pastern and coffin bone of a horse during trotting at a full gait cycle from 0% to 100% with 5% increment, data extracted from article by Clayton et al. (Part 2)

	Carpus			Fetlock			Pastern			Coffin		
	Flex/ext	Add/abd	Int/ext	Flex/ext	Add/abd	Int/ext	Flex/ext	Add/abd	Int/ext	Flex/ext	Add/abd	Int/ext
	Prox/dist: Fz	Med/lat: Fy	Cran/Caud: Fx	Prox/dist: Fz	Med/lat: Fy	Cran/Caud: Fx	Prox/dist: Fz	Med/lat: Fy	Cran/Caud: Fx	Prox/dist: Fz	Med/lat: Fy	Cran/Caud: Fx
	N/kg	N/kg	N/kg	N/kg	N/kg	N/kg	N/kg	N/kg	N/kg		N/kg	N/kg
0%	0.157	0.126	0.166	0.115	0.101	0.077	0.097	0.081	-0.019	0.049	0.041	-0.011
5%	0.095	0.197	0.166	0.064	0.035	0.105	0.111	0.080	0.023	0.061	0.043	0.011
10%	-0.020	-0.113	0.073	0.055	0.027	0.081	0.072	-0.024	0.066	0.045	-0.044	0.040
15%	0.011	-0.073	0.060	0.071	0.070	0.074	0.040	-0.015	0.035	0.026	0.001	0.026
20%	-0.024	0.029	0.082	0.065	0.069	0.074	0.032	0.044	0.006	0.019	0.024	0.008
25%	-0.060	0.015	0.031	0.062	0.067	0.066	0.020	0.030	0.011	0.016	0.019	0.006
30%	0.015	-0.024	0.033	0.073	0.045	0.056	0.023	0.018	-0.007	0.014	0.013	0.000
35%	0.002	-0.095	0.086	0.077	0.028	0.069	0.042	-0.024	-0.010	0.022	-0.008	0.001
40%	-0.020	-0.055	0.100	0.071	0.037	0.078	0.049	-0.025	0.008	0.026	-0.004	0.012
45%	0.029	-0.016	0.051	0.065	0.052	0.064	0.032	0.000	0.012	0.017	0.006	0.011
50%	0.060	0.002	0.038	0.069	0.064	0.052	0.013	0.015	-0.007	0.010	0.013	0.005
55%	0.055	-0.011	0.055	0.076	0.061	0.059	0.027	0.021	-0.010	0.019	0.013	0.003
60%	0.082	-0.095	-0.011	0.078	0.036	0.058	0.040	-0.007	-0.015	0.022	0.006	0.006
65%	0.122	-0.024	-0.086	0.077	0.039	0.039	0.018	-0.013	-0.027	0.013	0.007	-0.009
70%	0.166	0.100	-0.109	0.087	0.069	0.025	0.013	0.024	-0.056	0.010	0.022	-0.030
75%	0.131	0.064	-0.210	0.102	0.083	-0.006	0.008	0.037	-0.120	-0.006	0.016	-0.054
80%	-0.011	-0.122	-0.228	0.085	0.052	-0.086	-0.029	-0.016	-0.134	-0.013	-0.011	-0.036
85%	-0.016	-0.109	-0.109	0.044	0.013	-0.014	-0.031	-0.056	-0.005	0.000	-0.013	0.001
90%	0.131	0.069	-0.179	0.047	0.024	0.035	0.004	-0.012	-0.028	0.010	0.013	-0.024
95%	0.148	0.033	-0.268	0.085	0.070	-0.025	0.003	0.027	-0.111	0.016	0.011	-0.050
100%	0.139	-0.029	-0.126	0.083	0.049	0.032	0.036	-0.003	-0.004	0.020	0.005	-0.018

Figure 63 Joint forces of the carpus, fetlock, pastern and coffin bone of a horse during swing at a full gait cycle from 0% to 100% with 5% increment, data extracted from article by Clayton et al.

Appendix B: CAD Drawings of Horse Leg Protective Device [26]

Restrainer band Part Drawing

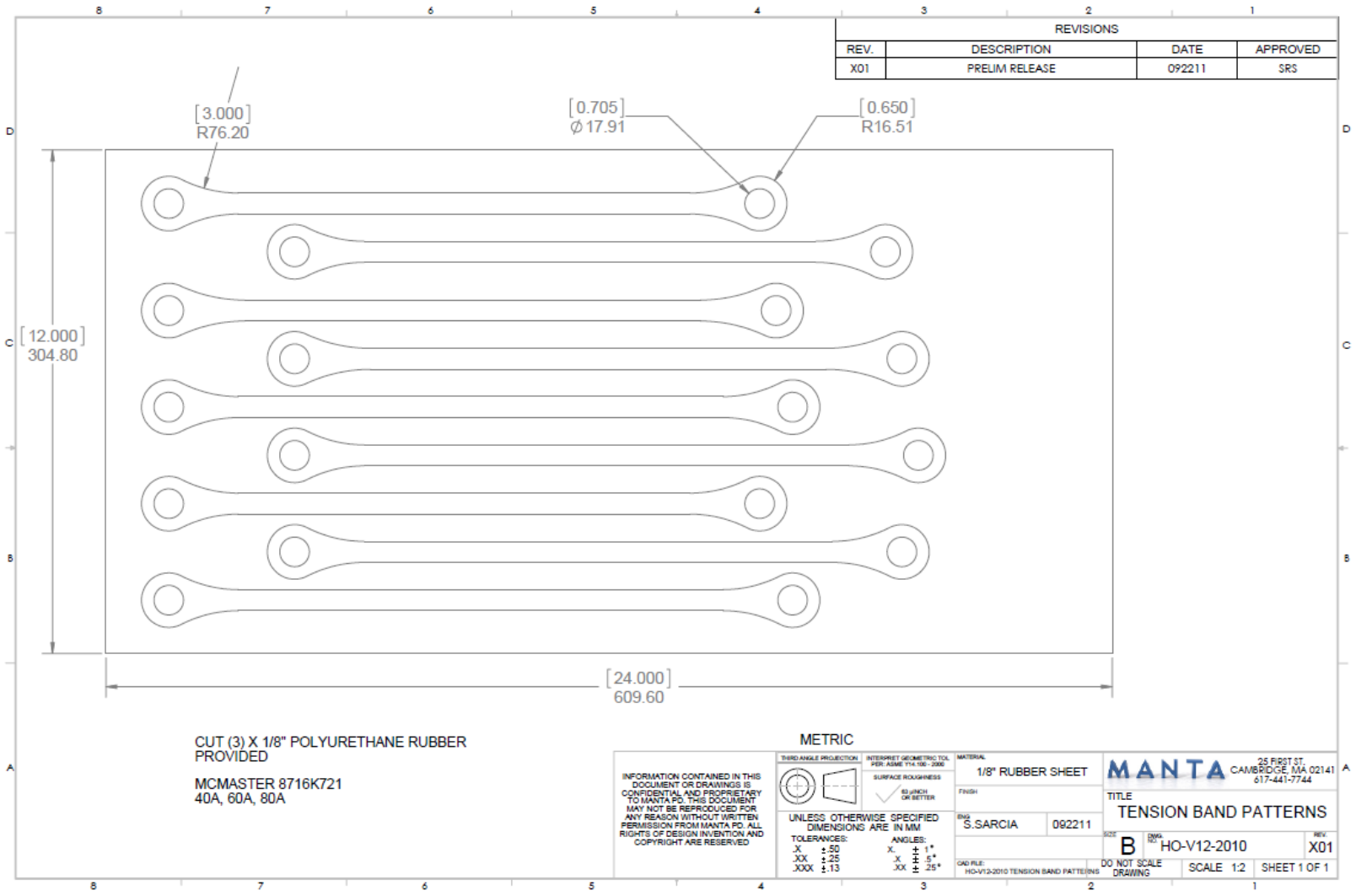

Horse Leg Protective Device Assembly Drawing

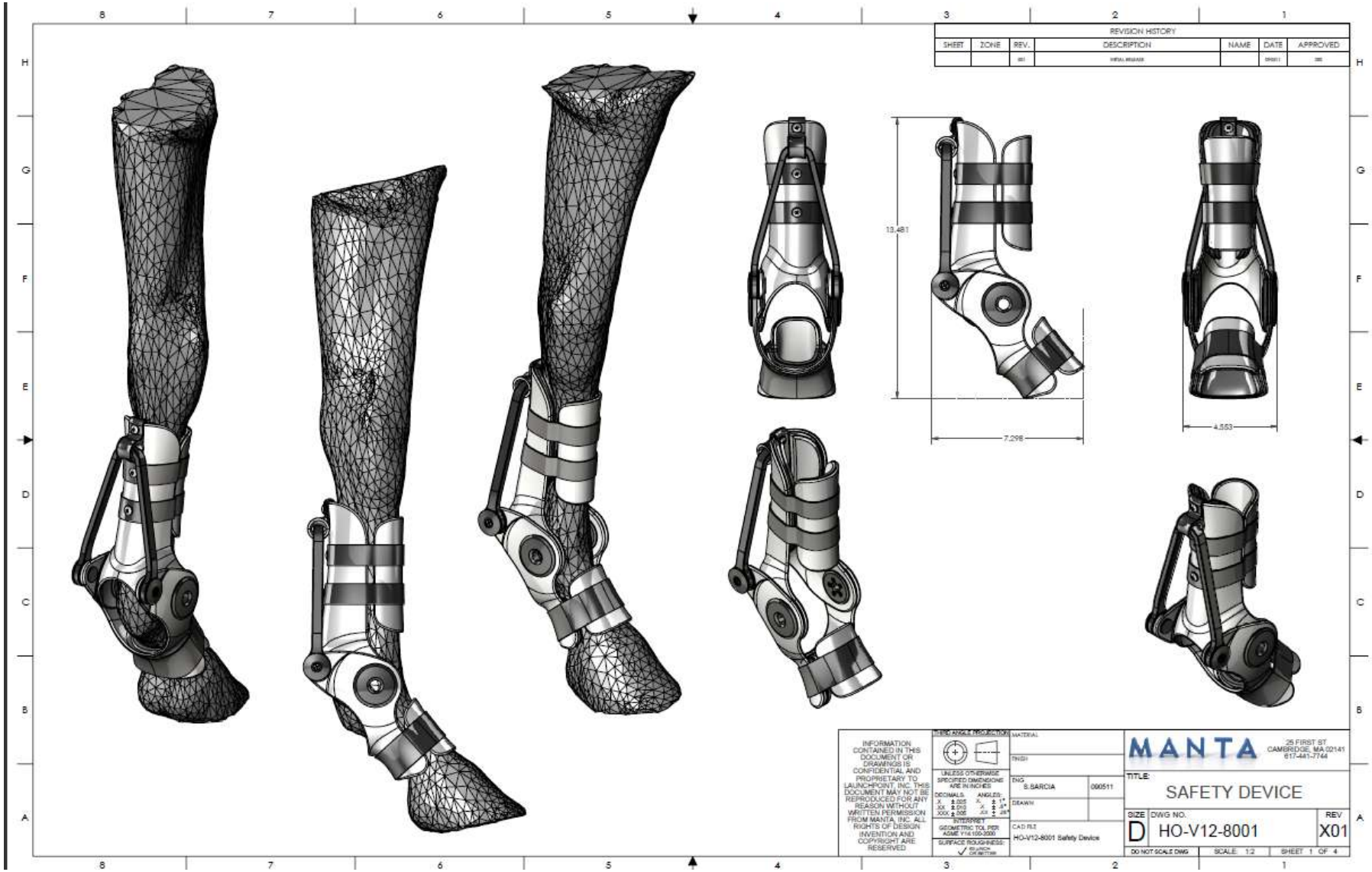

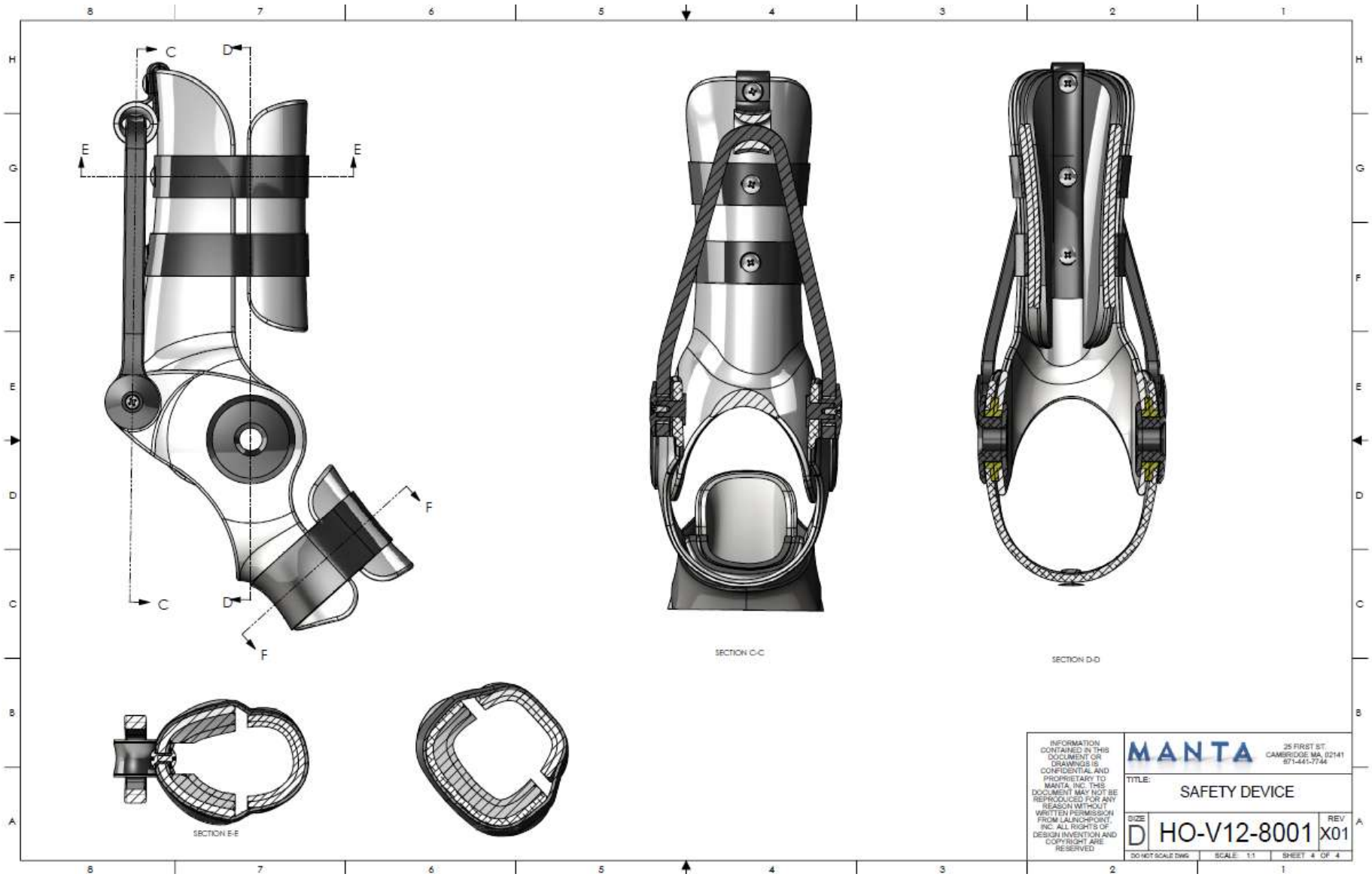
C
D
E
E
F
C
D
F
SECTION C-C
SECTION D-D
SECTION E-E
INFORMATION CONTAINED IN THIS DOCUMENT OR DRAWINGS IS CONFIDENTIAL AND PROPRIETARY TO MANTA, INC. THIS DOCUMENT MAY NOT BE REPRODUCED FOR ANY REASON WITHOUT WRITTEN PERMISSION FROM LAUNCHPOINT, INC. ALL RIGHTS OF DESIGN INVENTION AND COPYRIGHT ARE RESERVED
MANTA
25 FIRST ST. CAMBRIDGE, MA. 02141
671-441-7744
TITLE:
SAFETY DEVICE
SIZE
D
HO-V12-8001
REV
X01
DO NOT SCALE DWG
SCALE: 1:1
SHEET 4 OF 4